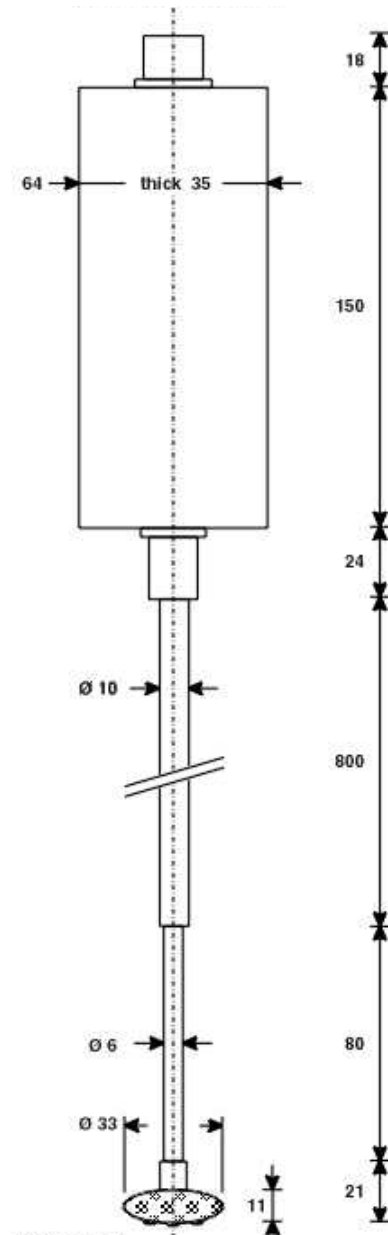


Influences of fluid accelerations on the threshold of motion

A graduation thesis by Maarten Tromp



Preface

This report is the final draft of my graduation thesis. This thesis is made within the framework of my master studies at the faculty of civil engineering, Delft University of Technology.

I would like to thank all co-workers of the Laboratory of fluid mechanics for their contribution on the realization of this thesis.

Finally I would like to thank the following members of the graduation commission for their support and dedication:

- Prof. dr. ir. M.J.F. Stive
- Ir. H.J. Verhagen
- Dr. ir. H.L. Fontijn
- Dr. ir. A.J.H.M. Reniers
- Ir. B. Hofland

Maarten Tromp
Delft, april 2004

Abstract

The hydraulic stability of rocks and other non-cohesive sediments is often described by so-called threshold conditions. These conditions describe the stability of the stones in terms of critical values of the velocity, wave height, or shear stress. The influence of fluid accelerations in most of these conventional design methods has been neglected or has been processed empirically.

For various purposes however (as bottom protection in constrictions, wave attack on a mild slope, or the behavior of sediments in the surf zone) the stability of stones does not only depend on the flow velocity (or shear stress) but also on the influence that fluid particle accelerations have on these sediments. As only little is known on the background of these processes a pilot experiment in a wave flume has been carried out to help identify key processes and to find out whether these fluid accelerations, do influence the threshold of motion.

During the experiment 78 test series have been performed with changing wave steepnesses in order to create scenarios of similar horizontal near-bed velocities, but with different accelerations. Another 22 of such tests series have been carried out with stones that have a smaller diameter. It has been assumed that if there is a relation between the threshold of motion and accelerations then for some combinations of a velocity and acceleration there are stones that move while in other cases with the same near-bed velocities, but a lower acceleration, there will be no movement of the same stones.

After analysis of the experimental data it appears that both the fluid accelerations and the fluid velocities influence the threshold of motion. This can be shown with the help of two different approaches

Usage of an instantaneous approach requires some skills and is very time-consuming, but leads to very satisfying results. With use of video monitoring it appears that the initial motion of stones starts somewhere between 0.15s and 0.05s before passage of the wave top. This interval also happens to be the interval at which the velocities and accelerations have large values in the direction of the wave propagation. Using these velocities and accelerations in a Morison-like equation proves that the threshold of motion is dependent on both the horizontal near-bed velocities and the accelerations.

The second used approach was by means of a waveform approach. Such an approach is easier to use and has no problems of finding the exact momentary forces.

Also with use of this approach it is possible to show that the threshold of motion depends in some measure on fluid accelerations in addition to fluid velocities.

A dimensional form of acceleration skewness as introduced by Drake and Calantoni (2001) is very use to show this.

Furthermore it is shown that the acceleration term becomes increasingly significant as the wave becomes more peaked.

Finally during the analysis an attempt has been made to find a stability relation, in which both accelerations and velocities are present. A dimensionless entrainment parameter and force parameter have been designed, in order to use this relation for various stone sizes. The relation does show an increase of entrainment when the wave forces are enlarged, but there is still a lot of scatter in the diagram.

Table of contents

PREFACE	1
ABSTRACT	2
TABLE OF CONTENTS	3
LIST OF FIGURES.....	5
1 PROBLEM DESCRIPTION	7
1.1 GENERAL INTRODUCTION	7
1.2 PROBLEM ANALYSIS	7
1.3 PROJECT DEFINITION	8
1.4 OBJECTIVE	8
2 THEORY.....	9
2.1 INTRODUCTION	9
2.2 INITIATION OF MOTION	9
2.3 SHIELDS, SLEATH AND JONSSON.....	10
2.4 MODEL THAT INCLUDES THE INFLUENCE OF ACCELERATIONS	12
2.4.1 Acceleration forces	12
2.4.2 Velocity forces	14
2.4.3 Model that combines pressure and velocity forces	14
2.4.4 Force balance	15
2.4.5 Values for C_M and C_D	17
3 THE EXPERIMENT	20
3.1 INTRODUCTION TO THE EXPERIMENT SET UP	20
3.2 THE WAVE FLUME AND WAVE GENERATOR	21
3.3 THE STONES	21
3.3.1 Testing area	21
3.3.2 Grain sizes	22
3.3.3 Placement of stones	23
3.4 MEASURING INSTRUMENTS AND EQUIPMENT	24
3.4.1 Physical parameters	24
3.4.2 Location of Measurements	24
3.4.3 Choice of instruments	25
3.4.4 Accuracy and reliability	25
3.4.5 Calibration of instruments	26
3.5 TESTING PROCEDURES	28
3.5.1 Tests to find the threshold of motion for various wave steepness	28
3.5.2 Measurements of near bed velocities, accelerations and wave heights	30
3.6 EVALUATION	31
4 WAVE ANALYSIS	32
4.1 INTRODUCTION	32
4.2 SHOALING	32
4.3 VELOCITY ANALYSIS	33
4.3.1 Validation of near-bed velocities	34
4.3.2 Behavior of near-bed velocities and phase lag	36
4.3.3 Phase shifts	37
4.4 ACCELERATIONS	38
4.5 EVALUATION	40

5	THRESHOLD OF MOTION	41
5.1	INTRODUCTION	41
5.2	INSTANTANEOUS APPROACH	41
5.2.1	<i>Force balance</i>	41
5.2.2	<i>Presence of velocity and acceleration forces</i>	42
5.2.3	<i>Relation between velocity and acceleration forces</i>	43
5.2.4	<i>Video observations</i>	48
5.2.5	<i>Critical wave forces</i>	53
5.2.6	<i>Bulk coefficient C_B and acceleration coefficient C_M</i>	56
5.2.7	<i>Results for using the Morison-like equation</i>	61
5.3	WAVEFORM APPROACH	64
5.4	ENTRAINMENT	70
5.4.1	<i>Entrainment parameter</i>	70
5.4.2	<i>Dimensionless parameters</i>	71
5.5	EVALUATION	74
6	CONCLUSIONS AND RECOMMENDATIONS	75
6.1	CONCLUSIONS	75
6.2	RECOMMENDATIONS	76
7	REFERENCES	77
	<i>ARTICLES:</i>	77

APPENDIXES:

1) SIGNAL PROCESSING AND DATA ANALYSIS FOR EMS	APPENDIX A
2) USED PARAMETERS AND DIMENSIONS	APPENDIX B
3) PICTURE OF EMS	APPENDIX C
4) SIEVE CURVES	APPENDIX D
5) M-FILES AND STONE LISTS	APPENDIX E
6) ENLARGED PLOTS OF CHAPTER 5	APPENDIX F
7) FLOW-TIME FOR ENTRAINMENT	APPENDIX G
8) DETAILED WAVE ANALYSIS	APPENDIX H

List of figures

Figure 2.2-1 Forces acting on grain	9
Figure 2.3-1 Critical shear stress according to Shields	11
Figure 2.4-1 Pressure differences in accelerating flow	12
Figure 2.4-2. Forces that act on a grain.	16
Figure 2.4-3 Lift and drag forces generated by current.....	17
Figure 2.4-4 inertia coefficient for a cylinder of ellipsoid cross section	18
Figure 3.1-1 Orbital motions; shallow water (A) and deep water (B).....	20
Figure 3.2-1 Dimensions of the wave flume used for the experiments	21
Table 3-1 Characteristics of the used stones	22
Figure 3.3-1 Plan that shows the locations and the placement of the bed material	23
Figure 4.2-1 Wave heights and wave forms at various locations.....	33
Figure 4.3-1 non linear orbital movements of water particles	33
Figure 4.3-2 amplitudes of horizontal velocities at various elevations.....	34
Figure 4.3-3 Near-bed velocity as waves travel into shallower water	36
Figure 4.3-5 Frequency-amplitude spectra and accompanying waveforms.	37
Figure 4.3-7 Growth of velocities in decreasing water depth for $H_0 = 0.125\text{m}$, $T = 2\text{s}$ and $h_0 = 55\text{cm}$	38
Figure 4.4-2 Accelerations at various locations for $H_0 = 0.125\text{m}$, $T = 2\text{s}$ and $h_0 = 0.55\text{m}$	39
Figure 4.4-3 Values of maximal accelerations obtained in the measuring area	39
Figure 5.2-2 Instantaneous values of near-bed horizontal velocities and accelerations	42
Figure 5.2-3 movement of the large stones versus instantaneous velocities and accelerations	45
Figure 5.2-4 Cumulative movement of at least 4 large stones plotted versus the momentary accelerations and the square of horizontal velocities.....	46
Figure 5.2-5 Movement of at least 1 small stone plotted versus the momentary accelerations and horizontal velocities	47
Figure 5.2-6 Movement of large stones plotted versus the momentary accelerations and the square of horizontal velocities.	48
Figure 5.2-7 Average times at which stone movement starts and ends.....	50
Figure 5.2-8 Graphical representation of the times at which stone movements starts and ends as a function of the surface elevation, the horizontal near-bed velocities and the accelerations for video 1.	52
Figure 5.2-9 Movement parameter plotted versus the maximum momentary velocity forces that were present for the movement parameter in question ($F = 1/2 C_{Bp} \rho A u^2$).....	54
Figure 5.2-10 Movement plotted versus the maximum momentary acceleration of forces ($F = 1/2 C_{Mp} V(du/dt)$), in which $C_M = 1$	55
Figure 5.2-11 Movement plotted versus the maximum momentary combined velocity and acceleration forces ($F = 1/2 C_{Bp} \rho A u^2 + 1/2 C_{Mp} V(du/dt)$), in which $C_B = 1$ and $C_M = 1$	55
Figure 5.2-12 Plot that shows the maximum forces and the movement parameters as found for all tested wave steepnesses. Movement of small stones and forces found with $C_B = 1$ and $C_M = 1$	56
Figure 5.2-13 Plot that shows the maximum forces and the movement parameters as found for all tested wave steepness. The forces have been found with use of equation 5.2 in which $C_B = 1$ and $C_M = 1$	57
Figure 5.2-14 Plot that shows the maximum forces and the movement parameters as found for all tested wave steepness. The forces have been found with use of equation 5.2 in which $C_B = 2$ and $C_M = 1$	57
Figure 5.2-15 Plot that shows the maximum forces and the movement parameters as found for all tested wave steepness. The forces have been found with use of equation 5.2 in which $C_B = 1$ and $C_M = 2$	58
Figure 5.2-16 velocity profile and the critical velocities found for both videos.....	59
Figure 5.2-16 Velocity profile and in it the critical velocity for both video 1 and video 2.....	59
Figure 5.2-17 acceleration profile and in it the critical acceleration for both video 1 and video 2.....	60

Figure 5.2-18 Plot that shows whether movement of large stones does occur for a certain maximum momentary wave force. The wave forces have been found with use of the Morison-like equation in which $C_B=0.55$ and $C_M=3.75$.	61
Figure 5.2-19 Plot that shows whether movement of large stones does occur for a certain maximum momentary wave force. The wave forces have been found with use of the Morison-like equation in which $C_B=0.4$ and $C_M=2.7$.	62
Figure 5.2-20 Plot that shows whether movement of stones did occur for a certain maximum momentary wave force. The wave forces have been found with use of the Morison-like equation in which $C_B=0.55$ and $C_M=3.75$. For small stones	63
Figure 5.2-21 Plot that shows whether movement of stones did occur for a certain maximum momentary wave force. The wave forces have been found with use of the Morison-like equation in which $C_B=0.4$ and $C_M=2.7$. For small stones	63
Figure 5.3-1 For each tested wave steepness with small stones, the movement has been plotted for maximal values of the near-bed velocities and maximum values of the acceleration	65
Figure 5.3-2 For each tested wave steepness with large stones, the movement has been plotted for the maximal values of the near-bed velocities and the maximum values of the acceleration.	65
Figure 5.3-3 For each wave steepness as tested with large stones, the movement has been plotted for values of u_{rms} and maximum values of a_{spike}	67
Figure 5.3-4 For each wave steepness as tested with small stones, the movement has been plotted for values of u_{rms} and maximum values of a_{spike}	67
Figure 5.3-5 forces and movement found for u_{rms} and a_{spike}	68
Figure 5.3-6 Movement plotted as a function of a_{spike} for tests performed with the small stones	69
Figure 5.3-7 Movement plotted as a function of a_{spike} for tests performed with the large stones	69
Figure 5.4-1 Entrainment as a function of the maximum wave force	71
Figure 5.4-2 Plot that shows the relation between the dimensionless entrainment parameter and the force parameters.	73

1 Problem description

1.1 General Introduction

Rocks, stones or sediments can only be moved if the water movement is strong enough to lift or to roll the particles from their initial position. Conventional design methods describe this hydraulic stability of rocks and sediments by the so-called threshold conditions. These conditions describe the stability of the stones in terms of critical values of the velocity, wave height, or shear stress.

The influence of fluid accelerations in most of these conventional design methods has been neglected or processed empirically. In order to get a better understanding into the influence of such accelerations research has to be carried out. Such research can be experimental, analytical or numerical. But before this research can be performed the goals of this research have to be defined. This will be done by means of a problem analysis and problem definition.

1.2 Problem analysis

Up to now the movement of stones in water has been ascribed to the exceedance of critical values of velocity or shear stress. Commonly used design methods are empirical formulae based on this principle. With the use of the graphs of Shields (Schierack, 2001 after Shields, 1936) and van Rijn (Schierack, 2001 after van Rijn, 1984) a so-called “threshold of motion” can be found. If the flow velocity exceeds this velocity, the water motion is strong enough to start moving the stones. For various stone diameters the critical velocities (and shear stresses) can be found in these graphs.

Under wave conditions this so-called “threshold of motion” can be determined with the use of the formulas and graphs of Sleath (Schierack, 2001 after Sleath, 1976) and Jonsson (Schierack, 2001 after Jonsson, 1967), who have developed a Shields-curve adapted for transport under waves. The horizontal velocity component of the orbital movement and the stone diameter are the two most important parameters in these formulae.

From investigations by Elgar and Hoefel (2003) and practice it became evident that in many non-uniform flow situations the stones would move while the flow and/or wave velocities were lower than the “required” critical velocity. Scientists (Stive and Reniers (2003), Calantoni and Drake (2001)) believe this type of movement can be ascribed to the existence of flow accelerations, which are present in non-uniform flows or in the orbital wave motion under waves.

In practice there are many occasions where the stones are subject to such accelerations. Some examples are:

- Accelerations under waves in the surf zone or on a mild slope.
- Accelerations of flow in rivers, channels, lakes or estuaries because of constrictions in the flow direction. These constrictions can be groin fields, columns of bridges, pier or other abutments.
- Accelerations due to flow through a barrage dam, lock or sluice.
- Accelerations that appear in the closure gap of a closure dam
- Water flows created by a bow thruster.

- Local turbulence

From the examples it occurs that these accelerations often appear at locations where bottom protection has been placed or will be required. A good insight into the influence of accelerations on stone stability is therefore required, in order to prevent spillage (optimization) of bottom protection material, or on the contrary to give the extra-required protection for the bottom and structures placed in constrictions or the surf zone.

The effects of accelerations on stones (and other non-cohesive sediments) are also very useful to get a better understanding of the processes of the surf zone. This knowledge can for example be used to predict onshore (and offshore) sediment transport rates. This can be very useful in forecasting the behavior of beach nourishments.

The goal of this thesis is to find effects of fluid accelerations on the stability of stones in an accelerating flow. As mentioned most previous research has processed this influence empirically and therefore very little is known on the background of these processes. During the investigations therefore a pilot experiment will be carried out to help identify key processes and to find whether these fluid accelerations, do influence the stability of stones.

In the experiment various accelerations will be generated by means of shoaling waves on a mild slope. The results of the experiment will also be compared to theoretically computed results. If the influence of accelerations turns out to be evitable the findings of the experiment can be used mathematically (first analytically and then numerically), to get even more insight in this matter. But that will be for future investigations and is beyond the scope of this thesis.

1.3 Project definition

For various purposes (as bottom protection in constrictions, wave attack on a mild slope, or the behavior of sediments in the surf zone) the stability of the stones/sediments will not only depend on the flow velocity (or shear stress) but also on the influence of fluid particle accelerations on these stones/sediments. Up to now little is known about the influence that accelerations have on the stability of stones that are placed in a flow or under waves.

1.4 Objective

The objective is to investigate, the influences that fluid accelerations have on the stability of stones, by means of an experiment. This experiment will be carried out in a wave flume. This will be done in order to control the wave climate. The orbital motion will create fluid accelerations and fluid velocities.

2 Theory

2.1 Introduction

In advance of the experiment a literature study has been performed. It became clear that various scientists have carried out a lot of research on the stability of stones in flowing water in the past. All this knowledge is still very empirical. In this chapter relevant findings of previous research will be discussed. And next some theory that will be used in the experiments will be described. This chapter only deals with the stability of loose non-cohesive grains, as the grains used in the experiment are loose non-cohesive grains.

2.2 Initiation of motion

Bed material can only be moved if the water movement is strong enough to lift or roll the grains from the bed. As mentioned in the introduction the experiment deals with the stability of loose non-cohesive grains. This leads to the assumption that the point of initiation of movement depends on the forces on each single grain, because there will be no cohesion between the various grains. The force acting on a single grain can be divided into forces that try to move the grain: the drag force (F_d), the lift force (F_l) and turbulence forces, and forces, which act to keep the grain in its place, the gravity force, (*Coastal engineering* (2000)). Once a sediment grain has begun moving, the influence of the lift component dies away rapidly and the frictional force influences movement increasingly.

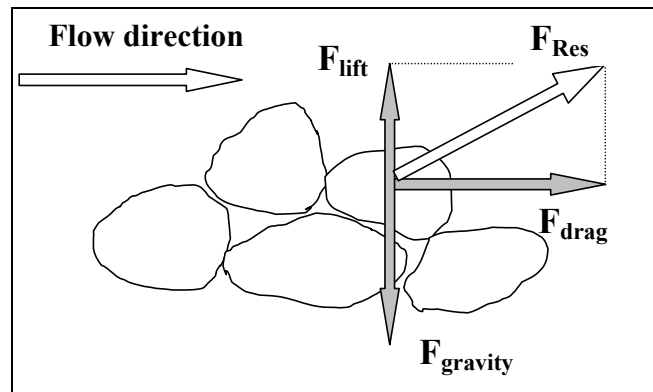


Figure 2.2-1 Forces acting on grain

The gravity force F_g is equal to the submerged mass of the stone multiplied by the gravitational acceleration.

$$F_g = ma = (p_s - \rho_w)d^3g \quad (2.1)$$

The drag force is caused by pressure and viscous skin friction. It always acts in the direction of the fluid motion. This is based on the assumption that for this case the viscous skin friction is negligible.

The lift force always acts perpendicular to the drag force. It is caused by a lower pressure at the top of the grain produced by the contraction of the water streamlines along the sides of the grain. Both forces are a product of the square of the flow velocity.

$$F_{drag} = \frac{1}{2} C_d \rho_w u^2 A_d \quad (2.2)$$

$$F_{lift} = \frac{1}{2} C_L \rho_w u^2 A_L \quad (2.3)$$

in which : C_d = drag coefficient
 C_L = lift coefficient
 A_d = grain surface on which drag forces work
 A_L = grain surface at which lift forces work

The asymmetry of shoaling waves has such a form that the maximum positive velocities are much greater than the maximum negative velocities. Therefore only movement of stones in the direction of wave propagation will be investigated during the experiments.

2.3 Shields, Sleath and Jonsson

Probably the most famous research on the stability of stones has been performed by Shields (Schierack after Shields, 2001). He found a critical value of shear stress for the initial movement of grains in a uniform current. He expressed this critical value as a function of the Reynolds number.

Shields chose the shear stress as the active force and gives a relation between a dimensionless shear stress (Ψ_c) and the so-called particle Reynolds number:

$$\Psi_c = \frac{\tau_c}{(\rho_s - \rho_w)gd} = \frac{u_{*c}^2}{\Delta gd} \quad (2.4)$$

In which: Ψ_c : Shields parameter [-]
 τ_c : critical shear stress [N/m²]
 u_{*c} : Critical shear velocity [m/s]

and $u_* = \sqrt{\frac{\tau_0}{\rho_w}}$

Figure 2.3-1 shows the presentation of the Shields relation in a graph:

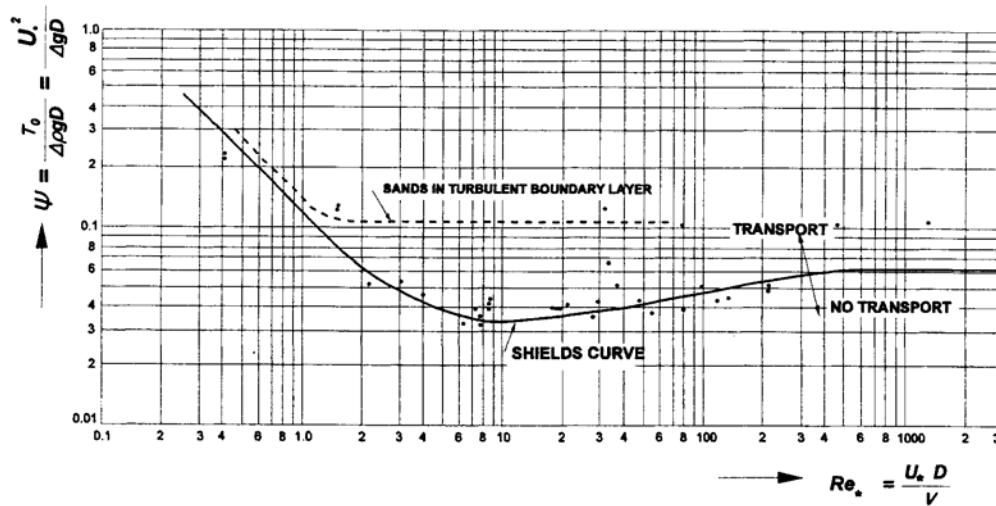


Figure 2.3-1 Critical shear stress according to Shields

Results below the curve indicate that no movement will occur and results above the curve indicate movement of the grains.

Jonsson (Schierack after Jonsson, 2001) carried out experiments to determine the bed shear stress under waves. He found out that this shear stress, τ_w , could be described in terms of near bed velocity amplitudes and the wave friction factor.

$$\tau_w = \frac{1}{2} \rho f_w \hat{u}_0^2 \sin^2(\omega t) \quad (2.5)$$

in which: τ_w = bottom shear-stress for waves

f_w = wave friction factor

Sleath (Schierack after Sleath, 2001) modified the Shields diagram for waves and stability of non-breaking waves, with use of Jonsson's values for τ_w . Comparing the results of the threshold of motion for a stationary flow to values for an oscillating flow, showed the same values for a large d_* (turbulent boundary layer). It seems odd that for both cases the same amount of stones will be in motion, because the potentially unstable stone in an oscillating flow cannot move in the same manner because of the changing flow regime for the same τ . Scientists believe this can be subscribed to an underestimation of the shear stresses under waves, which actually cause a bigger force on the stones, and they believe it occurs due to the influence of accelerations in oscillatory flows, which are neglected or processed in empirical factors in the traditional formulae.

2.4 Model that includes the influence of accelerations

From previous section becomes clear that most research has been based on the exceedance of a critical value of the shear stress. It also became clear that for an oscillating motion it can be hard to find a value for this shear stress and that the presence of accelerations is neglected (or processed in a constant empirical factor).

By means of this experiment an attempt will be made to investigate whether accelerations influence the threshold of motion. As mentioned the forces that try to move the grains are generated by wave motion. In this section a model will be described that will be used to invest the influence of accelerations on the stability of stones in an oscillating flow.

2.4.1 Acceleration forces

Fluid accelerations around a grain form horizontal acting pressure gradients. How this mechanism works can be explained with use of the following figure (*L.A.Schokking (2002)*). The figure represents a grain, which is placed in an accelerating flow.

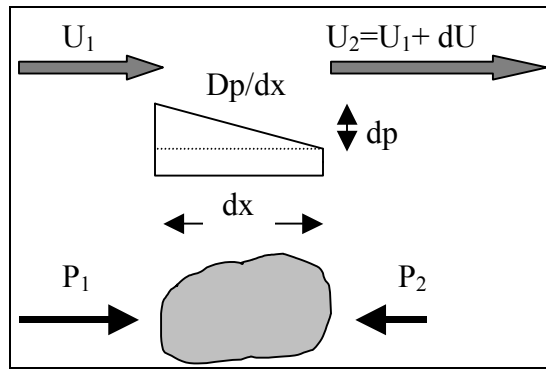


Figure 2.4-1 Pressure differences in accelerating flow

The tests are carried before the breaking of waves. And the energy dissipation by turbulence is assumed negligible. In this case Bernoulli leads to the following notation:

$$p_1 + \frac{1}{2} \rho u_1^2 = p_2 + \frac{1}{2} \rho u_2^2 \quad (2.6)$$

Which is equivalent to:

$$p_1 - p_2 = \frac{1}{2} \rho (u_2^2 - u_1^2) \quad (2.7)$$

Because the grains all have a very small length and all grains are equal we assume:

$$\frac{dp}{dx} = \text{constant} \quad (2.8)$$

So the force created by the difference in pressure and the difference in velocity (accelerations) will be equal to

$$F_p = \iiint \frac{dp}{dx} dx dy dz = V \frac{dp}{dx} \quad (2.9)$$

In which V is the volume of the stone and dp/dx is linear

From the Euler equation it is known that dp/dx can be replaced by $\rho (du/dt)$, which leads to

$$\nabla p = -\rho \frac{D\bar{u}}{Dt} \Rightarrow \frac{dp}{dx} = -\rho \left(\frac{\partial u}{\partial t} + \bar{u} \frac{\partial u}{\partial x} \right) \quad (2.10)$$

By doing so F can be rewritten as:

$$F = \rho \left(\frac{\partial u}{\partial t} + \bar{u} \frac{\partial u}{\partial x} \right) V \quad (2.11)$$

Because the length of a grains is very small the change of velocities along the length of the grain will also be very small, so

$$\frac{\partial u}{\partial x} \approx 0 \quad (2.12)$$

Therefore (..) reduces to:

$$F = \rho \left(\frac{\partial u}{\partial t} \right) V = \rho a V \quad (2.13)$$

In which a is the horizontal acceleration and V is the volume of the stone particle.

2.4.2 Velocity forces

The second type of forces, which try to move the stones from their initial position are forces created by the orbital horizontal velocities. These forces will be referred to as the drag, lift and turbulent forces and they are as seen in previous sections dependent on the square of the horizontal orbital velocity.

$$F = \frac{1}{2} \rho C_B A u^2 \quad (2.14)$$

in which: C_B = Bulk coefficient for all forces that are dependent upon the horizontal fluid velocity
 A = the surface of the stones the velocity force acts upon
 U = horizontal velocity of orbital horizontal motion that works on stones.

The horizontal velocities can be found from the measurements taken during the experiment. A disadvantage is that the EMS, which is used to measure the velocities, is not capable of measuring the velocities near the bed. The nearest point at which the velocity measurements can be taken is 4 cm above the bed and this is however not the height at which the velocity acts on the stones in the bed. That velocity would be lower due to the presence of the boundary layer.

The height of the boundary layer and the velocity distribution within this boundary layer depend among others on the bed roughness and is difficult to predict, especially for oscillating movement.

Booij (1992) approximated the growth of the boundary layer in the case of waves by:

$$\frac{d\delta}{dt} = \kappa u_* \approx 0.4 u_* \quad (2.15)$$

In which κ is the von Karman constant and $u_* \approx 0.1 * u_b$

The effect that this boundary layer has on the velocity profile will be investigated during the experiment.

2.4.3 Model that combines pressure and velocity forces

In a wave field both velocity forces, and pressure forces occur and they vary continuously in time. The stability of a grain under waves is dependent upon the extent of contribution of these hydraulic forces. Morison *et al.* (1950) proposed the following formula for the wave force; which is the sum of the two forces, drag and pressure.

$$F = F_{drag} + F_{acceleration} = \frac{1}{2} C_D \rho A u |u| + C_M \rho V \frac{Du}{Dt} \quad (2.16)$$

In which C_D is a drag coefficient and C_M is an acceleration coefficient, which also contains a contribution for the added mass.

The Morison formula lacks the influence of lift forces that act perpendicular to the drag forces and the influence of turbulence. As these lift and turbulent forces are also functions of the horizontal velocity U , it seems appropriate to change formula 2.16 into

$$F = F_{bulk} + F_{acceleration} = \frac{1}{2} C_B \rho A u |u| + C_M \rho V \frac{Du}{Dt} \quad (2.17)$$

In which the influence of drag, lift and turbulent forces are processed in a bulk coefficient C_B . When performing stability analysis on grains much attention should be paid to the determination of the coefficients C_B and C_M .

2.4.4 Force balance

From *Coastal engineering* (2000) is known that if the momentum of forces about the point of contact with the adjacent grain (point A in Figure 2.4-2) is positive then the grain will move. When resolving all forces into normal and tangential forces in the direction of expected movement, it arises that the tangential forces go through the pivot and therefore will have a contribution to the momentum of zero. This is valid when assuming that all forces have its origin in the centre of mass of the stones. Now only a balance of forces in the direction of movement can be made to check the stability of a stone.

Kirchner (1990). showed that the most common angle of first (easiest) movement, ϕ , for stones is between 30° and 45° . This is independent on whether the initial motion is a rolling or a sliding motion.

The force balance as seen in Figure 2.4-2 has been created by dissolving the gravity force and the wave forces into components that act in this direction of movement and in components that act in a direction tangential to this direction of movement.

The wave forces have been split into acceleration forces and velocity forces, just like the Morison equation does. The acceleration forces are assumed to act in a horizontal direction and the velocity forces act at an angle β . This angle β depends on the contribution of the lift, the drag and turbulence forces. This will be discussed further on.

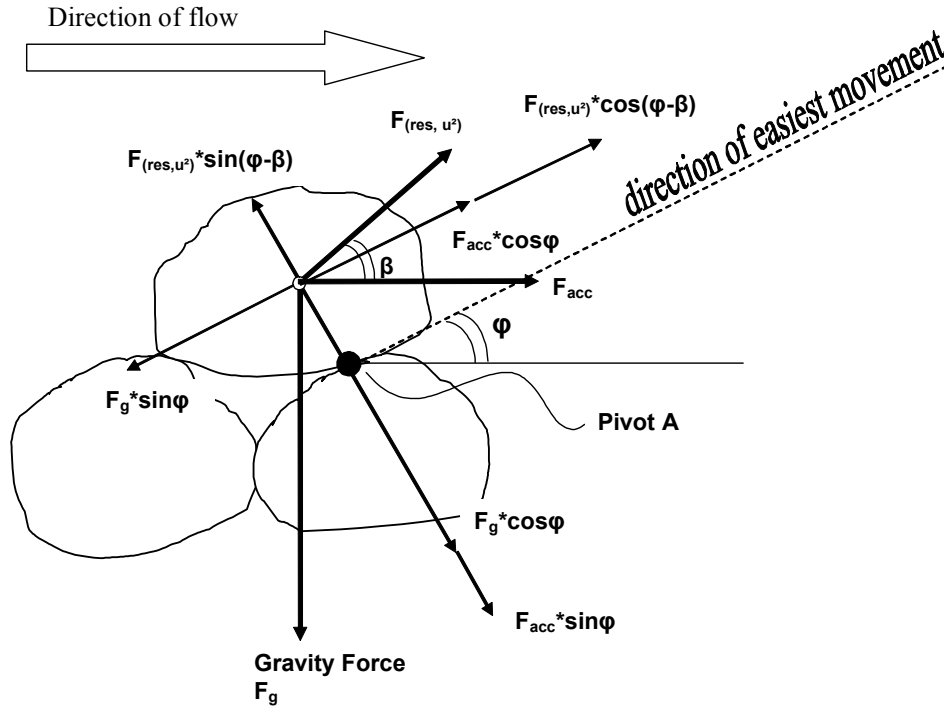


Figure 2.4-2. Forces that act on a grain. The resulting force $F_{(res, u)}$ is the resulting force of all forces that act on the grain and which depend on the square of the horizontal velocity. These forces are the drag force, the lift force and unknown turbulent forces. This resultant force acts at an angle of beta with the horizontal line.

At the critical point of movement the following applies:

$$F_{(res, u^2)} \cos(\varphi - \beta) + F_{acc} \cos(\varphi) = F_g \sin \varphi \quad (2.18)$$

in which :

$$F_{(res, u^2)} = F_{bulk} = \frac{1}{2} C_B \rho A u |u| \quad (2.19)$$

$$F_{acc} = C_M \rho V \frac{Du}{Dt} \quad (2.20)$$

Movement of the grain occurs when:

$$F_{(res, u^2)} \cos(\varphi - \beta) + F_{acc} \cos(\varphi) > F_g \sin \varphi \quad (2.21)$$

And no movement when:

$$F_{(res, u^2)} \cos(\varphi - \beta) + F_{acc} \cos(\varphi) < F_g \sin \varphi \quad (2.22)$$

2.4.5 Values for C_M and C_D

From the above balance of forces can be seen that a lot of attention has to be paid when determining values for C_M and C_D . From theory the following is known:

The bulk coefficient C_B

The bulk coefficient C_B must have such a value that it represents all forces, which are generated by the horizontal velocity in the direction of the stone movement. The presence of a horizontal velocity generates the following forces:

- Lift force
- Drag force
- Turbulence forces

The values and direction of the turbulent forces are very difficult to predict. Much research is nowadays performed to find out the behavior and the influence of these turbulence forces. By using non-breaking waves and a uniform bed profile it has been tried to reduce the turbulence to a minimum, but there will still be some influence of turbulences. The extent of this influence is still very hard to predict.

More is known about the influence of the lift and the drag forces. When a stone is subject to a current Figure 2.4-3 can be made. The presence of the current generates a lift force and a drag force that try to move the stone from its initial position.

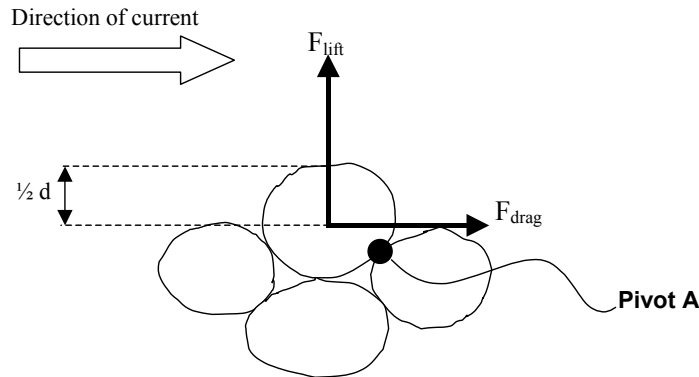


Figure 2.4-3 Lift and drag forces generated by current

The forces F_{lift} and F_{drag} can be written as follows:

$$F_{Lift} = \frac{1}{2} \rho C_L A u |u| \quad (2.23)$$

$$F_{drag} = \frac{1}{2} \rho C_d A u |u| \quad (2.24)$$

A represents the surface of the stone that is exposed to the current. It is assumed that only the upper half of the stone will be exposed to the current so the surface of half a stone should be considered. *Hofland et al* (2004) found:

$$C_L \approx 0.15 - 0.22$$

$$C_d \approx 0.25 - 0.35$$

With this information it is possible to determine the values of the lift and the drag forces. The only problem is that the forces are directed in a different direction.

Section 2.4.4 showed that the forces have to be dissolved into forces in the direction of movement and in a direction tangential to this direction. It also has been mentioned that the dissolved forces in the tangential direction go through the pivot, so when looking for the critical forces that make a stone move, only the balance of forces in the direction of movement can be considered.

Dissolving the drag and the lift forces in the direction of movement makes it possible to find their contribution in the Morison-like equation. When this is done it appears that the joint contribution C_B of the lift and drag forces must be in the order of $K^*(C_L + C_D)$, in which K is a factor that is dependent on the angle for which the forces must be dissolved. So $K \leq 1$.

The acceleration coefficient C_M

The acceleration coefficient C_M can be discussed meaningfully as the sum of two terms (Dean and Dalrymple, 1991)

$$C_M = 1 + k_m \quad (2.25)$$

Where the second term k_m is called the added mass, which depends on the shape of the object. The interpretation of added mass is an additional local pressure gradient, which exists in order to accelerate the neighboring fluid around the grain. The force necessary for this acceleration of the fluid around the grain yields the added mass term, k_M .

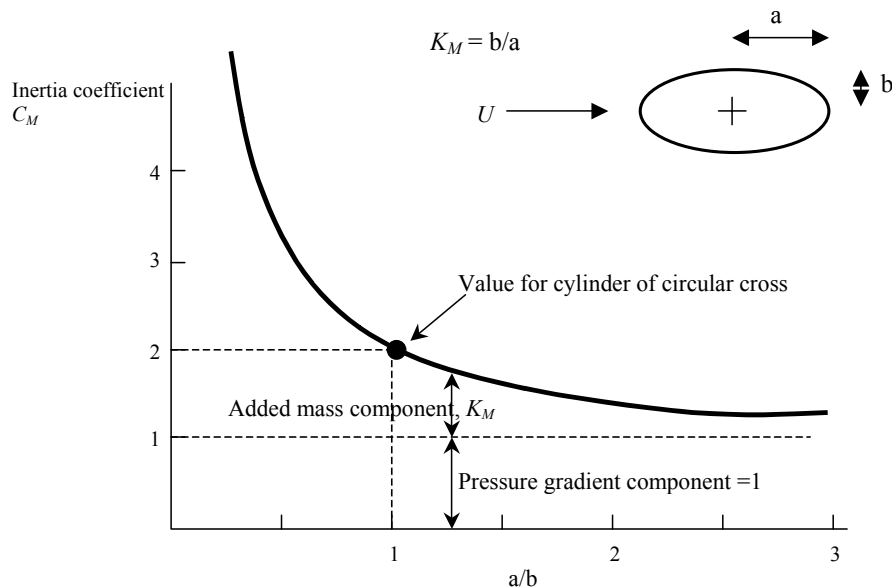


Figure 2.4-4 inertia coefficient for a cylinder of ellipsoid cross section

From Figure 2.4-4 can be seen that for a sphere k_M has a value of 1. The stones used in the experiment are no spheres, but are more edged. This leads to larger values for a/b . Figure 2.4-4 gives values that are larger than 1 for these types of objects. A value for k_M of at least two seems therefore reasonable.

The added mass however is only present in the accelerating fluid around the grain. Because no accelerations are present within the bed, this added mass will only be of importance for that part of the grain that protrudes out of the bed, where there are fluid particle accelerations. It is assumed that half of the stone is placed in the bed and the other half has a free surface. Therefore only half the value of k_M will be available in the acceleration coefficient.

So it appears that in all cases C_m should be greater than unity. When looking at the above explanation a reasonable value for the coefficient C_M will be in the order of 2 to 3..

3 The experiment

3.1 Introduction to the experiment set up

The previous chapter showed a model that can be used to describe all wave forces. It became clear how velocity generated forces and acceleration generated forces tried to move a stone.

When assuming that acceleration generated forces influence the threshold of motion then there have to be combinations of horizontal velocities and accelerations that don't lead to movement of stones, while other combinations that have similar velocities, but different accelerations do lead to movement of grains. This experiment will be therefore be used to create various combinations of horizontal velocities with different accelerations. In the experiments the orbital wave motion will be responsible for the presence of the horizontal velocities and accelerations.

The displacements, velocities and accelerations of water particles under waves describe an oscillating movement. Near the water surface the water particles describe an elliptical movement and near the bottom they make a horizontal orbital movement. This implies that from the water surface to the bottom the vertical displacements of the water particles reduce to zero. In deep water the horizontal movement will not reach towards the bed, but as the water gets shallower this oscillating movement will reach entirely towards the bottom. In fact the more depth decreases; the stronger this horizontal oscillating movement will reach towards the bottom. (Battjes, 1991).

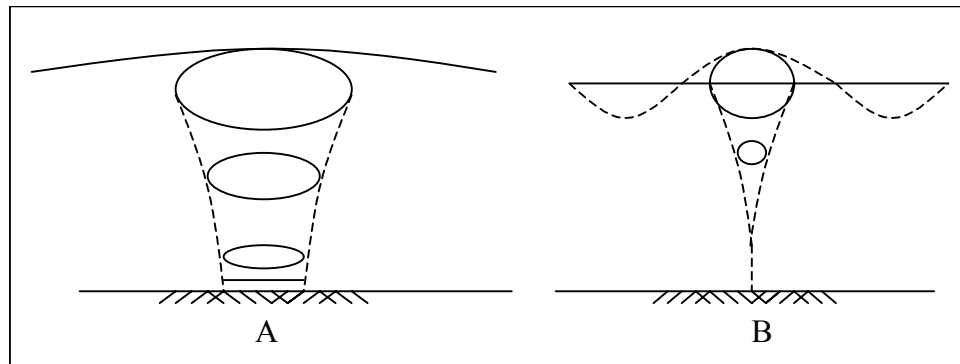


Figure 3.1-1 Orbital motions; shallow water (A) and deep water (B)

Making use of this depth-dependency of the orbital motion can create many combinations of velocities and accelerations. Stones of equal diameter and density therefore have to be placed on a sloping bed. If the stones are small enough, the orbital velocities and accelerations from a certain point on the slope become strong enough to move some of the placed stones. So varying the wave steepness and water depths creates for all locations on the slope different scenarios of horizontal velocities and accelerations.

In this chapter the composition of such an experiment and the testing procedures will be described.

It can therefore be used as a manual to build up and carry out a similar experiment. It can also be used as a guide to construct a new experiment for testing the influence of accelerations

3.2 The wave flume and wave generator

The experiments are to be carried out in a wave flume in the Fluid mechanics Laboratory of the Department of Hydraulic and Geotechnical Engineering of the faculty of Civil Engineering and Geosciences of Delft University of Technology. The wave flume is a (sediment) transport flume with an effective length of 42.00 m, a width of 0.80 m and a maximum depth of 1.00 m. It can flow in both directions and at one end of the flume an irregular, piston-type, electro-mechanically driven wave generator is placed with automatic reflection compensation and a stroke length of 2.00 meters. An impression and some dimension of the wave flume can be seen in Figure 3.2-1

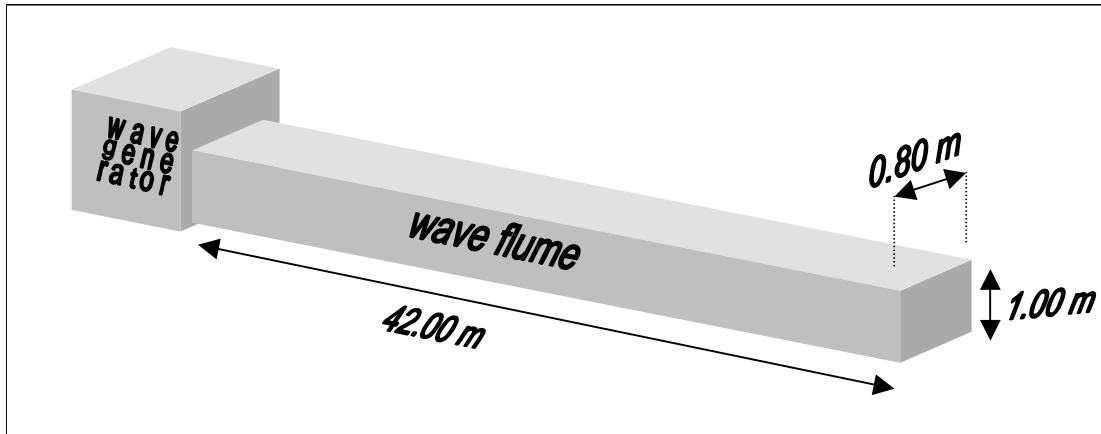


Figure 3.2-1 Dimensions of the wave flume used for the experiments

On the bottom of the flume a concrete slope has been constructed with a gradient of 1:30. The starting point of the slope is located at 8,70 m from the central position of the wave board and this slope reaches towards the end of the flume (this is the end opposite of the wave generator). The slope has been constructed at a certain distance of the wave generator in order to allow the waves to develop completely in water of sufficient and constant depth.

For the experiment only regular waves are used. As the water depth decreases in the flume due to the slope, the waves are traveling in shallow water and non-linear wave effects will be of importance. The wave generator therefore has to be programmed to produce regular 2nd order Stokes waves. The wave generator also must be instructed to use the active reflection compensation. Because the waves traveling in the flume cannot travel infinitely into one direction the water has to return and this gives irregularities in the newly generated waves; in order to compensate this influence of reflecting waves in the flume this ARC function is be used.

3.3 The stones

3.3.1 Testing area

Multiple layers of stones are to be placed on the slope. But as the flume is 42.00 meters long it will not be necessary to cover the entire bed with stones. The used stones are all rubble stones. The places where the measurements will take place are located between $X=16.5$ and $X=22$ meters; this location is chosen from trial experiments and practical considerations, like easy access to that

part of the flume (X is the horizontal distance upstream from the central position of the wave board). In this area all the placed stones must be of the same density and size.

It is important to create a good approaching flow area, so that the flow conditions under the waves only change in the measurement area because of shoaling and not due to differences in bed roughness. Therefore stones are also to be placed in front of the measuring area.

The velocity profile in a current (in shallow water) is affected by the bottom shear stress over the entire depth. When this bottom friction (created by the bed roughness) is changed, then the velocity profile will also change over the entire depth. This however, takes time. Under waves there is not enough time to build up a fully developed boundary layer. This is because of the ever-changing oscillating velocity profile near the bed (*Coastal engineering*, 2000). An advantage of this changing oscillating velocity profile is that the approach flow area is not to be very long. Half the maximum wavelength will be sufficient. This is approximately 4 m.

At the end of the measurement area the stones are affected by the oscillating wave flows and by the return current. This return current is a uniform flow. This implies that upstream of the measurement area the same stones as in the measurement area have to be placed, so that this return current will not be affected by a sudden change in bottom friction and then influence the measurement area. So after the measuring area there has to be an extra 1.5-meter of the same stone layers.

In Figure 3.3-1a plan of the placement of the stones is shown.

3.3.2 Grain sizes

As the waves travel along the slope, the wave becomes steeper due to shoaling. Because of this and because of the declining water depth the velocities and accelerations near the bed become stronger. From a certain point on the slope these forces become strong enough to start moving the grains. In Figure 3.3-1 it can be seen that the testing area is located between $X=22\text{m}$ and $X=16.5\text{m}$. So the threshold of motion of the grains has to be within this area for the various wave scenarios. With the use of the linear wave theory and the moving criteria of Izbash and Shields, required grain sizes for the experiment have been found. Yet it turned out that the calculated grains were too small for conducting the experiment. By trial the grain sizes now had to be found, but the calculated values were a good guide to start the trail from.

To get a good insight in the behavior of accelerations on stone movement various grain sizes have to be tested in the wave flume, but because of the limited time for the experiments only two grain sizes will be tested.

The stones used in the experiment are obtained by sieving and the stones have the following characteristics.

Stone type	dn50	Av density	W50	Grading
Small stones	0.0074 m	2656,01 kg/m ³	1.100 gr	Narrow
Large stones	0.0096 m	2679,63 kg/m ³	2.511 gr	Narrow

Table 3-1 Characteristics of the used stones

The sieve curves of the two stone types can be seen in appendix D.

3.3.3 Placement of stones

Preliminary tests in the wave flume showed that stone layers, which were placed loosely on the bottom, started to slide over the bottom. This is not allowed during the tests and the following will prevent it:

In the testing area only small strips of colored stones are placed directly on the bed. The length of these strips is 15 cm and they cover the entire width of the flume. The strips are placed at a distance of 50 cm from each other. Between these strips 50 cm long and 5 mm thick PVC plates are placed and attached to the concrete slope.

A first layer of stones has to be glued with aqua silicone to these PVC plates. Each plate has a width equal to (or just a little bit smaller) the width of the wave flume. A second layer of stones will then be attached onto these plates. The strips of loosely placed stones are then to be raised to the same level. The design can be seen in Figure 3.3-1.

A possible side effect of this solution is that the stones on the boundaries of the strips are placed next to the attached stones and are because of that interfered in their movement. But this effect has only an effect on less than 1% of the stones (the ones at the edges of the strips) and is therefore assumed negligible.

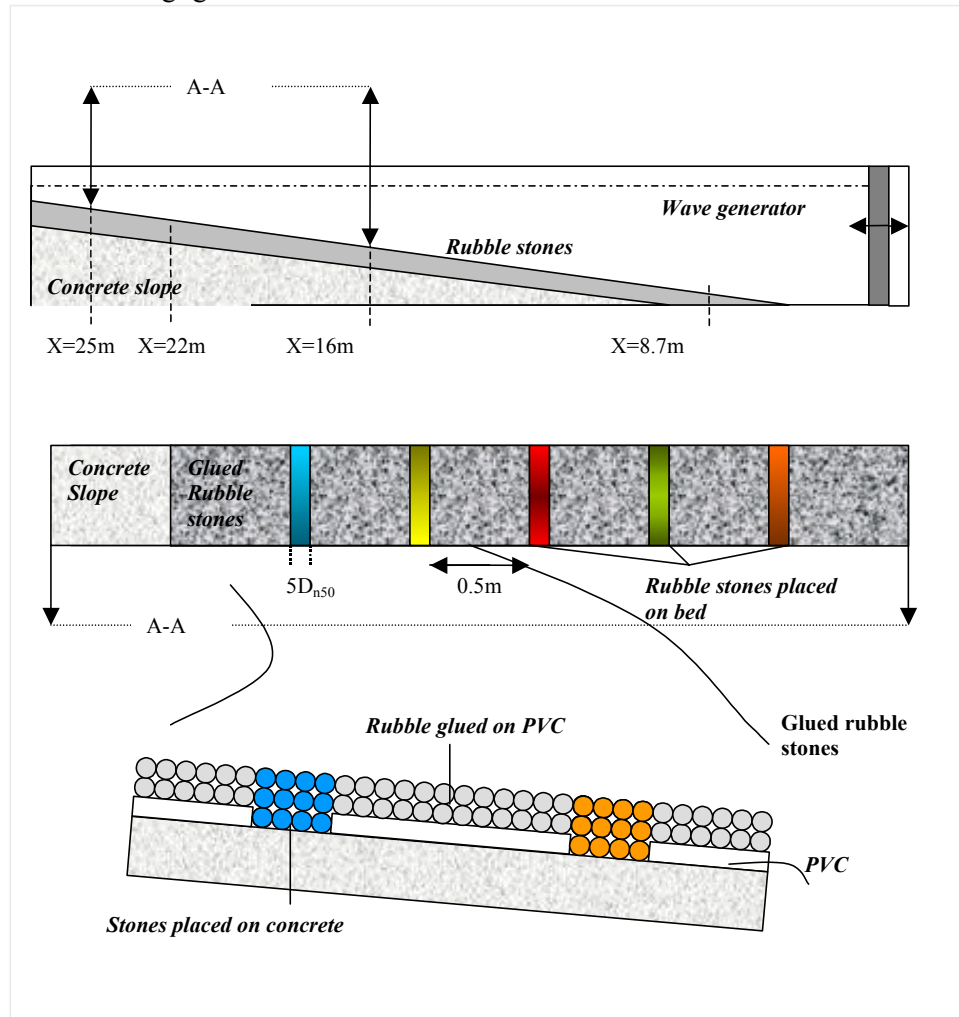


Figure 3.3-1 Plan that shows the locations and the placement of the bed material

3.4 Measuring instruments and equipment

A successful experiment depends among other things on selecting appropriate instrumentation to acquire the necessary measurement (*ASCE*, 2000)

The choice of instruments depends on four questions that must be answered.

1. Which physical parameters must be measured to make a meaningful interpretation of the physical processes?
2. At which locations should the measurements be taken?
3. Which instruments are suitable for the measurements?
4. Which is the required accuracy and what is the reliability of the measurements?
5. Which instruments are available?

The following sections answer these questions and explain the pick of the instruments and equipment.

3.4.1 Physical parameters

The measurements can be categorized in a number of different ways. Here we shall group the measurements according to the following divisions.

The geometrical measurements:

- Dimensions of the wave flume
- Different positions and elevations in the flume relative to a fixed coordinate system (the slope).
- Before every test the still-water level
- Particle grain size
- Variations in water surface elevations (waves)

Fluid motion measurements:

- Fluid velocities
- Wave period
- Fluid accelerations

Transport measurements:

- Number of moved grains

And other items:

- Water-working time
- Time for every experiment
- Density of water
- Water temperature

3.4.2 Location of Measurements

Many of the geometrical measurements can be done in advance of the tests. Only the variations of the water level and the measurement of the still water level have to be measured during the

experiment. The water surface elevation measurements have to be carried out at various places in the flume in order to get a good insight into the behavior of the shoaling waves. The measurements also have to be done before the initiation point of the slope to control the height of the waves the wave generator makes.

The transport and fluid motion measurements will be done in the measurement area located between $X=16$ and $X=22$ m..

The other measurements are not location-bounded, so they have to be done regardless of the place.

3.4.3 Choice of instruments

Laboratory studies involve measurement of static and dynamic quantities (Hughes, 1993). Static quantities, such as dimensions, or slowly changing quantities, such as steady flow speeds, are relatively easy to measure and most of this can be done before the experiment starts.

This type of measurements contains nearly all geometrical measurements except the variation in water level measurements. All these measurements will be done with a ruler or a tapeline and they will be done before the experiment starts. Other static measurements like the density and temperature of water will be measured by weighing and by thermo metering before the experiments start and are believed to remain constant.

The slowly changing quantities, as water-working time and number of moved stones will be registered at the end of each test. The water-working time will be checked with a watch and the number of moved stones will be counted.

Measurements of dynamic quantities, such as force, and kinematic quantities, such as unsteady flows and turbulence, are harder to get and are usually obtained by using specialized electronic equipment interfaced to a computer.

Measurements of rapidly changing water surface levels are from now on referred to as wave measurements. And the machines used to obtain the measurements are called 'wave gauges'. In the wave flume six resistance wave gauges will be placed on movable trestles. The wave gauges are able to measure the water level with a frequency of 20 Hz. By doing so it is possible to check the wave heights and the wave periods at all times. They also help making a still water level measurement.

The gauges are placed in pairs of two for getting an increased accuracy. One pair of wave gauges is to be placed in front of the slope to check the generated wave height.

The fluid motion is measured with the use of an EMS (Electro Magnetic Flow sensor). This EMS is based on Faraday's principle of electro magnetic induction. Such an EMS can perform velocity measurements in two directions. And has therefore two channels

As only waves perpendicular to the wave flume are used there are only velocities in one direction have to be measured. So the other channel can be used to register the accelerations of this flow. This acceleration is obtained by the derivative of the stream in time.

3.4.4 Accuracy and reliability

The character and reliability of the measurements depends on the accuracy and precision provided by the instruments with the operator's dependability and skill (Hudson, 1979).

The extent, to which measurement and operator's errors impact the results, depends of course on the magnitude of the error. Quantifying these errors is very important, in order to establish the reliability of the experiment.

In Table 3-1 all measuring instruments are listed with their known errors. Other errors, which can arise due to external factors that cannot be controlled, like the inability to repeat exactly a flow condition, can be found during the test. If a sufficient number of tests is performed, then it is possible to establish the statistical range of error.

Other errors, like reading errors and incorrect instrument usage can only be eliminated through careful and continual checking of the experiments (*ASCE*, 2000).

Instrument	Used for measuring	Possible errors
Ruler	Stone diameter,	Accuracy & reading errors; $\pm 0.5\text{mm}$
Tapeline	Dimensions of flume, still water level	Accuracy & reading errors; $\pm 5\text{mm}$
Balance	Stone weight, density of water	Accuracy & reading errors; ± 0.1 gr
Thermometer	Water temperature	Accuracy & reading errors; $\pm 0.5^\circ\text{C}$
Stopwatch	Water working time, experiment duration	Skills & handling speed: ± 1 s
Wave gauges	Wave heights, wave periods	Accuracy & reading errors; $\pm 0.2\text{cm}$
EMS	Flow velocities, flow accelerations	Accuracy & reading errors; ± 0.02 m/s

Table 3-2 Measuring instruments and their errors

Because it is difficult to know whether the values obtained with the EMS are correct a manual on the use of EMS data has been made. This manual can be seen in appendix A.

3.4.5 Calibration of instruments

Finally all the wave gauges and the EMS must be calibrated each time before measurements can be taken. Generally there are two types of calibrations that have to be performed at all times, in case of doubt other calibrations can be done to verify the obtained data.

3.4.5.1 Calibration of EMS

It is very hard to know whether the measured values of the orbital velocities are correct. From physical models values can be obtained that estimate the actual velocities, but there will always be differences.

The data obtained with an EMS are constructed in the following way:

$$\text{Velocity} = \text{Offset} + \text{gain factor} \times \text{signal}$$

Differences between the measured velocity and the actual velocity can be attributed to the Offset, the gain factor or the signal. If there are problems with the signal the EMS is broken and cannot be used anymore.

Differences in the gain factor however do not always yield to rejection of the data. The gain factor can change due to a difference of water temperature, pollution of the water, or by means of dirt on the probe. By doing calibration tests the deviation of the gain factor can be found. How this should be done is described in the following steps.

This test has to be carried out in advance of velocity and acceleration measurements and after these measurements, in order to check whether a constant error in the EMS signal occurred during all measurements done at that day. If the values of the calibration tests have varied over the day the data obtained at that day has to be rejected.

Required for these calibration tests are 1 EMS and a moving trestle, which has to be driven electronically or mechanically and which can move with various constant speeds over the wave flume.

- step 1. Make sure the water is absolutely still. No water movement is allowed.
- step 2. Drag the EMS with a constant speed of 5cm/s along the flume and have the EMS take a measurement during the drive. As there is no movement of the water and the EMS is dragged through the flume with a constant speed, the EMS should record a signal that corresponds to a constant flow of 5cm/s along the probe.
- step 3. When the trestle is stopped wait till the water movement created by dragging of the EMS has stopped.
- step 4. Drag the EMS with a velocity of -5 cm/s and let the EMS take a measurement of the ride
- step 5. Do the same thing for drag velocities of 10, 20 and 30 cm/s, respectively -10, -20 and -30 m/s.
- step 6. Check the measured data and compare its values to the dragging velocities and examine if the data required before the tests is the same as the data required after the tests.

3.4.5.2 Calibration of the offset

Both the EMS and the wave gauge have an offset. This offset depends among others on the water temperature, but also on the location in the vertical and on the location in the flume.

Because the offset is dependent on a lot of factors it is important to check the offset before every measurement to be performed with an EMS or a wave gauge.

The offset can be checked as follows.

- step 1. Have the EMS and the wave gauges placed at the required position.
- step 2. Wait till there is no more water movement.
- step 3. Record the signal of all wave gauges and of the EMS in non-moving water
- step 4. Register the offset of the EMS, so later on the signal can be corrected with the offset.
- step 5. For the wave gauges turn the offset on the signal conditioner to zero. This means that the still water level has an elevation of 0 cm and that no correcting factors for the offset are required when analyzing the data.

3.5 Testing procedures

All tests have to be carried out under the same conditions and with a similar approach. From now on this approach of the various tests will be referred to as the plan of work. This plan of work for the experiment has to be clearly defined before the experiment can start. In it all steps, which have to be taken and executed during the tests, will be defined. It will also explain why certain steps are to be taken and how they should be carried out.

Not all tests are the same, because there are different things to look for. They can be categorized in the following way.

1. Tests to find the threshold of motion for the various wave steepness
2. Velocity, acceleration and wave height measurements
3. Calibration of the instruments
4. Vertical distribution of horizontal velocities
5. Slope reflection measurements
6. Video monitoring

In this section the plan of work for all 5 different tests will be given.

3.5.1 Tests to find the threshold of motion for various wave steepness

The threshold of motion can be defined in a lot of ways. In this thesis the threshold of motion will be defined as the movement of at least four stones from a colored strip. Using the movement of at least 4 stones will reduce the influence that stones can have which are placed in a unfavorable position.

As explained in previous sections, the forces acting on stones in the bed depend among others on the wave steepness. By increasing the wave steepness, the drag and pressure forces acting on the bed material will also increase, see section 2.4 The tests therefore will be split into series of regular waves with increasing wave steepness. Because it is difficult to change the water depth or the wave height during a test, only the wave period will be enlarged in order to change the wave steepness. Each of these series is to be repeated multiple times, in order to eliminate possible errors.

In a new test series it is now possible to do the same with a different wave height or a different water depth. By doing so many scenario of wave steepness can be created at various locations along the bed.

The plan of work for one test series with a varying wave period will be as follows:

- step 1. Choose a wave height H_0 and water depth h_0 for the given test
- step 2. Place the colored stones in the strips
- step 3. Create the required water level in the wave flume
- step 4. Let the wave board generate a wave that is 2.5 cm higher then the chosen H_0 and which has a very short period of 1.5 seconds.
- step 5. Have this series of waves run through the flume for at least one hour. This must be done for the water working. A high wave with a relative short period creates stronger

forces than required during the experiment, but only for a very short time. The colored stones, which are placed manually in the strips, are not all in a favorable position. By streaming with a large wave with a short period the stones can find a more stable and favorable position, but because this force is only working for a short time on the stones, the stones will not be transported but will find a favorable place almost at the same location.

- step 6. Stop the wave generator after one hour
- step 7. Take out all the colored stones, that have moved out of the strips during the water working
- step 8. Let the wave board generate a series of regular waves with a wave height of H_0 and a period of T seconds as chosen in step 1. T should be chosen such that almost none or only a couple of stones in the strips will move.
- step 9. After 50 waves check how many stones have moved out of the strips of colored stones and register this on a form as seen in appendix E.
- step 10. Stop the wave generator after it has generated 100 waves. Register the number of colored stones that have moved out of the strips and remove those stones from the flume.
- step 11. Let the wave generator make waves with H_0 as in step 1 and 8 and a period of $T + \Delta T$. This period should be a little longer then the previously used period. By enlarging the period the wave forces near the bed become stronger and therefore more stones will start moving. More details can be found in the note *
- step 12. After 50 waves register how many stones have moved. After 100 waves the wave generator must be stopped and the transported stones should be registered and removed from the flume.
- step 13. Return to step 11. This has to be done until the period becomes longer then the boundary value of T which is set at 4s. Waves with a longer period cannot be generated properly in the wave flume.
- step 14. When the boundary period has been reached the test series has been completed.

*Note: The velocities and accelerations increase along the slope until the waves break. As the wave period becomes longer the waves will become higher along the slope and the breaking point of the waves shifts towards the wave board. So by increasing the wave period different bed velocities and accelerations will arise along the strips.

The value ΔT is not a constant value. By changing the step size in various tests a lot of different scenarios can be created. While taking very small steps of ΔT , it will be impossible to find the threshold of motion, because with every step only one stone will move and after a lot of those small steps all stones have moved, but according to the criterion [see section..] there was no threshold of motion, because the number of moved stones was smaller then 5 for every created wave steepness.

When ΔT is chosen very large, there will be a lot of movement in every strip and this is also of no use. Because then the criteria will be valid at all locations of the strips, but at each strip the

velocities and accelerations have different values and therefore it will be impossible to find a relation for the influence of accelerations on the stability of stones.

According to the above a value for ΔT is impossible to find, so many values have to be tested. Sometimes small steps have to be made and sometimes the steps for ΔT have to be taken bigger. During the experiments, the values of ΔT have varied from 0.2 sec to 1 sec.

3.5.2 Measurements of near bed velocities, accelerations and wave heights

Stones in the bed can only be moved if the water movement is strong enough to lift or roll the grains along the bottom. Forces (created by the water movement) that cause the stone movement can be subdivided into drag forces (created by the horizontal orbital velocity) and pressure forces (created by the accelerations under the wave motion). These forces are being increased during the test series, this in order to find the influence of these forces on the threshold of motion. To find values for the drag and the pressure forces, near-bed velocity and acceleration measurements are required. As mentioned in section 3.4, these measurements will be performed with an EMS. To check the output of the EMS and to get a good insight into the growth of the waves along the slope (shoaling) the wave heights at the location of the EMS measurement will also be checked. Finally during all measurements the elevations of the water surface before the toe of the slope have to be recorded in order to control the generated waves.

The approach for these measurements will be described in the plan of work as shown beneath. Required for the measurements are 6 wave gauges and one EMS. The program Daisylab will be used for registering and recording of the measured data. The measurements must be carried out for all wave heights and water depths as used in the threshold test described in the previous section.

- step 1. Placement of the wave gauges. Place 2 wave gauges just before the toe. Place 2 wave gauges at respectively $15\frac{1}{2}$ and 16 m distance from the wave board. And finally place two wave gauges at the end of the measurement area at respectively 22.3 and 22m distance from the wave board. The EMS has to be placed at the end of the measuring area at a distance of 22 m from the wave board. By installing the EMS at the reversed side of the trestle it will be possible to place a wave gauge and the EMS at the same location. The wave gauges will be placed in pairs in order to correct possible deviations of the instruments
- step 2. Create the required water depth h_0 and have the wave board generate waves with the required wave height H_0 with a period of 2 seconds.
- step 3. After 75 waves (the wave pattern has to be completely adjusted to the newly created waves), the near-bed velocities, the accelerations and surface elevations have to be recorded for at least 10 wave periods. Multiple periods must be recorded in order to see deviating patterns, which can indicate possible measuring errors, irregular waves or even breaking waves.
- step 4. Stop the wave generator and let it generate new waves with height H_0 and a period of $T+\Delta T$. The value of ΔT should be the same as used in the tests to find the threshold of motion.
- step 5. After 75 waves the near-bed velocities, accelerations and surface elevations have to be recorded for at least 10 wave periods.
- step 6. Stop the wave generator and let it generate new waves with height H_0 and a period that is ΔT longer then the previously used wave period.

- step 7. After 75 waves, the near-bed velocities, accelerations and surface elevations must be recorded for at least 10 wave periods.
- step 8. Return to step 6. This must be done until T becomes as long as the given boundary period of 4s
- step 9. After the test with a period of 4s has been completed the EMS and the 2 wave gauges placed near the EMS should be moved half a meter forward, to respectively 21.5m for the EMS and one wave gauge and 21.8 m distance of the wave board for the other wave gauge.
- step 10. Return to step 2. The water depth has to be controlled again to check whether there is no leakage out of the flume that can influence the measurements. When step 9 will be reached the EMS and the 2 wave gauges have to be moved half a meter towards the wave board and one should return to step 2
- step 11. Do this until the EMS and the wave gauge next to the EMS are at a distance of 16.5m from the wave board.

3.6 Evaluation

In this chapter has been shown how the experiment has to be built up. During the description of the construction plan and the plan of work all relevant parameters have been introduced. It has been told why they are used and what their expected values must be. As help, in appendix C all parameters are listed that will be used during the experiments.

The measuring techniques have also been discussed. It appeared that attention has to be paid when analyzing data obtained with EMS or wave gauges. It is important that calibrations steps are performed before and after measurements are taken. If this calibration is executed correctly then no significant problems are to be expected.

An extended manual that describes the usage of EMS and wave gauges can be found in appendix A. This manual also gives information on how to process such digital data and how to verify this digital data.

Finally the plan of work for the various experiments has been discussed. Repeating each test series multiple times will reduce the experimental character of the data. Finally when performing a similar test this chapter can be used as reference.

4 Wave analysis

4.1 Introduction

During the experiments lots of wave data have been collected. As seen in the previous chapter, these data are not directly applicable. The electrical signals of the wave gauges and EMS are converted from analogue into digital signals, which are subsequently recorded by a computer. While transforming the data, modifications in the signals can arise due the instruments filters. How to deal with such modifications is explained in a manual that can be seen in appendix A.

Previous chapters showed that waves generate the forces, which try to move the stones from their initially stable positions. This implies that a thorough knowledge of the hydraulic wave processes is essential when determining and analyzing the wave forces that act on the bed material.

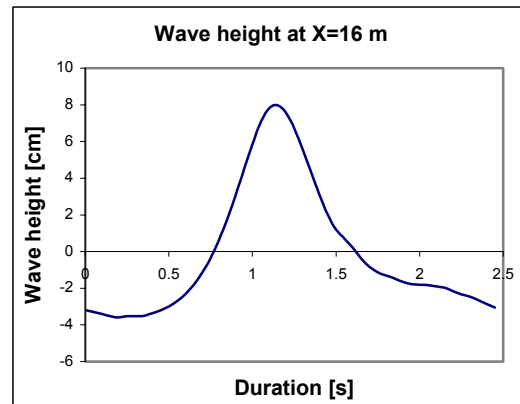
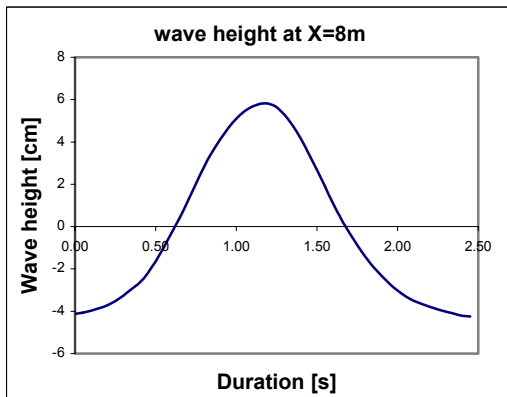
So before analyzing the influence that fluid accelerations have on the threshold of motion it is important that all wave process that take place in the wave flume are known.

With use of the wave data a thorough wave analysis has been performed. The most relevant findings of the wave behavior in the flume are presented in this chapter. The entire wave analysis can be seen in appendix H.

4.2 Shoaling

As waves travel into water of decreasing depth the wave height increases and the wave profiles become more peaked. This effect is known as shoaling. The waves used in the experiments will also shoal due to the presence of the slope.

An example of such a shoaling wave in the wave flume can be seen in Figure 4.2-1.



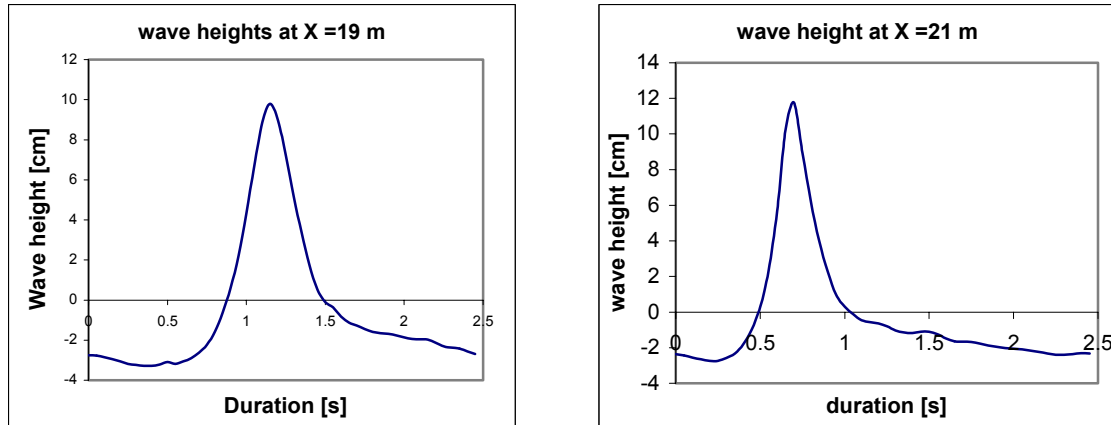


Figure 4.2-1 Wave heights and wave forms at various locations for $H=0.1$ m, $T=2.5$ sec and $h=0.55$ m

It can be clearly seen that an asymmetric wave pattern develops as the water depth decreases. The wave front (the left side of the wave) becomes steeper and the wave tops grow, while the troughs get smaller amplitudes. It can also be seen that the waveform becomes skewed. This will be discussed later.

4.3 Velocity analysis

The vertical and horizontal fluid motion differ 90° in phase. This corresponds to a revolving turn along a circle, the so-called orbital motion, (Battjes, 1991). Due to non-linear movement, these circles are not entirely closed, but describe in one period a relative small net horizontal movement.

The values of kh (the product of the wave number and water depth) determine the relative quantities of the water motion velocities.

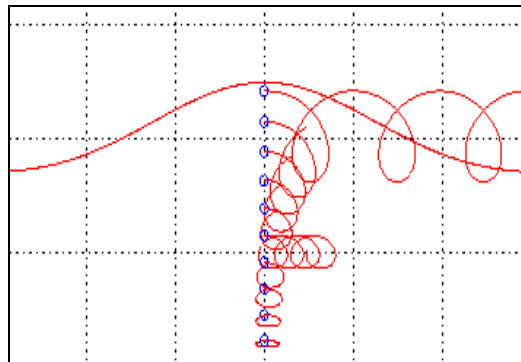


Figure 4.3-1 non linear orbital movements of water particles

The vertical water motion reduces to zero near the bottom. The vertical accelerations on the bed are also assumed to be infinitely small, and can therefore also be neglected. This doesn't mean that no vertical water motion forces try to move the grains in the bed. Turbulent movements near the bed due to irregularities of the bed and flow irregularities create turbulent forces that can act

on the grains and try to lift up the grains. Creating a uniform slope, with carefully placed grains of the same size and by sufficient water working time this influence can be minimized.

In the experiment it is assumed that the horizontal water motion generates the forces that try to move the grains. With an EMS the horizontal flow velocities have been measured during all the tests at various locations near the bed for all types of generated regular waves. The accelerations follow from differentiating these velocities.

4.3.1 Validation of near-bed velocities

The force acting on the stones can be directly related to the orbital horizontal fluid motion near the bed. So the most logical thing to measure will be the horizontal orbital velocity at the bed. This is though, not possible with the EMS. The EMS is based on the Faraday principle of electromagnetic induction. For accurate measurements the probe, in which the measuring electrodes are situated, must be surrounded by a sufficiently big body of water in order to prevent disturbances in the created the electronically fields. This implies for the EMS that it cannot be placed too close to the bed. The minimum height at which the EMS can do its measurements without disturbances of the electronically field is approximately 4 cm above the bed. It is of course important to know whether the values measured at 4 cm above the bed are representative for the near-bed velocities.

The vertical distribution of orbital horizontal velocities can give an insight in this representation of the measurements at 4 cm altitude.

For two waves the horizontal velocities have been measured at an elevation of respectively 4, 6, 8, 10 and 12 cm above the bed. The amplitude of those horizontal velocities at every elevation shows the development of the horizontal distribution in the vertical. If the increase of velocities is gradually between the various heights, then we are dealing with velocities outside the boundary layer. On the contrary if the increase of velocities is very big between the various heights then we know that most of the previously done near-bed measurements have been taken, within the boundary layer.

Note that under waves the boundary layer is growing and declining due to the orbital motion. Therefore the amplitude is a good criterion, because it is the largest value, and hence the biggest boundary layer.

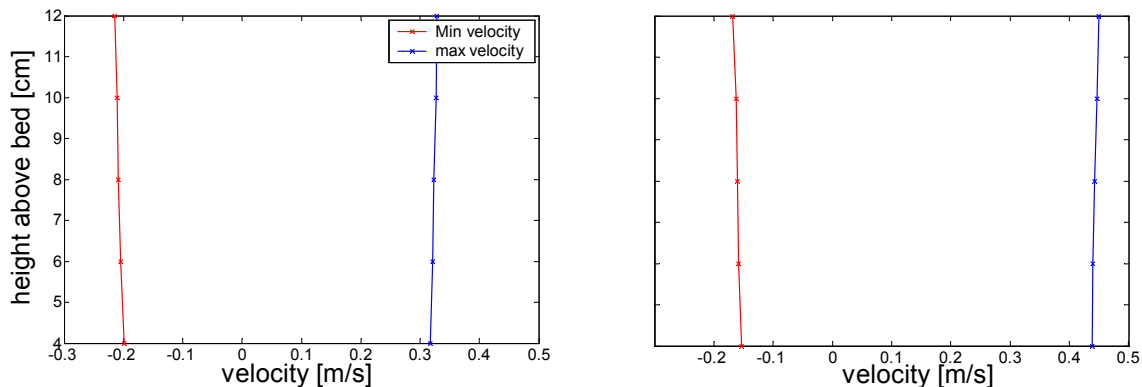


Figure 4.3-2 amplitudes of horizontal velocities at various elevations at 18m for a wave of $H_0=0.1\text{m}$, $h_0=55\text{cm}$ and on the left $T=2\text{s}$ and in the right graph $T=3\text{s}$.

Both graphs show a very small increase of velocities and therefore it can be assumed that the near-bed velocity measurements have been taken outside the boundary layer. The fact that all near-bed velocities have been taken outside the boundary layer means that it's assumable that no velocity fluctuations can be expected due to irregularities in the bed.

It will also be very useful for determining the velocities at the bed, because now common accepted relations can be used to determine the velocities within the boundary layer at the height of the stones.

In section 2.4 a formula found by (Booij, 1992) has been shown that could help finding an approximate height of this boundary layer.

$$\frac{d\delta}{dt} = \kappa u_* \approx 0.4u_* \quad (4.1)$$

In which $u_* \approx 0.1 * u_b$

For the above two examples this leads to a maximum boundary layer height of respectively 1.2cm for the 2s wave and 1.8cm for the 3s wave. This is indeed be very small and verifies the assumption that the velocities that have been measured at 4cm above the bed, were taken outside the boundary layer.

4.3.2 Behavior of near-bed velocities and phase lag

In section 4.2 has been shown that the wave front becomes steeper due to shoaling. This shoaling also influences the horizontal velocities and accelerations. Figure 4.3-2 shows the growth of the near-bed horizontal velocity profile at various locations along the slope. The distances are distances from the wave board, which leads to a decreasing water depth.

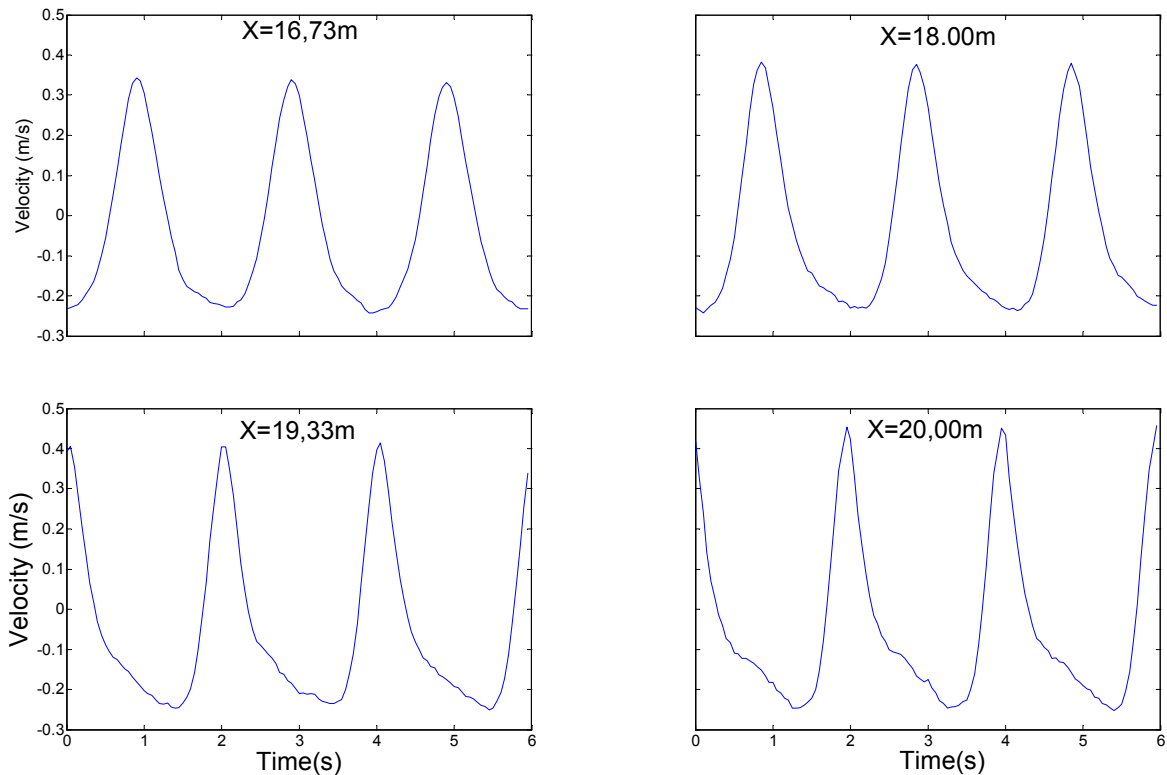


Figure 4.3-3 Near-bed velocity as waves travel into shallower water for $H=0.125\text{m}$, $T=2\text{s}$ and $h=55\text{cm}$

It can be seen that just like the wave profiles, the velocity profile becomes more peaked at the top and gets a flatter trough. The waves break at $X=20\text{ m}$, this can also be seen in the velocity profile around $X=20\text{m}$. The profile there is very sharply peaked.

It also seems that the velocities will keep increasing due to shoaling. This is however not exactly true. The reason for this is the occurrence of phase shifts.

4.3.3 Phase shifts

The shape of deep-water waves is sinusoidal. The reason for this is that waves in deep water are constructed of only one frequency component. As waves travel into water of decreasing depth the influence of the higher order frequency components becomes more and more evitable and the wave evolves to a more peaked and skewed form. This is represented in figure 4.3-4.

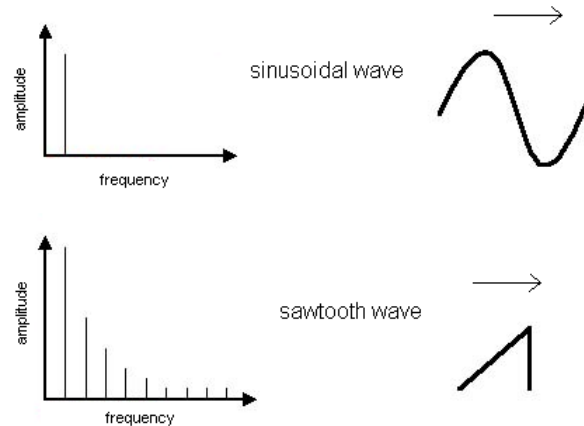


Figure 4.3-5 Frequency-amplitude spectra and accompanying waveforms.

From harmonical analysis (see appendix A) it is known that every continuous periodic function can be represented as an infinite sum of harmonic signals with differing angular frequencies ω_0 , whose amplitudes c_n , and phases φ , may also differ, but not necessarily.

So in the experiment the waves can be represented by an infinite sum of harmonic components of water surface elevations and the corresponding velocities under the waves can be made out of an infinite sum of harmonic components of wave velocities.

All these harmonical components of the surface elevations and the near-bed velocities have an amplitude and a phase. The phases of the harmonical components are however not always equal. As the waves travel into water of decreasing depth the phases of the various harmonical components will change independently of each other.

This implies that, as the harmonical components are in phase that they will strengthen each other and a large value of the horizontal near-bed velocities can be found. While at other locations the harmonical components are out of phase and the signal will be weakened by the harmonical components.

Due to these changing phases of the various harmonical order components, the horizontal near-bed velocities will not grow linearly towards the breaking point of the waves, where the surface elevation of the wave is maximal. The graph that represents the increase of velocities can look very bumpy due to these ever changing phase lags. This is represented in figure 4.3-6.

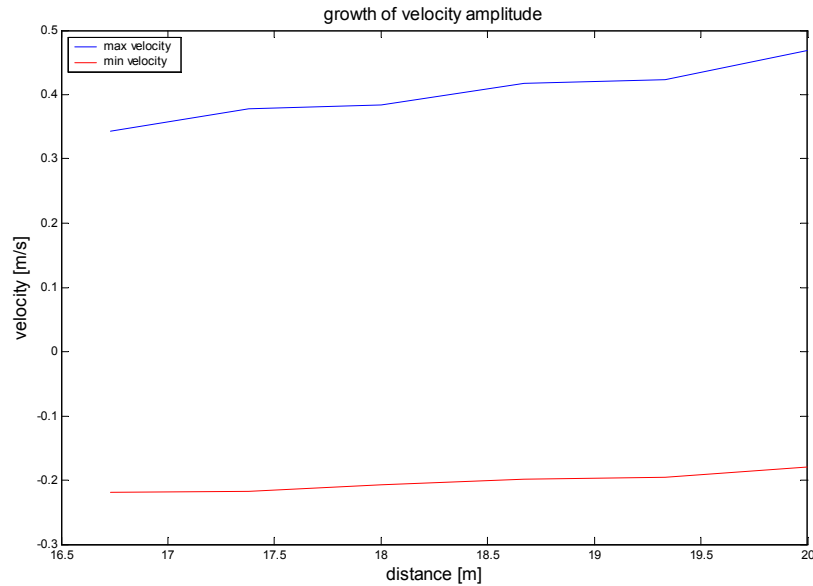


Figure 4.3-7 Growth of velocities in decreasing water depth for $H_0=0.125\text{m}$, $T=2\text{s}$ and $h_0=55\text{cm}$

A more detailed explanation of the behavior and occurrence of phase lags can be found in appendix H, which shows a detailed wave analysis.

4.4 Accelerations

As mentioned the velocities are not the only forces that act upon the grains. Accelerations create pressure gradients that also try to move the grains from their initial position. The accelerations are found by differentiating the velocities profile as a function of the time. As said in the previous section the changing waveform leads to changing bed velocities. Therefore also the bed accelerations will change. As seen in the previous section, the near-bed horizontal velocity profile becomes steeper at the wave front for a decreasing water depth. This will therefore yield to increasing accelerations in water of decreasing depth, because the derivative of a steeper profile has a larger value, then the derivative of a mild slope.

The increase of accelerations along the slope can be seen in figure 4.4-1. The accelerations are found from derivation of the velocity profile that has been shown in Figure 4.3-2.

From the plots it becomes clear that in the experiment the biggest acceleration (or pressure) gradients can be found just before breaking of the waves. After breaking these accelerations still increase, but the experiment only deals with waves that haven't broken yet.

In the plots the measured waves did break at a distance of 20 m from the wave board. This can be seen in the plot of $X=20\text{m}$ as it shows a lot of turbulence.

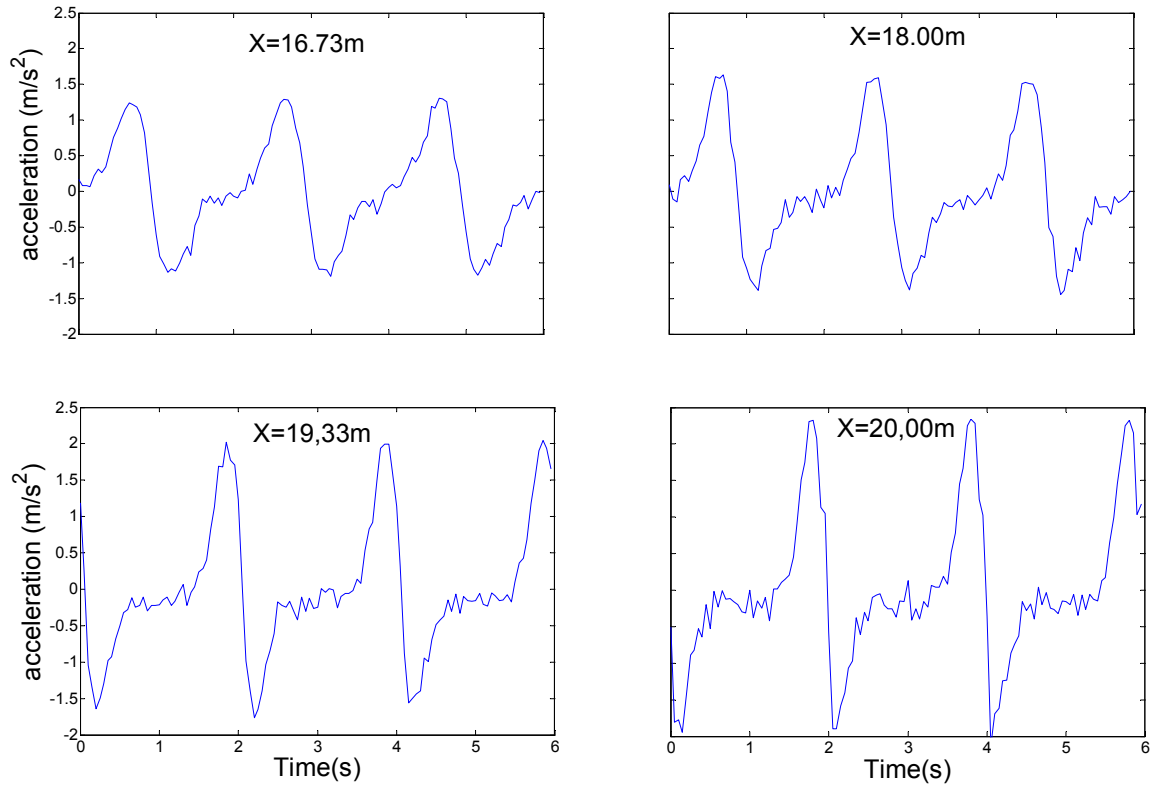


Figure 4.4-2 Accelerations at various locations for $H_0=0.125\text{m}$, $T=2\text{s}$ and $h_0=0.55\text{m}$

The growth of accelerations increases more rapidly as the waves near their breaking point, this is shown in the following figure. Values before the measuring area are not available. This is because the values are all taken from the measurements with the new EMS and there was little time, so only the measurements in the measuring area have been taken.

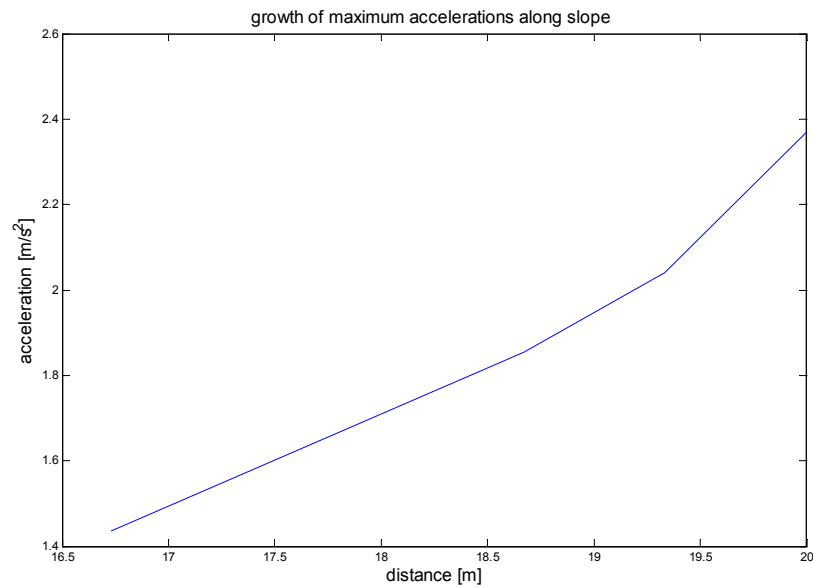


Figure 4.4-3 Values of maximal accelerations obtained in the measuring area for $H_0=0.125\text{m}$, $T=2\text{s}$ and $h_0=55\text{cm}$. Waves break around 20m.

4.5 Evaluation

In this chapter the most relevant results of the performed wave analysis have been described.

It appeared that the sloping bed in the wave flume has the desired effect.

As expected the waves become bigger due to shoaling effects. This also implies for the horizontal near-bed velocities and the accelerations. However due to phase shifts it is very difficult to predict the increase of these velocities and accelerations.

The phase shifts are very difficult to describe. Besides the phase shifts make it difficult to predict the velocities and accelerations with use of wave theory. (This is explained in appendix H).

Nonetheless the wave analysis confirmed the experimental approach of creating numerous combinations of velocities and accelerations by means of waves on a slope.

5 Threshold of motion

5.1 Introduction

The goal of this thesis was to investigate whether fluid accelerations have an effect on the threshold of motion of stones placed on a bed. In this chapter the presence of such a relation will be analyzed and discussed.

If there is a relation between the threshold of motion and accelerations then for some combinations of a velocity and acceleration there will be no movement, while in other cases with the same near-bed velocities, but a different acceleration, there will be movement of the same stones.

An experiment has been carried out to find out whether accelerations influence the threshold of motion. During the experiments 78 test series have been performed at various locations and with changing wave steepness in order to create scenarios of similar horizontal near-bed velocities, but with different accelerations. Due to the arisen problems with the EMS only the tests carried out at an initial water depth of 55cm will be analyzed in this theses.

During the tests the number of stones that moved have been observed for all different waves and locations along the slope. Using the EMS data for the same tested locations and wave steepness now leads to a wide range of horizontal velocities, accelerations and accompanying number of moved stones. So by knowing the number of stones that moved and the horizontal velocities and accelerations it becomes possible to find a relation between the velocity generated forces, the acceleration forces and the threshold of motion.

5.2 Instantaneous approach

One way to find the effect that fluid accelerations have on the threshold of motion is with use of an instantaneous approach. Whether this is a correct approach will be discussed later on. An instantaneous approach assumes that a stone will start to move once the momentary forces that act on the stones exceed a certain critical value.

5.2.1 Force balance

Grains placed in a bed can only be moved if the force created by the water movement is strong enough to lift or roll the grains from their initial position. From section 2.4.3 is known that the forces, which act on a single grain can be divided into forces that try to move the grain and forces, which act to keep the grain in its place.

For non-cohesive grains the gravity force is the force that tries to keep a grain at place. This force remains constant during each test.

The horizontal water particle velocities and accelerations generate the forces that try to move the stone. As this water motion describes an orbital motion under waves, the forces that try the move the stones will do the same and will therefore never have a constant value. So when using an instantaneous approach a relation between the times at which a stone starts to move and the momentary wave forces that occur at that moment have to be considered.

The sample rate of the measurements performed with the EMS has been 20 Hz, so it is possible to determine the wave forces for every 0.05s. With use of the force balance as seen in section 2.4.4 it is now possible to find for every 0.05s whether the stone will remain stable or that it will start to move.

5.2.2 Presence of velocity and acceleration forces

Just like the water particles under waves, the velocity and acceleration profiles also describe an orbital motion. In appendix H has been shown that at the moment when the wave top passes the EMS, the value of the near-bed horizontal velocity will have its maximum.

The accelerations are obtained from deriving the velocity profile. This implies that the maximum value of acceleration never occurs at the same moment as the maximum value of velocity. To see whether there are moments where the velocity forces and the acceleration forces strengthen each other, the following plots have been made. In the plots both the velocity profile and the acceleration profile have been set out. In the first plot a dark point indicates the value of the acceleration at the time the wave top passes the EMS and a light point indicates the value of the horizontal near-bed velocity at that same time. The second plot indicates in the same manner the values 0.05s in advance of this passage of the wave top. The value 0.05s has been taken because the sample rate of the EMS was 20HZ, so this was the smallest time step available.

The third plot highlights the values taken at 0.10s before passage of the wave top and the last plot has been made for the values of acceleration and velocity at 0.15s before passage of the wave top.

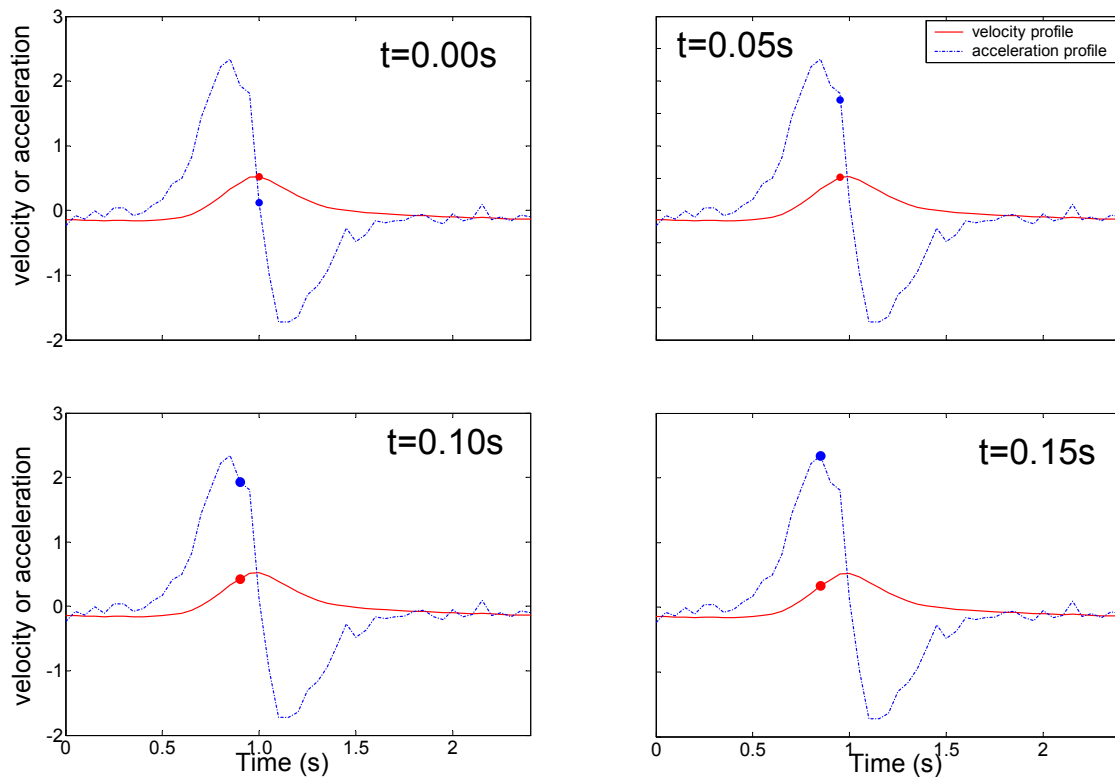


Figure 5.2-1 Instantaneous values of near-bed horizontal velocities and accelerations for a wave with $H_0=12.5\text{cm}$, $h_0=55\text{cm}$, $T=2.5\text{s}$ and $X=18.68\text{m}$. The solid line represents the orbital velocity motion and the dash-dotted line the orbital acceleration motion. The time in the title of the plots is the time before passage of the wave top.

The above has been done for many waves and all non-broken waves show the same pattern. At the passage of the wave top the velocity has a maximum value and the acceleration has a very small value. At 0.05s seconds the velocities still has a large value and the accelerations have a larger positive value. At 0.010s before the wave top passes the values of the near-bed horizontal velocity are somewhat smaller and the values of the accelerations are large. Finally at 0.15s before passage of the wave top the values of the accelerations are very big and the values of the velocities are getting small, but nonetheless remain positive.

The reason that the values of the horizontal velocities and accelerations have been plotted for the given time intervals is that for these situations the accelerations and the velocities both have positive values in the direction of wave propagation. As the experiment only considers movement of stones in the direction of the wave propagation, the forces on the stones will only act in the right direction somewhere at this interval, which is between the passage of the wave top and 0.15s before this passage.

For waves with a large period (i.e. 3.4s) the maximum value of acceleration did already pass at 0.15s before the top of the waves. For waves with a short period the maximum value was not reached yet, but it still turned out that the maximum instantaneous forces would occur during this time interval.

The forces that try to move a stone are generated by both the horizontal velocities and the accelerations, when a Morison-like equation is to be considered (see section 2.4) From Figure 5.2-1 can be clearly seen that on the interval just before the passage of the wave top the accelerations and velocities have not just the same direction but also large values and will therefore fortify each other. So when looking at the graphs in Figure 5.2-1 it seems reasonable to believe that the accelerations do have an influence on the threshold of motion

5.2.3 Relation between velocity and acceleration forces

Many combinations of near-bed velocities and accelerations have been created by changing the wave steepness during a test and also by testing at various locations along the slope. During all these tests the movement of stones under the changing wave steepness and at various locations has been examined and registered on lists. An example of such a list can be seen in appendix E. After the completion of the experiment these forms give information on the number of moved stones for a given wave height, wave period and location.

A second objective during the experiment was to find the near-bed velocity and acceleration profiles for every wave height, wave period and location as tested for movement. With use of an EMS this data has been collected.

Section 2.4 made clear that the forces, which try to move the stones are generated by the near-bed horizontal velocity u and the accompanying accelerations a . In addition the previous section showed that every wave has an interval at which the acceleration and velocity forces near the bed strengthen each other in the direction of wave propagation.

When bearing in mind the above two relations, a good indication for the influence of acceleration forces can be obtained by plotting the movement of stones against the momentary velocities and accelerations. This has been done for the velocities and accelerations that were measured at respectively 0.15s, 0.10s and 0.05s before passage of the wave top and at the time the wave top was passed the EMS ($t=0.00s$).

As all tests have been repeated multiple times it is possible to find statistical values of movement. An advantage of this classification is, that sometimes movement occurs due to insufficient water

working time or an unfavorable position of a stone, repeating the tests will reduce the effects of these errors.

Making a long list that contains all locations and all tested wave steepnesses can create such a statistical approach. It has been shown that for all locations, the number of stones that did move during a test have been registered on a list. Combining the information from those movement lists with the long list that contains all measured locations makes it easy to see how many tests for a given wave steepness have been performed and how often movement of stones did occur. From here on the movement of stones will be categorized into the following classes:

- If for certain location and wave steepness a stone did move during more then 75% of all tests performed with those parameters then movement will be classified as *always*.
- When movement occurred during 25%-75% of all performed tests, then movement is classified as *sometimes*,
- If movement occurred in less then 25% of all tests then the movement parameter is equal to *none*.

Literature study showed that a definition for the threshold of motion turned out to be rather vague. Previously done researches all used different criteria for this threshold of motion. To get optimal results during this thesis multiple criteria will be compared. The plots of Figure 5.2-2 have used as criterion the movement of at least one stone. Other criteria will be shown and discussed further on.

In Figure 5.2-2 it is can be seen that the centre of gravity of all points at $t=0.00s$ lies near the bottom right corner. The other plots show that the cloud of marker symbols shifts towards the upper left corner for increasing values of t . This means that for higher values of t the values of the velocity become smaller and the values of the accelerations increase. This is of course only valid for the small interval that lies between the wave top and 0.15s before this passage of the wave top.

The plots as seen in Figure 5.2-2 have to be interpreted in the following manner.

- A vertical dividing line between the movement and no movement symbols means that there will be no movement of stones until the velocity exceeds a critical velocity. Because of the vertical borderline, it indicates that the accelerations don't influence the threshold of motion
- A horizontal dividing line between movement and no movement implies that there is only a critical value for accelerations. Only if this critical acceleration is exceeded there will be movement of stones. So for this case the threshold of motion depends just on accelerations.
-

A diagonal dividing line indicates that the threshold of motion is dependent on both accelerations and velocities.

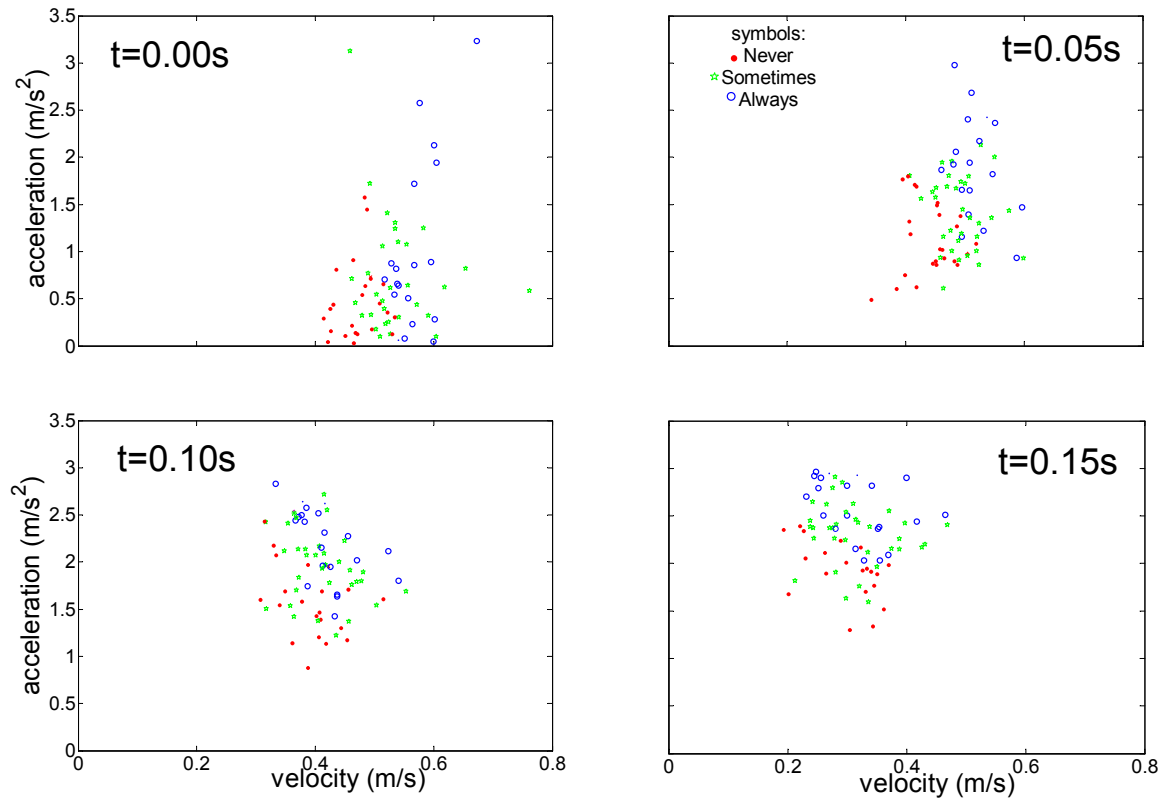


Figure 5.2-2 movement of the large stones plotted versus instantaneous velocities and accelerations that try to move the stones at $t=0.00s$, $t=0.05s$, $t=0.10s$ and $t=0.15s$ before passage of the wave top. Each symbol represents the statistical movement of wave steepness. Larger plots can be seen in appendix F.

The plots in Figure 5.2-2 show for $t=0.00s$ and $t=0.05s$ a rather vertical distinction line between movement and no movement. This would imply that the accelerations have very small or even no influence on the threshold of motion.

The plots for $t=0.10s$ and $t=0.15s$ however show a diagonal line between movement and no movement. This means that the threshold of motion is dependent on both the horizontal velocities and the accelerations.

A possible cause for such differences between the plots is that the stones already start to move before the wave top passes. With an instantaneous approach it is assumed that stones start to move when the wave forces that cause the threshold of motion exceed a critical value. If the stones start to move somewhere between $t=0.15s$ and $t=0.10s$ then at that interval the combined forces generated by the accelerations and horizontal velocities are larger than the critical force. This combination of forces therefore leads to a diagonal dividing line. In this case the stones have already left their initial positions at $t=0.00s$ or at $t=0.05s$, so the combination of forces at that time is no longer responsible for moving the stones from their initial positions. So the velocities and accelerations at those times don't give much information about the influence of accelerations and/or velocities.

A cause for some scatter in the plots can be as follows:

The sample rate of the measurements is 20Hz so a measurement is taken at every 0.05s. The actual occurring velocities and accelerations are continuous functions, so it can happen that

therefore not the exact velocities and accelerations that were required have been measured, but a velocity or acceleration just before or just after this point. This is not a big problem for profiles with a mild slope. The slopes of the velocity and acceleration profiles however are steep. This can therefore lead to distorted values of velocities and accelerations and give a wrong impression. Especially the acceleration profile at $t=0.00\text{s}$ and $t=0.05\text{s}$ is very steep. The error of the measured accelerations at this interval will therefore be very big and can lead to much scatter.

Another criterion that can be used for the threshold of motion is the cumulative motion of at least four stones. Considering at least four stones reduces the influence of stones that are placed in unfavorable positions. And a cumulative summation will be made because it is assumed that the wave force increases each time, the wave steepness is enlarged during a test. So it is considered that during a test series the wave forces will continue to increase and therefore once the threshold of motion has been reached only more and more stones will start to move during a test series. Figure 5.2-3 shows plots in which the movement of stones is plotted against the momentary velocity and accelerations. Movement has now been defined as the cumulative movement of at least four stones.

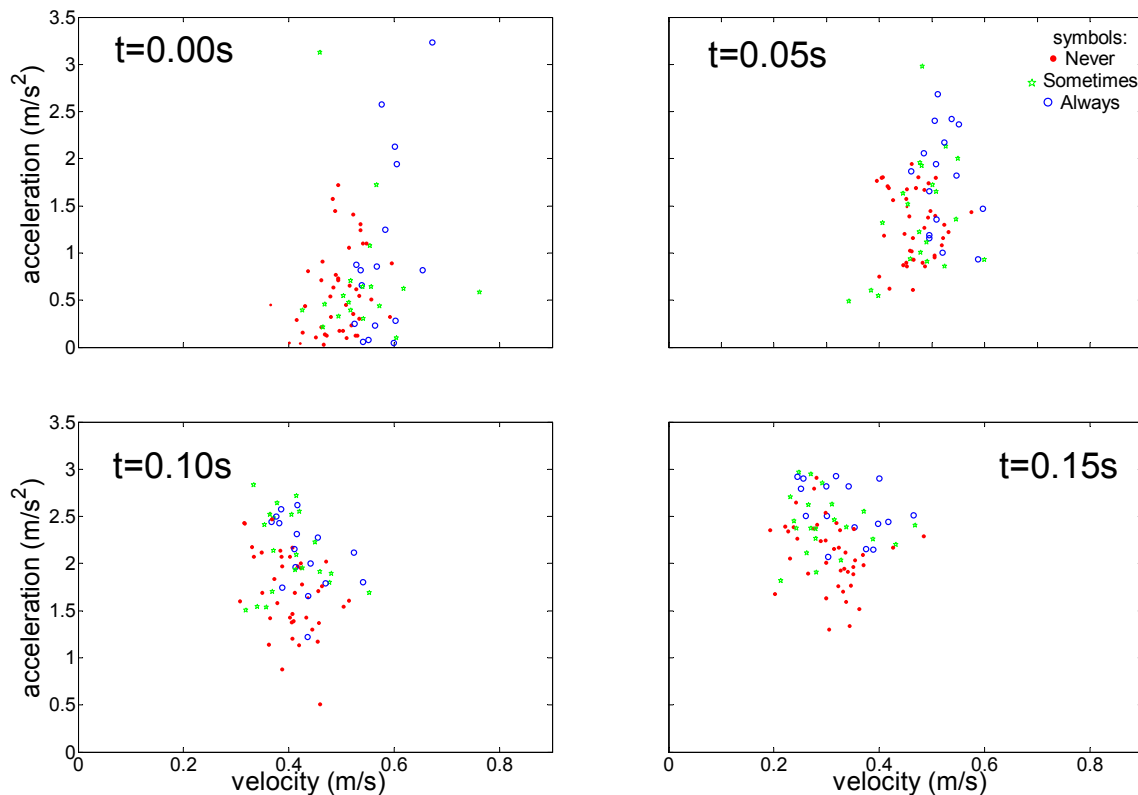


Figure 5.2-3 Cumulative movement of at least 4 large stones plotted versus the momentary accelerations and the square of horizontal velocities that try the move the stones at $t=0.00\text{s}$, $t=0.05\text{s}$, $t=0.10\text{s}$ and $t=0.15\text{s}$ before passage of the wave top. Each symbol represents the statistical movement of wave steepness. Larger plots can be seen in appendix H.

The plots in Figure 5.2-3 show for $t=0.00\text{s}$ and $t=0.05\text{s}$ again a vertical dividing line between movement and no movement and the plots taken at $t=0.10\text{s}$ and $t=0.15\text{s}$ show a diagonal distinction between movement and no movement. This is similar to the findings in Figure 5.2-2. The scatter however is somewhat bigger for the plots in Figure 5.2-3. This seems surprising

because the criterion of at least 4 stones was taken to reduce the influence of badly placed stones. The reason of the extra scatter turns out to be caused by an incorrect assumption. It was assumed that the wave force would increase for each time that the wave steepness was increased. Because of the presence of phase shifts this is not always true. The summation of the amplitudes of all harmonical components did indeed increase, but because of the phase shifts the horizontal velocities and accelerations did not always grow (phase shifts have been discussed in section 4.3). So sometimes stones were classified to have moved, while the velocities and accelerations forces turned out to be smaller then the critical force.

More plots with different movement criterion can be seen in appendix F. They all show comparable findings. The small stones as used in the experiment also show similar findings. In Figure 5.2-4 the movement of at least one stone has been plotted at $t=0.00$, 0.05 , 0.10 and 0.15 s.

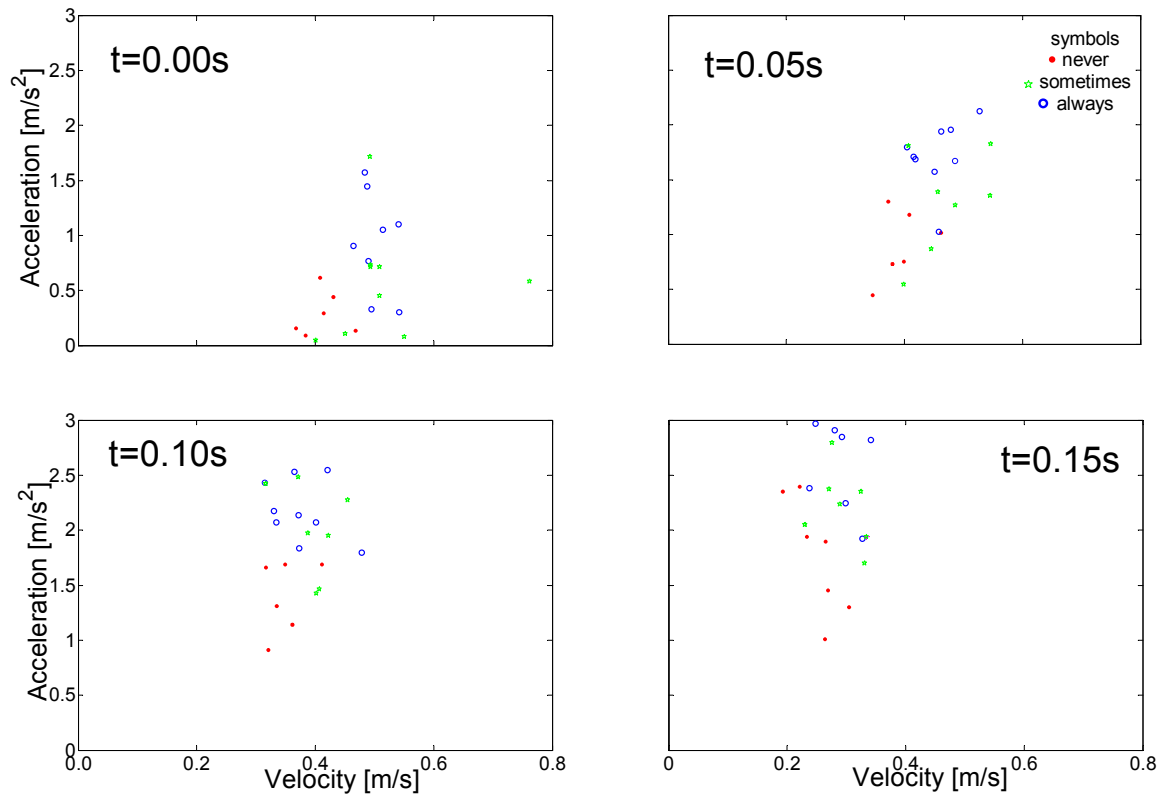


Figure 5.2-4 Movement of at least 1 small stone plotted versus the momentary accelerations and horizontal velocities that try to move the stones at $t=0.00s$, $t=0.05s$, $t=0.10s$ and $t=0.15s$ before passage of the wave top. Each symbol represents the statistical movement of wave steepness. Larger plots can be seen in appendix H.

The most important finding so far are that for all used movement criteria, the plots of $t=0.10s$ and $t=0.15s$ all show a diagonal dividing line between movement and no movement. This implies that at $0.10s$ to $0.15s$ before passage of the wave top both the accelerations and the velocities influence the threshold of motion.

All shown plots still have a lot of scatter. When using the Morison-like equation the influence of the velocity forces is proportional to u^2 and the influence of the accelerations is proportional to a . Plotting the movement of stones versus the square of the horizontal velocity u^2 and the

acceleration a might therefore reduce the amount of scatter. In Figure 5.2-5 this has been done for the threshold of at least one large stone.

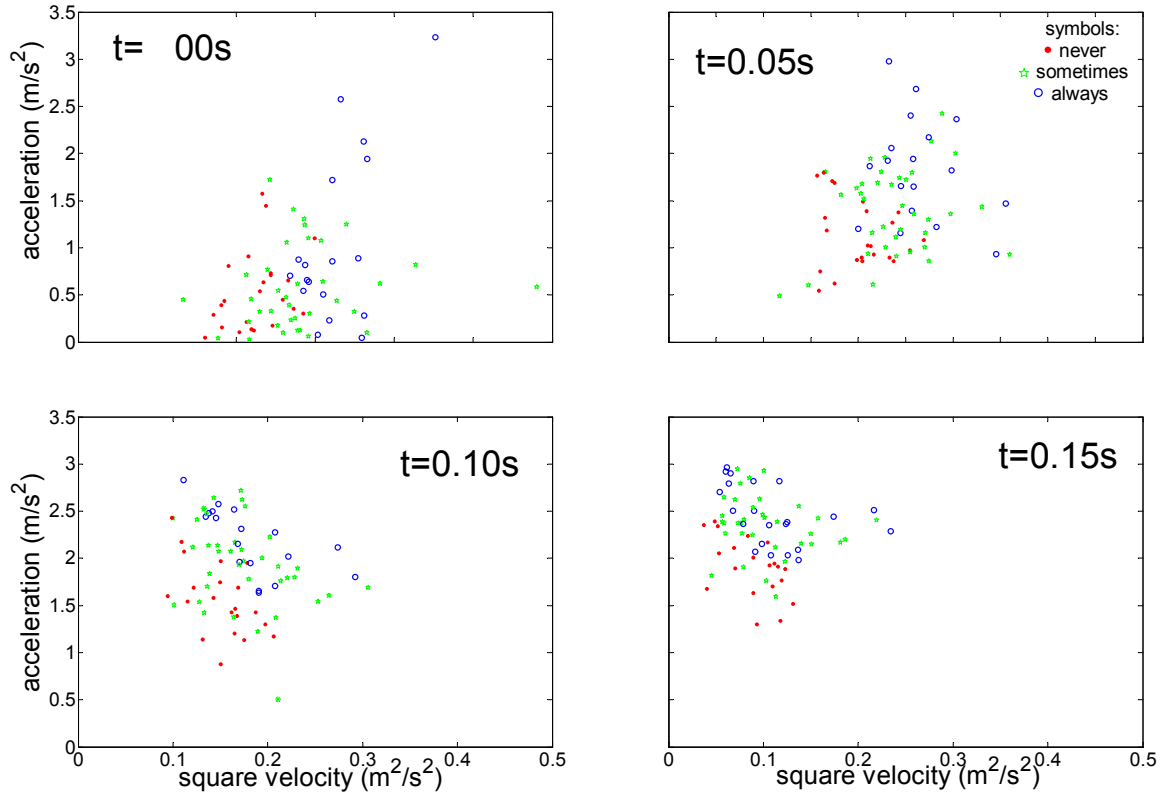


Figure 5.2-5 Movement of large stones plotted versus the momentary accelerations and the square of horizontal velocities that try the move the stones at $t=0.00s$, $t=0.05s$, $t=0.10s$ and $t=0.15s$ before passage of the wave top. Each symbol represents the statistical movement of wave steepness.

Yet the same pattern is still visible. At $t=0.00s$ and $t=0.05s$ no influence of accelerations can be found but when looking at the diagrams plotted at $t=0.10s$ and $t=0.15s$ a diagonal border line between movement and no movement occurs, while the amount of scatter remains rather big.

5.2.4 Video observations

It has been shown that somewhere between 0.10s and at 0.15s before the wave top passes, a relation between the threshold of motion and the velocity forces and acceleration forces can be found. However it is still unknown whether the velocities and accelerations that are present at these times are responsible for the movement of the stones. So the next step to be taken is to find out at what time the stones start to move. For this purpose video observations have been made.

A video camera can be used to record the movement of the stones. In the video images both the waves and the stones have to be visible. Once a stone starts to move the video image has to be frozen. Doing so makes it possible to see the elevation of the wave at the time the stone starts to move.

Because a wave gauge is always placed next to the EMS, the horizontal velocities and accelerations are known for all wave elevations. So knowing the surface elevation at the time the

stones start to move, makes it possible to find the horizontal velocities and accelerations that are present at that same moment.

In previous sections, the used velocities and accelerations have been represented as a function of the time. To prevent confusion the same representation of the surface elevation as function of the time will be used for the video analysis. So the time at which the wave peak passes (which is the maximum surface elevation) is known as $t=0.00s$. As an aid to find the relevant time at which the stones start to move a digital clock must be used, that is accurate up to $1/100s$. The display of this clock also has to be in the video images. By first determining the time at which the wave top passes it then becomes possible to know the time at which the stones started to move, relative to the time the wave top passes. The same can be done for the end of movement.

This observation method can be used for every wave steepness and location. This is however not feasible, due to shortage of time. Therefore only for a couple of locations and few wave steepness videos have been made.

Only videos in which multiple stone movements occurred while observing them can be used for the video analysis. This is a requirement that must be met, in order to find out whether all stones started to move under the same interval of surface elevation.

When the stones all start to move under very different surface elevations it becomes impossible to use an instantaneous approach, because in that case every time completely different velocities and accelerations are present at the time of first movement. If this happens it can be concluded that there must be another mechanism, which is responsible for the initiation of movement.

If multiple stones start to move under the same interval of surface elevations then the video analysis can be continued.

For each usable video a table has been made that shows the times at which the various stones started to move. The times at which the movement of each stone ended have also been registered in these tables. As this theses only deals with the experiments carried out at an initial water depth of 55cm, an example of a table from a video made at this depth is shown in Figure 5.2-6.

Video 1 has been made at a distance of 18.00m from the wave board. The occurring wave steepness was created by the following parameters:

- $H_0 = 15cm$
- $T = 2.5s$

During the video observations it was possible to follow the movement of 5 stones from their initial positions. The times at which this movement started and ended has been shown in table 5.1

Stone nr.	1	2	3	4	5	Average
Tim of passage wave top	1.25	1.25	1.25	1.25	1.25	1.25
Time of 1 st movement	1.15	1.11	1.12	1.18	1.12	1.13
Time of end of movement	1.55	1.33	1.42	1.45	1.33	1.42

Table 5-1 Time at which movement started and ended found in video 1

Note that the time at which the wave top passes is 1.25s instead of 0.00s. In the analysis this time at which the wave top passes will however be known as $t=0.00s$. The time 1.25s has been taken because that was the time at the display when the wave top did pass for the first time.

The average time at which the movement of the stones begins and ends can also be represented graphically. This has been shown for the surface elevations as present in video 1.

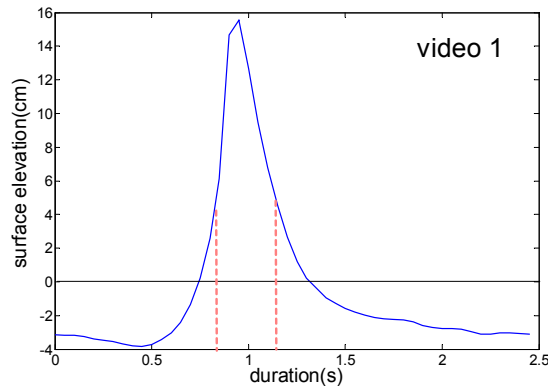


Figure 5.2-6 Average times at which stone movement starts and ends

It can be seen that the time at which a stone started to move was about the same for all the stones. This implies that the use of the instantaneous approach still can be justified. The times for the end of movement of the various stones however are less uniform. The same phenomenon can be seen for the other videos.

Figure 5.2-7 also shows that the first movement starts at 0.12s before the wave top passes. This moment is within the interval that showed a diagonal dividing line between movement and no movement (see section 5.1). So it seems like that for this case both the horizontal velocities and the accelerations influence the threshold of motion.

To find out whether this time of first movement is uniform for different wave steepness the average values of the first movement of all videos have been listed in table 4.2.

As not all the times of first movement are exactly the same, a classification between the various wave steepnesses has been made. The categories are just used, as reference and no physical importance should be attached to it. Plotting the surface elevation of all waves and subsequently comparing the steepness of the profiles to each other have obtained the classification. The flattest profiles have been classified as very mild and the steepest profiles as very steep. Mild and rather steep has been used to classify a profile that was somewhere between the very steep and the flat profiles.

Video	Wave				Classification	Time of 1 st movement (± 0.02 s)
	h_0 [cm]	T[s]	H_0 [m]	X		
1	55	2.5	0.15	18.00	Mild	0.12s
2	55	2.25	0.15	18.00	Very mild	0.12s
3	55	3	0.125	18.67	Rather steep	0.08s
4	55	3.8	0.125	18.67	Very steep	0.10s
5	60	2.5	0.15	17.38	Very mild	0.10s
6	60	3	0.175	18.00	Rather steep	0.08s
7	60	2.5	0.15	18.67	Mild	0.12s
8	60	3	0.15	18.67	Rather steep	0.08s
9	60	3.4	0.15	18.67	Very steep	0.09s
10	60	3.6	0.15	18.67	Breaking	0.10s
11	65	3	0.15	19.00	Mild	0.12s
12	65	3.4	0.15	19.00	Rather steep	0.08s
13	65	2	0.15	20.00	Very mild	0.11s
14	65	3	0.15	20.00	Mild	0.12s
15	65	3.4	0.15	20.00	Rather steep	0.09s
16	65	4	0.15	20.00	Very steep	0.08s

Table 5-2 Average times before passage of the wave top at which stones started to move. The times have been found with use of video observations.

Table 5.2 shows that for every wave steepness the average time at which the stones start to move is between 0.08s and 0.13s before passage of the wave top. This means that the EMS measurement taken at 0.10s before passage of the wave top will probably give the best approximation of the velocities and accelerations that make a stone move (sample rate is 20Hz, therefore only every 0.05s a measurement will be taken).

The classification of the observed waves shows that for steep waves a stone starts to move between 0.08 and 0.10s before the wave top passes, while for mild slopes a stone starts to move between 0.10 and 0.12 s before passage of the wave top. The difference between these times is 0.05s, which is exactly the same as the time between two measurements. Therefore attention has to be paid when assuming that the forces that make the stones move come from the wave forces measured at $t=0.10$ s.

From table 5.2 can also be seen that only 4 videos have been taken at an initial water depth of 55cm. For these videos the exact time at which the stones start to move are known. The EMS that has been placed next to the wave gauge can now be used to find the horizontal velocities and accelerations that are present at the time the stone movement starts. With an instantaneous approach it is assumed that these velocities and accelerations generate the forces, which are responsible for the stone movement.

For video 1 these critical horizontal velocity and acceleration are represented graphically. This is shown on the next page.

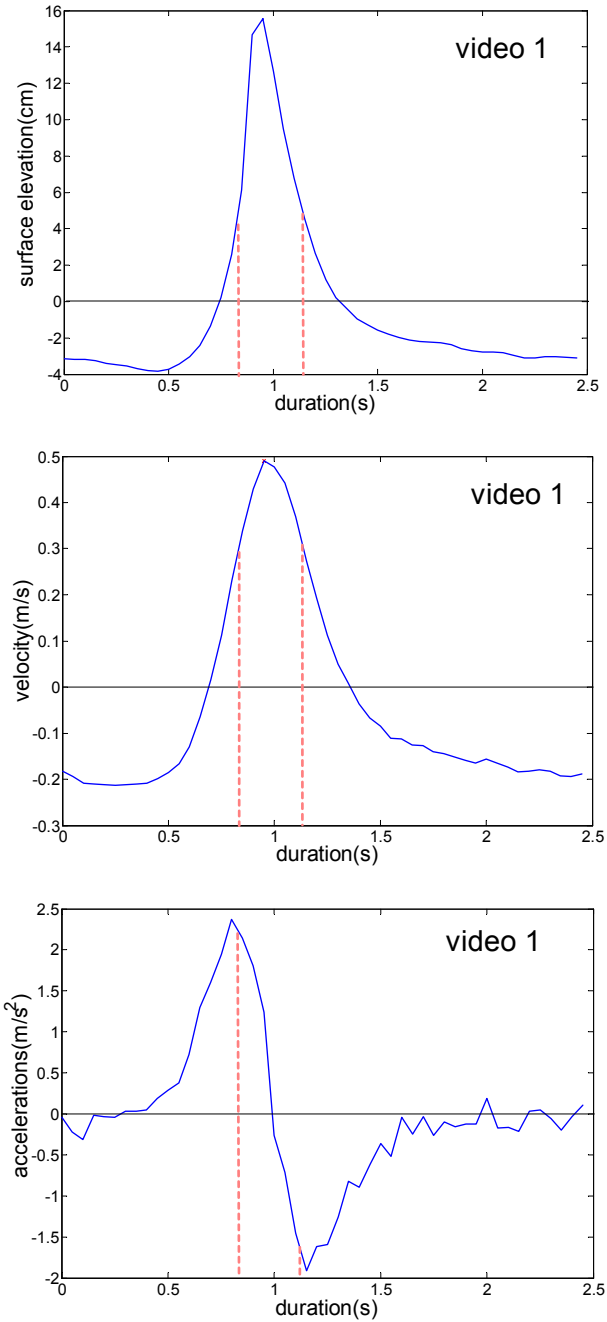


Figure 5.2-8 Graphical representation of the times at which stone movements starts and ends as a function of the surface elevation, the horizontal near-bed velocities and the accelerations for video 1.

From these graphical representations, it can be clearly seen that both the velocities and the accelerations have large positive values at the time a stones starts to move. The other videos showed the same.

5.2.5 Critical wave forces

In the previous section has been shown that video observations can be used to find the critical horizontal near-bed velocities and the critical accelerations. It also became clear that only four video observations were made for the tests carried out at an initial water depth of 55cm, while 78 different wave steepness and locations have been tested. It will be a waist of data to continue just with the four videos and reject the other data. So a different approach has to be found for analyzing the data.

The videos did prove that the forces, which are responsible for stone movement occur at the time interval between $t=0.00s$ and $t=0.15s$ before passage of the wave top. In order to use all data, it will therefore be assumed that the maximum force that occurs at this interval will be responsible for the movement of a stone.

For all 78 different locations and wave steepnesses the horizontal velocities and accelerations are known for every time step Δt (the sample rate of the EMS which is equal to 0.05s). These velocities and accelerations are therefore also known at the mentioned time interval. With use of these values it is possible to compute the instantaneous wave forces for every Δt at this interval. Later on the correctness of the assumption can be verified by checking whether the maximum of forces occurred at the same time as the time found with the four video observations.

The momentary maximum forces will be found with a Morison-like equation. This equation represents the wave forces as a function of the near-bed horizontal velocities and accelerations. A bulk coefficient C_B is used to represent all forces that are generated by the horizontal velocities and the coefficient C_M is used to represent all forces that are generated by the horizontal accelerations. The equation has the following form:

$$F = \frac{1}{2} C_B \rho A u |u| + C_M \rho V \frac{Du}{Dt} \quad (5.1)$$

From section 2.4 it became clear that the force required to move a stone from its initial position has to be greater then $F_g * \sin \varphi$. This value is also known as the critical value. So when movement of a stone occurs, the forces (in the direction of movement) found with the Morison-like equation have to be bigger then this critical value.

Previous sections already proved that it is plausible to believe that the threshold of motion is caused by a combination of accelerations and horizontal velocities. More evidence can be found by showing that only for a combination of acceleration forces and horizontal velocity forces there will be movement once a “critical” force is exceeded. This can be explained as follows.

If a combination of the accelerations and the horizontal velocities influences the threshold of motion then a critical force can be found with use of the correct values of the coefficient C_B and C_M . For forces smaller then this critical force no movement should occur and for larger forces there will be movement. If there is no relation between the threshold of motion and accelerations there will also be a critical force, but this force will then only depend on $1/2 C_B \rho A u |u|$.

On the contrary if only accelerations are responsible for movement the critical force will be an acceleration-generated force.

For the large stones 78 different wave steepnesses have been tested. For all these 78-tested wave steepnesses it is known whether movement did occur *always*, *sometimes* or *never* (see section 5.2.3). Also all the instantaneous velocities and accelerations are known. It also has been mentioned that in order to use all data it is assumed that the maximum wave force that occurs at the interval between $t=0.00s$ and $t=0.15s$ before passage of the wave top is responsible for the movement of a stone. In order to find this maximum force that is present for each of the 78 different wave steepnesses, a program has been written in Matlab. The program listing and information on the usage can be found in appendix E.

In the first plot the movement parameters (none, always or always) as found for the 78 different wave steepnesses have been plotted versus the maximal instantaneous velocity forces that were present for each wave steepness. In the second plot the same has been done only instead of the maximal velocity force the maximal acceleration force will be used. Finally in the third plot a combined force of both velocity forces and acceleration forces has been plotted versus the movement parameters.

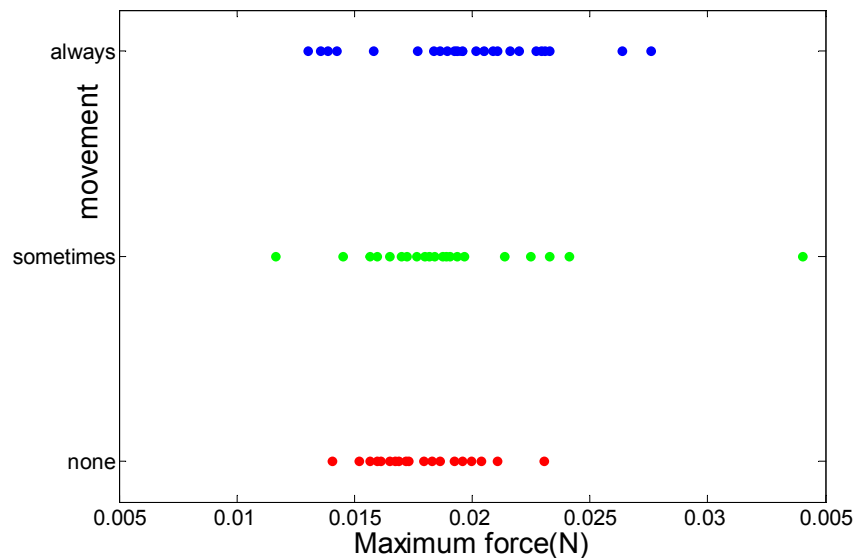


Figure 5.2-9 Movement parameter plotted versus the maximum momentary velocity forces that were present for the movement parameter in question ($F=1/2C_B\rho Au^2$).

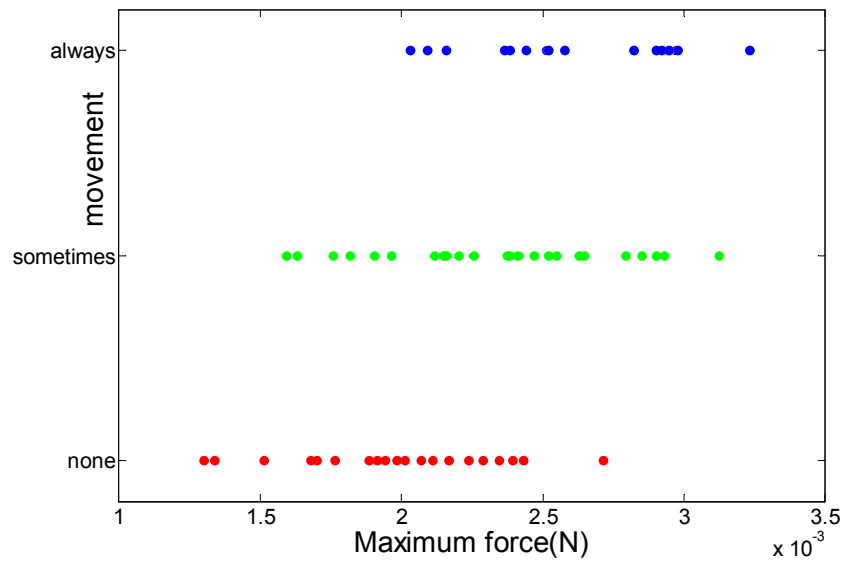


Figure 5.2-10 Movement plotted versus the maximum momentary acceleration of forces ($F=1/2C_M\rho V(du/dt)$), in which $C_M=1$.

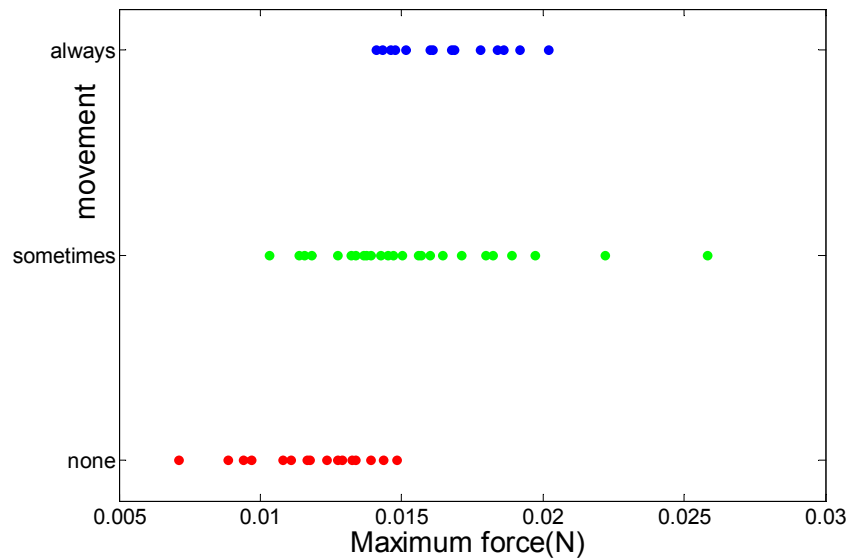


Figure 5.2-11 Movement plotted versus the maximum momentary combined velocity and acceleration forces ($F=1/2C_B\rho Au^2+1/2C_M\rho V(du/dt)$), in which $C_B=1$ and $C_M=1$.

The figure that shows the velocity-generated forces has absolutely no critical force that will lead to movement when exceeded. For all values of this force there can be movement or no movement. The figure that shows forces generated by the accelerations shows for low forces no movement of the stones and for large forces it shows movement. There is however a large overlap of forces that can result in both movement or in no movement. It appears that only for the combined acceleration and horizontal velocity forces a critical force can be found that gives a good distinction between movement and no movement. This proves that the threshold of motion is dependent of both the horizontal velocities and the accelerations.

For the tests performed with the small stones the same comparison can be made. Also for these tests it turns out that only for a combined force (generated by both horizontal velocities and accelerations) a critical force can be found that shows a clear distinction between movement and no movement.

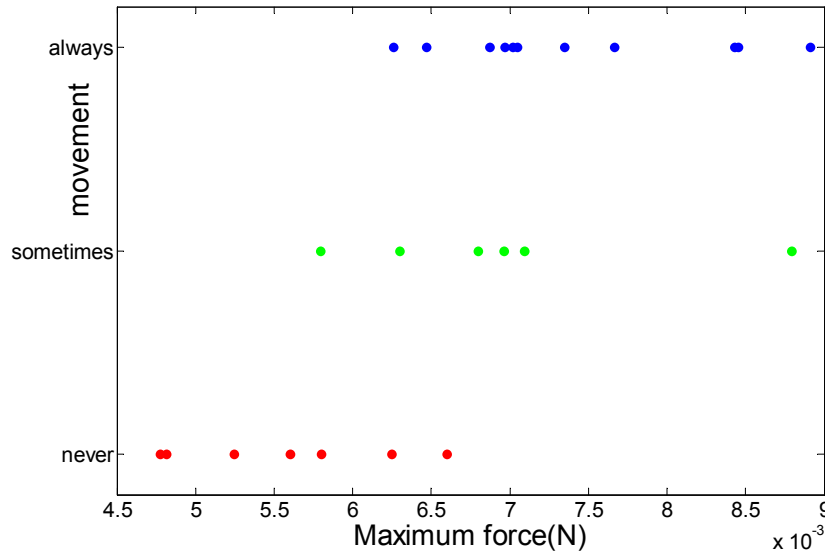


Figure 5.2-12 Plot that shows the maximum forces and the movement parameters as found for all tested wave steepnesses. Movement of small stones and forces found with $C_B=1$ and $C_M=1$.

5.2.6 Bulk coefficient C_B and acceleration coefficient C_M

It appears from the previous section that a Morison-like equation can be used to predict the stability of stones under wave motion. Yet before it can be used, the values of the coefficients C_B and C_M have to be determined. Values of the wave forces depend greatly on the ratio between these coefficients and on the values of these coefficients. This section will determine these coefficients.

The plots in Figure 5.2-13 to Figure 5.2-15 have been made in order to see the effects that different values of the coefficients C_B and C_M can have. In the plots the maximum instantaneous forces that were present during each of the tested wave steepnesses have been plotted versus the value of the movement parameter of the same wave steepness. The maximum instantaneous forces in the plots are found with the Morison-like equation.

$$F = \frac{1}{2} C_B \rho A u |u| + C_M \rho V \frac{Du}{Dt} \quad (5.2)$$

In the plots various values of C_B and C_M have been used. Figure 5.2-13 shows equal values for both C_M and C_B . In Figure 5.2-14 the influence of the velocity coefficient is assumed dominant and C_B is chosen larger than C_M . subsequently in Figure 5.2-15 the opposite has been done and the acceleration coefficient C_M has been chosen bigger than C_B .

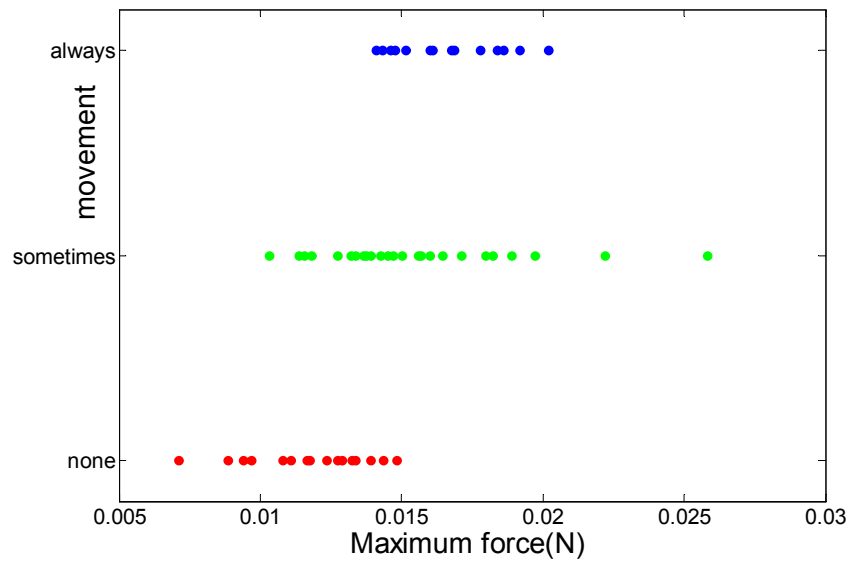


Figure 5.2-13 Plot that shows the maximum forces and the movement parameters as found for all tested wave steepness. The forces have been found with use of equation 5.2 in which $C_B=1$ and $C_M=1$.

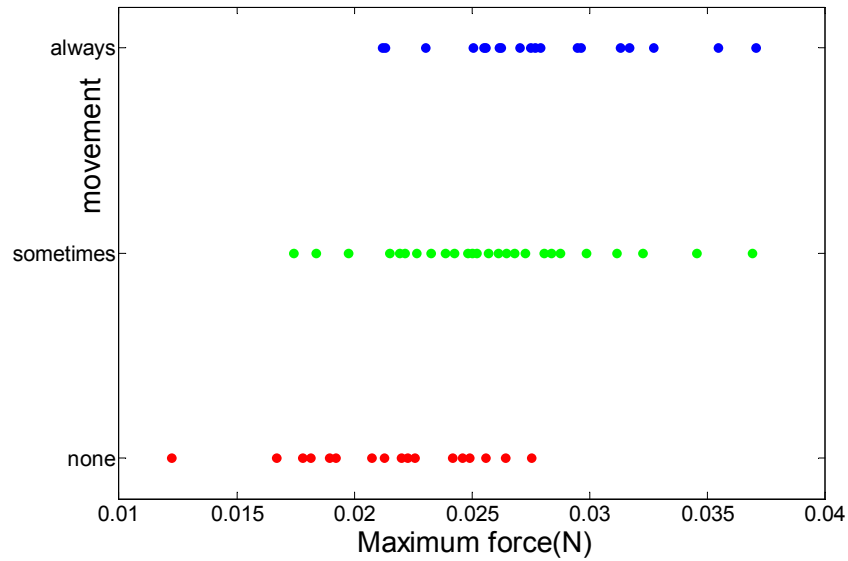


Figure 5.2-14 Plot that shows the maximum forces and the movement parameters as found for all tested wave steepness. The forces have been found with use of equation 5.2 in which $C_B=2$ and $C_M=1$.

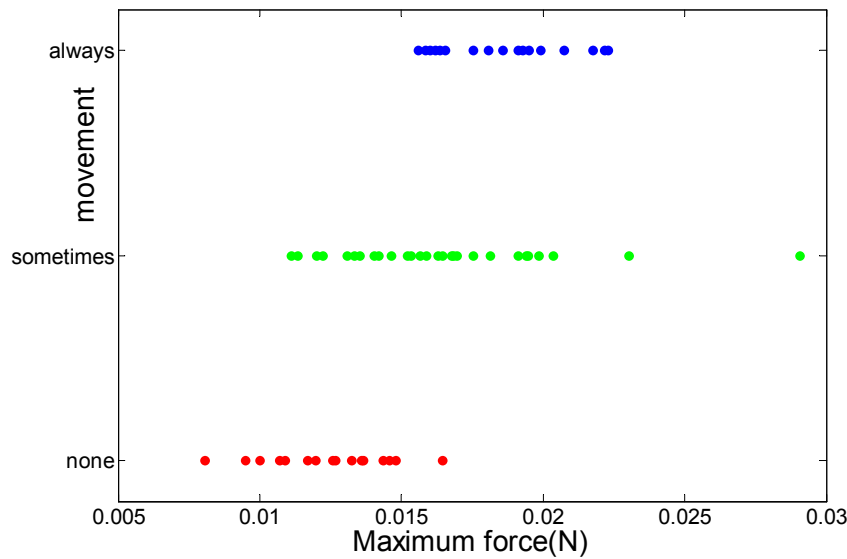


Figure 5.2-15 Plot that shows the maximum forces and the movement parameters as found for all tested wave steepness. The forces have been found with use of equation 5.2 in which $C_B=1$ and $C_M=2$.

It appears that a clear distinction between movement and no movement can no longer be seen when C_B is chosen larger then C_M . It also appears that the clearest distinction between movement and no movement can be seen when C_M is chosen larger then C_B . So apparently $C_B \leq C_M$.

The next step will be to determine exact values of the coefficients C_B and C_M . For this purpose the video observations will be used.

Usage of video observations

From the balance of forces as shown in section 2.4.4 can be seen that a stone will start to move once the wave forces exceed the value of the gravity force. It also has been shown that the balance of forces has to be considered in the direction of movement. So at the threshold of motion the following applies:

$$F_{(res,u^2)} + F_{acc} > F_g \sin \varphi \quad (5.3)$$

Note that the values of F_{u^2} and F_{acc} are the values of the acceleration forces and the values of the velocity forces in the direction of movement. The values of these forces will however be obtained from the horizontal accelerations and horizontal velocities. These horizontal velocity- and acceleration-generated forces do not all act in the same direction. In this thesis all adaptations that have to be made while dissolving the various forces will be processed in the bulk factors C_B and C_M . So all forces that are obtained with use of the Morison-like equation are assumed to work in the direction of movement.

As seen above the critical force that has to be exceeded before movement occurs, can be found with use of the gravity force. The video observations have been made for tests that have large stones as bed material. Therefore the gravity force (and the critical force) will be the same for all video observations. *Kirchner et al* (1990) showed that the direction of first movement, φ , is

between 30° and 45° with the horizon. Using this leads to values of the gravitational force in the direction of movement. These values vary between:

$$F_{crit} = F_g \sin \varphi = F_g \sin(30^\circ - 45^\circ) \approx 7.2 - 10.1 \cdot 10^{-3} N \quad (5.4)$$

As mentioned, horizontal velocities and accelerations generate the wave forces, which lead to the initial movement. The velocities and accelerations that are present at the initiation of movement will be referred to as the critical velocity and the critical accelerations. Values of these critical velocities and critical accelerations can be found with the use of video observations. Section 5.2.4 showed how to find the surface elevation, the near-bed horizontal velocity and the acceleration that were present at the time of initial movement. As each video has been made with different wave steepness, each video will show different values of the critical velocity and different values of the critical accelerations.

Video 1 and video 2 have both been shot in water with an initial depth of 55cm. As this thesis only deals with tests performed at this initial water depth these two videos will be used to find values for C_B and C_M . Both videos made observations of movement at a distance of 18.00m from the wave board and have an initial wave height of $H_0 = 15$ cm. Video 1 has a period of 2.5s and video 2 has a period of 2.25s.

Figure 5.2-16 shows the velocity profile and the critical velocities found for both videos.

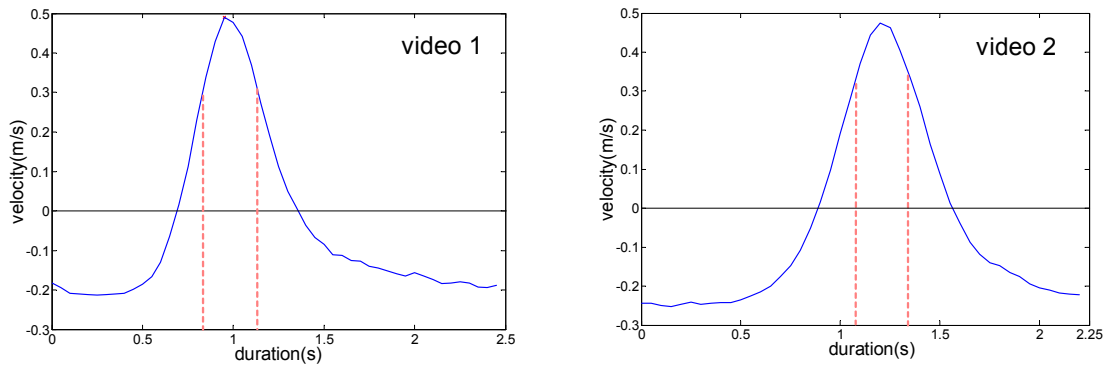


Figure 5.2-17 Velocity profile and in it the critical velocity for both video 1 and video 2.

It appears that the two videos have different critical velocities. The same plots have been made for the acceleration profiles and the critical accelerations as found for the two videos. This can be seen in Figure 5.2-17

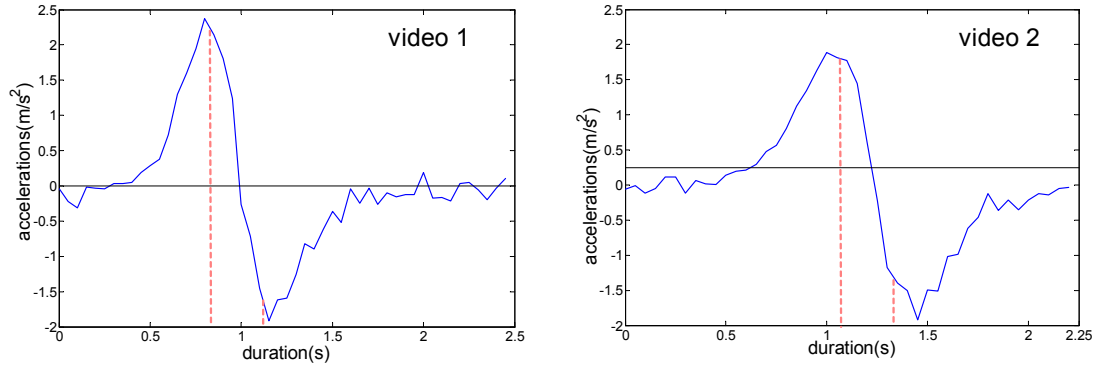


Figure 5.2-18 acceleration profile and in it the critical acceleration for both video 1 and video 2.

Also from Figure 5.2-19 it appears that different critical values are found for the two videos. The values of the critical horizontal velocities and accelerations as found for the 2 video observations are:

Video 1: Critical velocity = 0.3191m/s
Critical acceleration = 2.232m/s²

Video 2: Critical velocity = 0.389 m/s
Critical acceleration = 1.845 m/s²

The force that tries to keep the stones in place is constant for both videos. So by using the critical velocities and the critical acceleration in the Morison-like equation, two equations will be present and two unknown factors, C_B and C_M . And this can be solved. This will be shown.

The force required to move a stone from its initial position are known. See equation 5.4

The wave forces as described with a Morison-like equation. See equation 5.2

At the initiation of motion the following applies:

$$F_{crit} = F_u^2 + F_{acc} \quad (5.4)$$

So at the initial moment of movement the following applies:

$$\frac{1}{2} C_B \rho d^2 u_{crit,1}^2 + C_m \rho d^3 a_{crit,1} = \frac{1}{2} C_B \rho d^2 u_{crit,2}^2 + C_m \rho d^3 a_{crit,2} \quad (5.5)$$

Solving this equation gives the values for C_B and C_M .

$$C_B = 0.40 - 0.55$$

$$C_M = 2.67 - 3.75$$

These values of C_B and C_M are of the same dimension as values for C_B and C_M found in section 2.4.5. In appendix E a statistical method has been used to find the ratio of C_B/C_M that shows the smallest standard deviation error. Values of C_B/C_M that have a ratio between 0.20 and 0.10 show the smallest deviation. Also this is in the same dimension as the values that have been found with the video observations.

5.2.7 Results for using the Morison-like equation

As a final check, to see whether an instantaneous approach can be used, plots will be made that show the maximum forces and the movement parameters as found for all tested wave steepnesses. The value of the maximum forces will be obtained with use of the values of C_B and C_M as found with the video observations. If the critical force found for the plots is the same as the critical force found with use of the balance of forces, then the usage of the instantaneous approach seems justified. Figure 5.2-20 and Figure 5.2-21 show this for the large stones and Figure 5.2-22 and Figure 5.2-23 for the small stones.

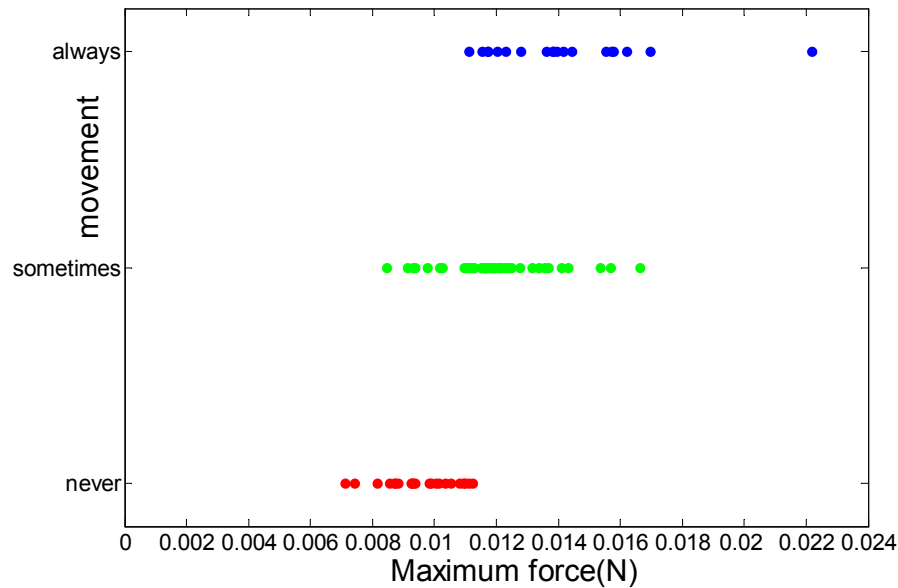


Figure 5.2-24 Plot that shows whether movement of large stones does occur for a certain maximum momentary wave force. The wave forces have been found with use of the Morison-like equation in which $C_B=0.55$ and $C_M=3.75$.

These values of C_B and C_M have been found for a critical force of $10.126 \cdot 10^{-3}$ N, which has been found for a direction of movement of 45° . In Figure 5.2-25 the critical force seems to be a little larger, but it is almost the same, so for this case usage of an instantaneous approach seems to be justified. The somewhat larger values found in Figure 5.2-26 can be do to scatter.

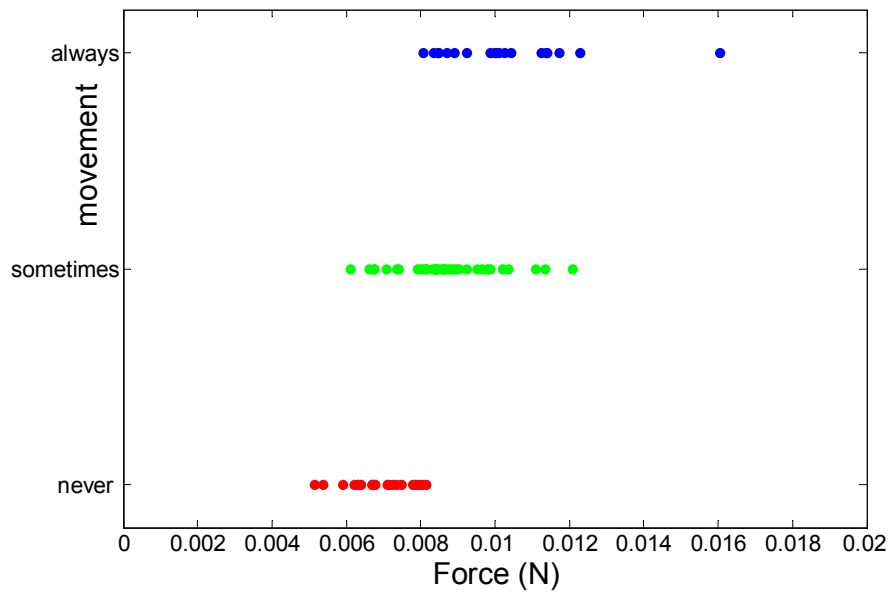


Figure 5.2-27 Plot that shows whether movement of large stones does occur for a certain maximum momentary wave force. The wave forces have been found with use of the Morison-like equation in which $C_B=0.4$ and $C_M=2.7$.

The critical force that has been used to find these values of C_B and C_M was equal to $7.2 \cdot 10^{-3}$ N. This is the value found with use of a direction of movement of 30° . The critical force as seen in the figure is almost the same.

Two definitions will be used to help finding the critical forces from Figure 5.2-28 and Figure 5.2-29. In the first definition the critical force is defined as the biggest force that leads to no movement.

The second definition of the critical force defines the critical force as the smallest force required to make a stone move.

Using the first criterion leads to critical forces of respectively $11.2 \cdot 10^{-3}$ N for Figure 5.2-30 and $8.1 \cdot 10^{-3}$ N for Figure 5.2-31. When the second criterion is used the critical forces have values of respectively $11.1 \cdot 10^{-3}$ N for Figure 5.2-32 and $8.0 \cdot 10^{-3}$ N for Figure 5.2-33. For each figure the values found with both the criterion are almost identical. This proves the existence of a critical force that leads to movement when exceeded.

For the tests performed with the small stones, no video observations are available. The critical forces will therefore be shown graphically with use of the values for C_B and C_M as found for the large stones.

Figure 5.2-34 and Figure 5.2-21 show these plots. Also for the small stones a clear distinction between movement and no movement can be seen. It is recommended to do more tests with other wave steepness, because these plots show very little data.

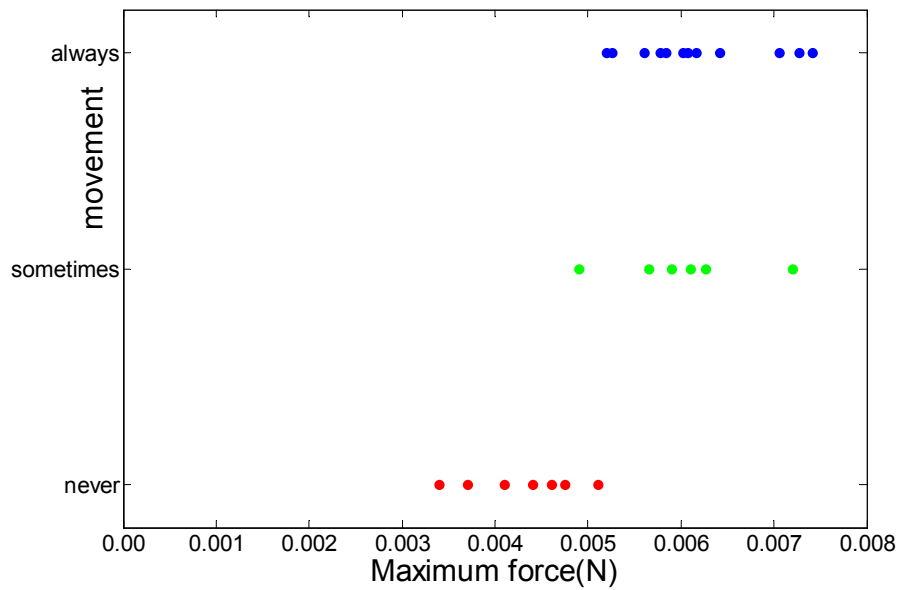


Figure 5.2-35 Plot that shows whether movement of stones did occur for a certain maximum momentary wave force. The wave forces have been found with use of the Morison-like equation in which $C_B=0.55$ and $C_M=3.75$. For small stones

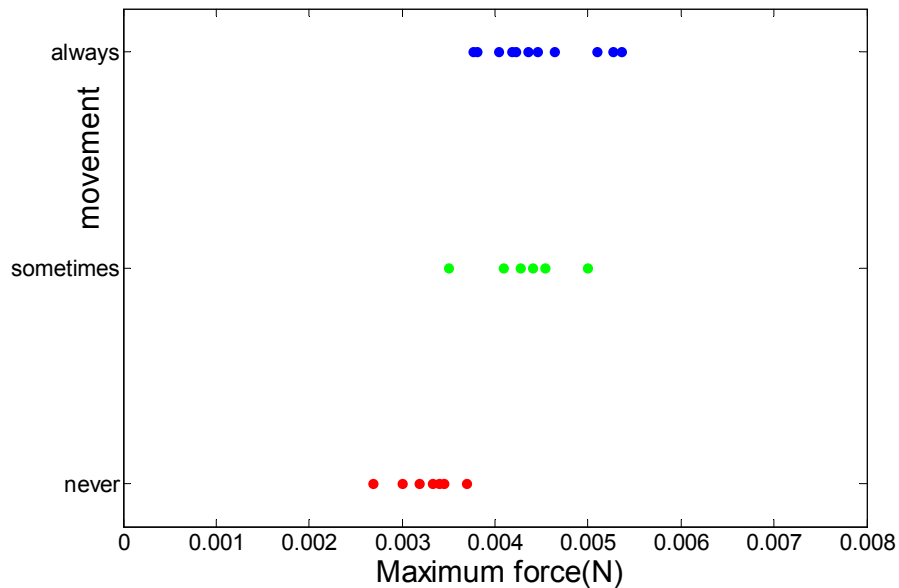


Figure 5.2-36 Plot that shows whether movement of stones did occur for a certain maximum momentary wave force. The wave forces have been found with use of the Morison-like equation in which $C_B=0.4$ and $C_M=2.7$. For small stones

Finally the differences between the critical forces found with the plots and with the balance of forces for

$C_B=0.4$ and $C_M=2.7$ are smaller then the same differences for of $C_B=0.55$ and $C_M=3.75$. This will probably imply that the direction of movement in the experiments was less then 45° .

5.3 Waveform approach

A second method that can be used to find the effect that fluid accelerations have on the threshold of motion is with use of a waveform approach. An advantage of a waveform approach is that it is easier to use. When a momentary approach is used, the instantaneous wave forces have to be known. These instantaneous wave forces can only be found by measuring or by analysis of the surface elevation. This requires skills and is time-consuming. So it would be more convenient to use an approach, which is dependent on the waveform. The existence of such a relation is subject of this section.

5.3.1.1 Maximum horizontal velocity and accelerations

It has been shown in the previous section that the maximum value of the horizontal velocities and the accelerations do never arise at the same moment. When using an instantaneous approach however, the values of the accelerations and the horizontal velocities that generate the maximum momentary force are mostly just a little bit smaller than the maximal values of these fluid motions (see section 5.2).

So maybe it is possible to see whether a relation can be found between the maximum values of acceleration, the maximum values of horizontal velocities and movement. Such a relation would be very convenient because with use of wave theory it is possible to find the maximum values of the horizontal near-bed velocities and accelerations. And then no momentary maximal forces have to be found when looking for stability.

For each tested wave steepness a statistical value of movement has been found in section 5.2.3. A classification was made between movement, sometimes movement and no movement. The same classification will be used in this section. In Figure 5.3-1 this movement parameter (of every tested wave steepness) of the small stones has been plotted against the maximum occurring velocities and maximum occurring accelerations. The same has been done in Figure 5.3-2 for tests performed with the large stones.

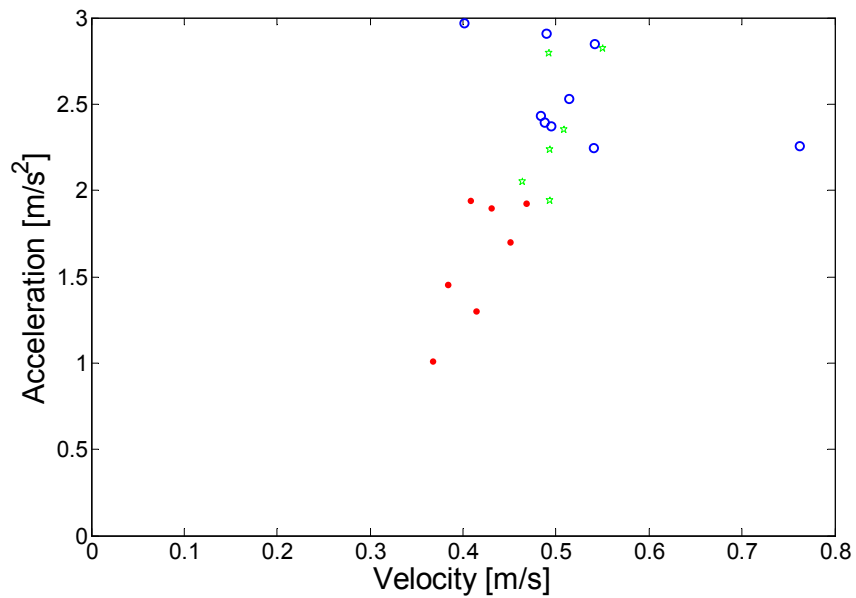


Figure 5.3-3 For each tested wave steepness with small stones, the movement has been plotted for maximal values of the near-bed velocities and maximum values of the acceleration

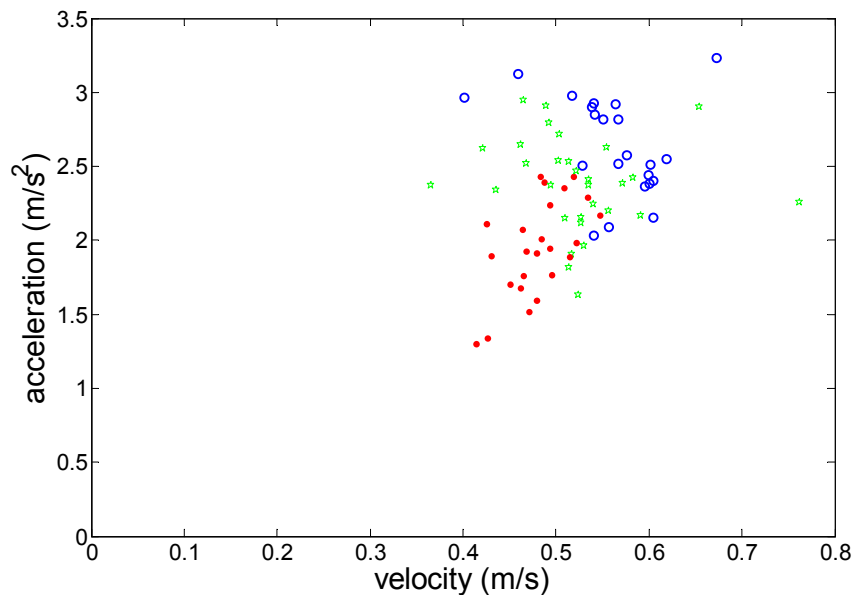


Figure 5.3-4 For each tested wave steepness with large stones, the movement has been plotted for the maximal values of the near-bed velocities and the maximum values of the acceleration.

When looking at Figure 5.3-5 it is hard to detect whether there is a horizontal or a diagonal dividing line between movement and no movement. And In Figure 5.3-6 it is hard to say whether the dividing line is diagonal or vertical. This implies that for the given tests there is not enough data to say whether this method can be used. So more tests have to be performed.

5.3.1.2 Wave peakedness

The shape of waves entering shallow water evolves from sinusoidal to peaky, with sharp wave crests and flat wave troughs. Water rapidly accelerates under these wave fronts generating strong horizontal pressure gradients. Some scientists (Elgar and Hoefel (2003), Drake and Calantoni (2001)), did already suggest that transport of sediments depend in some measure on these fluid accelerations in addition to fluid velocity.

Drake and Calantoni (2001) introduced as a parameter for the effects that accelerations have in peaked waves a dimensional form of acceleration skewness. They named it a_{spike}

$$a_{spike} = \frac{\langle a^3 \rangle}{\langle a^2 \rangle} \quad (5.6)$$

Where a is the time series of acceleration and angle brackets denote averaging. With use of a discrete particle model they found a critical value a_{crit} for a_{spike} that must be exceeded before accelerations enhance transport.

To see whether such a critical value of the acceleration skewness would also be applicable to find the threshold of motion, the a_{spike} of all tested wave steepnesses has been computed. The dimension of a_{spike} is m/s^2 . This is the same dimension as normal accelerations have.

As mentioned before, in previous sections a classification has been made between movement, sometimes movement and no movement for the stability of stones tested with various wave steepnesses. This classification has been referred to as the movement parameter and this classification was then used to show whether there was a relation between the threshold of motion and the forces acting upon them. The same will be done for a_{spike} .

In section 5.2 the instantaneous approach showed that the threshold of motion was dependent on a combination of both horizontal velocities and accelerations. Therefore besides the time averaged acceleration a_{spike} a time-averaged value of the velocity will be created. A good value for a time-averaged velocity is u_{rms} , so for every tested wave steepness also the u_{rms} has been computed.

As a first indication a plot will serve that shows for each wave steepness the movement parameter. This movement parameter will be plotted as a function of a_{spike} and u_{rms} . In Figure 5.3-7 this has been done for the large stones and in Figure 5.3-8 this has been done for the small stones.

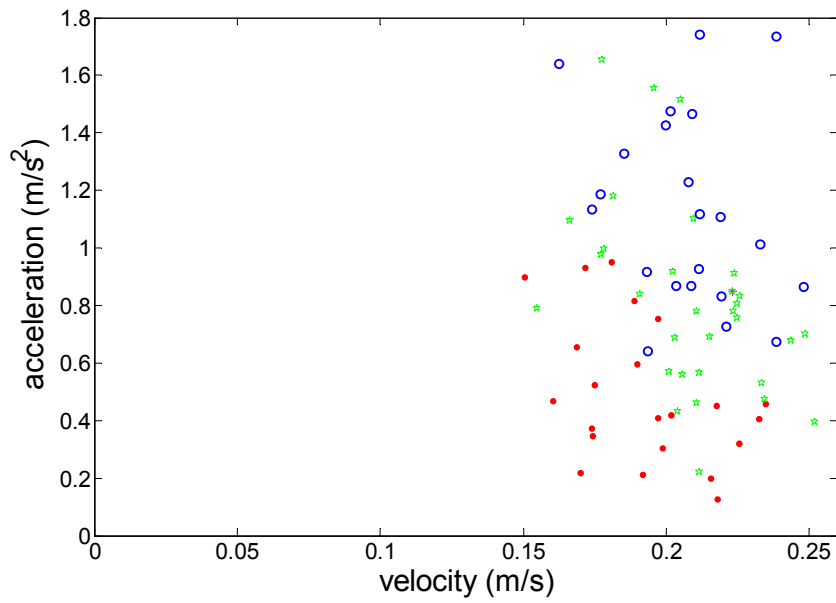


Figure 5.3-9 For each wave steepness as tested with large stones, the movement has been plotted for values of u_{rms} and maximum values of a_{spike}

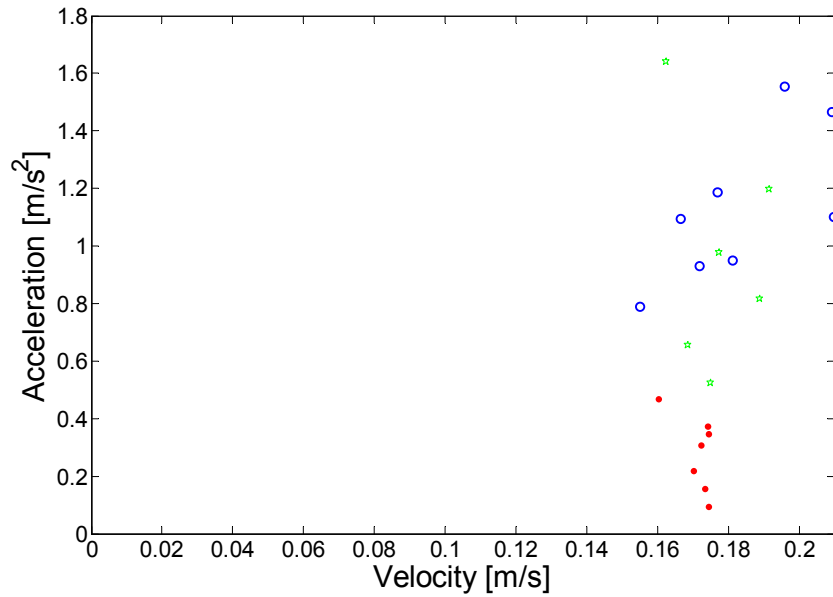


Figure 5.3-10 For each wave steepness as tested with small stones, the movement has been plotted for values of u_{rms} and maximum values of a_{spike} .

The plot that has been made with the data of the small stones shows a clear distinction between movement and no movement. yet it is to little data to draw conclusions from, because it is not clear whether the dividing line is horizontal or diagonal.

From Figure 5.3-11 and Figure 5.3-12 can be seen that there is a diagonal distinction line between movement and no movement. This implies that the threshold of motion is a combination of a_{spike} and u_{rms} . This is somehow what *Drake* and *Calantoni* discovered. As mentioned they found with use of computer modeling a critical value of a_{spike} that has to be exceeded before accelerations enhance transport. They also found that once this critical value was exceeded that transport became a combination of both velocities and accelerations.

Plotting the maximum occurring wave forces for all tested waves resulted in the previous sections in a critical force that made a clear distinction between movement and no movement. For a waveform approach this has also been tried.

For each wave steepness the values of a_{pspike} and u_{rms} have been processed in a Morison-like equation (see equation 5.2).

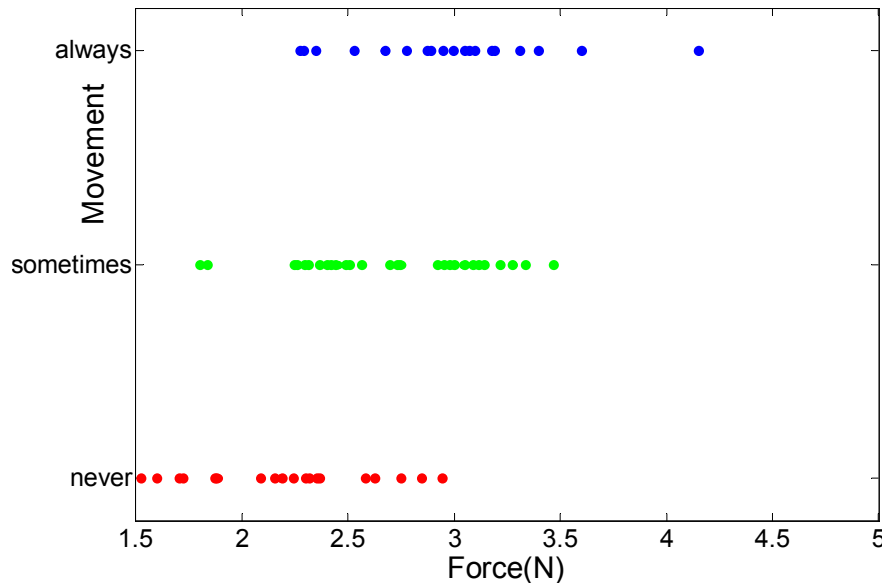


Figure 5.3-13 forces and movement found for u_{rms} and a_{spike}

In Figure 5.3-14 can be seen that there is not a critical force that leads to movement once exceeded. So this approach seems not to be valid

a_{spike} is a parameter that gives information on the skewness of the waves. But it also gives information about the magnitude of the present accelerations. For small waves that have little accelerations the values of a_{spike} will never become large. As the accelerations are derived from the velocity profile a_{spike} will therefore also give information about the magnitude of the velocities. Because a_{spike} gives information of both the skewness, the magnitude of accelerations and the magnitude of velocities there might be a relation between values of a_{spike} and the threshold of motion. So maybe there is a critical value of a_{spike} , which will lead to movement of a stone when exceeded. Whether such a critical value exists can be shown with use of following plots. In it the values of a_{spike} for all tested wave steepness have been plotted versus the movement parameter. This has been done for tests performed with the small stones and for tests performed with the big stones

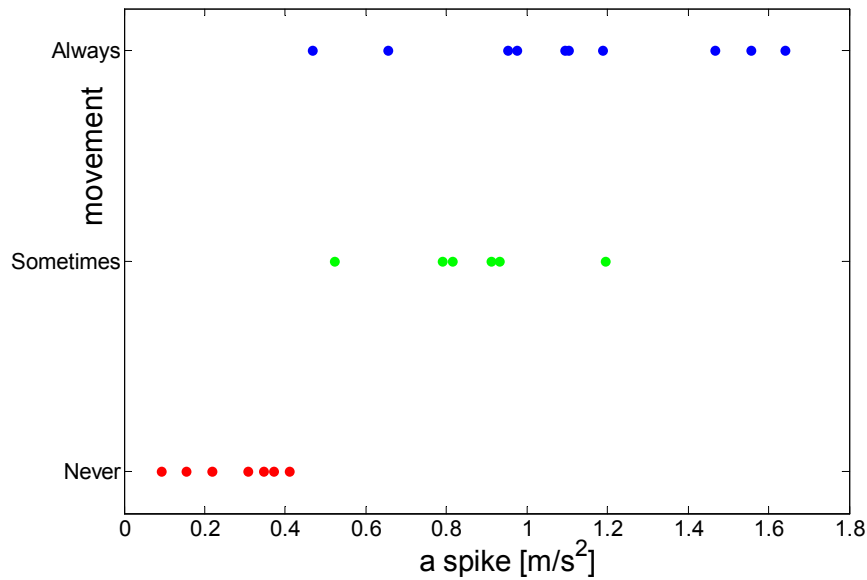


Figure 5.3-15 Movement plotted as a function of a_{spike} for tests performed with the small stones

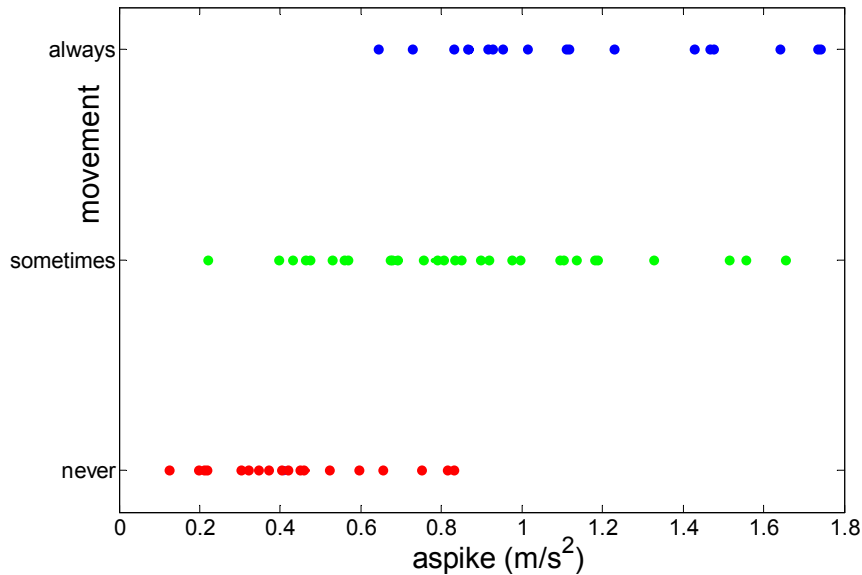


Figure 5.3-16 Movement plotted as a function of a_{spike} for tests performed with the large stones

It appears that there is indeed a value of a_{spike} that will always lead to movement of stones once exceeded. For the small stones this borderline is very easy to see. The bigger stones show some overlap.

A reason for this overlap is that some waves approach a sawtooth form before breaking. The values of a_{spike} will increase significant as the wave shape approaches this sawtooth form. Small waves that would not be able to move a stone from its initial position now also have large values for a_{spike} , due to this extreme skewness of the waves. And this results in the overlap.

In spite of this overlap the above figures show that the acceleration term becomes increasingly significant as the waves become more peaked. So this also proves that the threshold of motion is also influenced by accelerations.

5.4 Entrainment

Previous sections showed that accelerations do influence the threshold of motion. This is very useful to know when designing at locations where both fluid accelerations and horizontal fluid velocities are present. Such information however gives no information on how this new information can be used in future designs. In this section an attempt will be made to find a stability relation, in which both accelerations and velocities and a stability parameter are present, and which can be used to define the stability of objects.

5.4.1 Entrainment parameter

During the experiment it has not only been registered whether stones did move for various wave steepnesses. Also, the number of stones that moved has been registered, for each tested wave steepness.

This makes it possible to describe the number of moved stones as a function of the wave force that acts upon them. Making such a relation time-dependent will lead to an entrainment function. An advantage of having such a time-dependent function is that it's a statistical value and therefore the scatter will probably be reduced. For each different wave steepness many tests have been repeated, but they all showed different values. Making it time-dependent now will lead to an average value.

Entrainment can be defined as the number of stones that move per unit area per unit time:

$$E = \frac{n}{AT} \quad (5.7)$$

All parameters that are required for usage of this formula are available, so it is possible to find the entrainment of each tested wave steepness. The exact manner how this should be done can be found in appendix G.

For increased wave forces it is expected that the entrainment will also increase. Whether this happened during the experiments can be shown graphically. In Figure 5.4-1 for every tested wave steepness the entrainment has been plotted versus the maximum momentary wave force. This has been done for both the large stones and the small stones. The maximum forces have been found with a Morison-like equation as seen in section 5.2.7, in which $C_B=0.4$ and $C_M=2.7$.

Both stone diameters show that the entrainment will grow for larger values of the maximum wave force. Yet the scatter that both figures show is rather large (especially for the large stone sizes). The experimental character of the performed tests probably causes this. Performing more tests can find better statistical values and therefore reduce the amount of scatter.

As seen logarithmic values have been used for the y-axis. The cloud of points was very wide when using a linear axis. Using a logarithmic axis showed a better relation, so probably entrainment can be described as an exponential function of the wave force.

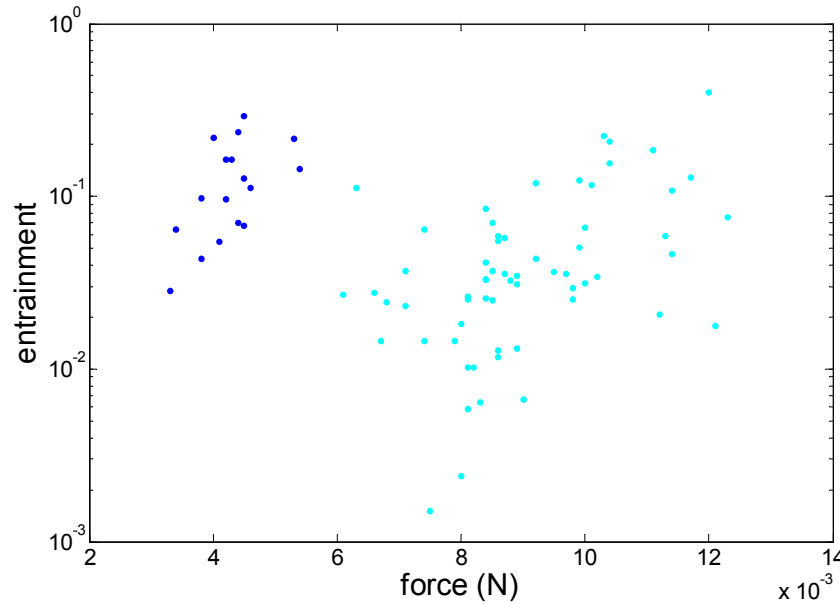


Figure 5.4-2 Entrainment as a function of the maximum wave force for all tests performed with the large stones (the light-colored points) and tests performed with the small stones (dark-colored points)

It occurs that the range of entrainment is similar for both tested stone diameters. The range of the forces are however not equal.

Causes for these differences between the forces are the following:

- The gravity force is the force, which tries to keep the stones in place. The value of the gravity force depends on the weight of a stone. If stones are used with the same density, the stones with a smaller diameter have less weight than stones with a larger diameter.. So smaller forces are required to move the stones with a small diameter. And bigger forces are required to move stones with a larger diameter.
- The forces are found with a Morison-like equation that makes use of the surface area and the volume of the used stones. So this will also lead to different forces for stones of various diameters when using velocities and accelerations of similar magnitude.

When designing for stability, Figure 5.4-3 can be used to find values of expected entrainment for different values of acting wave forces. Yet a problem arises, because this graph can only be used for the two tested stone diameters. A designer wants to have this information for many more stone diameters. To make an entrainment graph for every existing stone diameter is not an option. So the next step is to find an entrainment parameter, which is independent of the stone diameter.

5.4.2 Dimensionless parameters

As seen in the previous chapter it can be very useful to describe entrainment as a function of the wave forces. It will be even more useful if such a relation can be found that is independent of the stone diameter.

Both the wave forces and the entrainment parameter as used in Figure 5.4-4 make use of the stone diameter d . The entrainment parameter does this because the numbers of moved stones for each wave steepness are only valid for the tested stone diameter. And the wave forces from Figure

5.4-5 are dependent on the stone diameter, because they are found with use of the Morison-like equation (see section 5.2.7), which uses the stone diameter as a parameter.

However, the stone diameter is not the only parameter that is used in above parameters. The entrainment parameter and the wave forces are also dependent on the density of the stones, on the fluid density and other parameters. It will be ideal to find a relation that is valid for all purposes. Making relations dimensionless can do this.

So both the entrainment parameter and the force parameter from Figure 5.4-6 have to be made dimensionless.

There are multiple manners that can make both parameters dimensionless. It is therefore necessary that it will be done with the use of parameters that are relevant. The goal of a dimensionless relation between entrainment and wave forces is to find the amount of stones (or other materials) that will move for a certain wave force. This amount of moving stones will depend greatly on the:

- Stone diameter
- Density of water
- Density of stones
- Wave forces

Processing these 4 parameters into a dimensionless entrainment relation makes it possible to use one graph for different values of these parameters. As the wave force-parameter is already used on the x-axis, the other three parameters will be used to make the relation dimensionless. When this is done properly the relation can also be used to find entrainment in i.e. seawater or for plastic structures placed on the seabed.

The force parameter will be made dimensionless by dividing it through $\rho \Delta g d^3$. So the dimensionless parameter \tilde{F} is:

$$\tilde{F} = \frac{\frac{1}{2} C_B \rho d^2 u^2 + C_M \rho d^3 a}{\rho \Delta g d^3} \quad (5.8)$$

The entrainment parameter will be made dimensionless by:

$$\tilde{E} = E d^2 \sqrt{\frac{d}{g}} \quad (5.9)$$

With use of these dimensionless parameters it is now possible to plot the entrainment of both the small stones and the large stones in one figure. This is done in Figure 5.4-7 for the dimensionless parameters as found above. Again the clearest results were obtained when using linear x-axis and logarithmic y-axis.

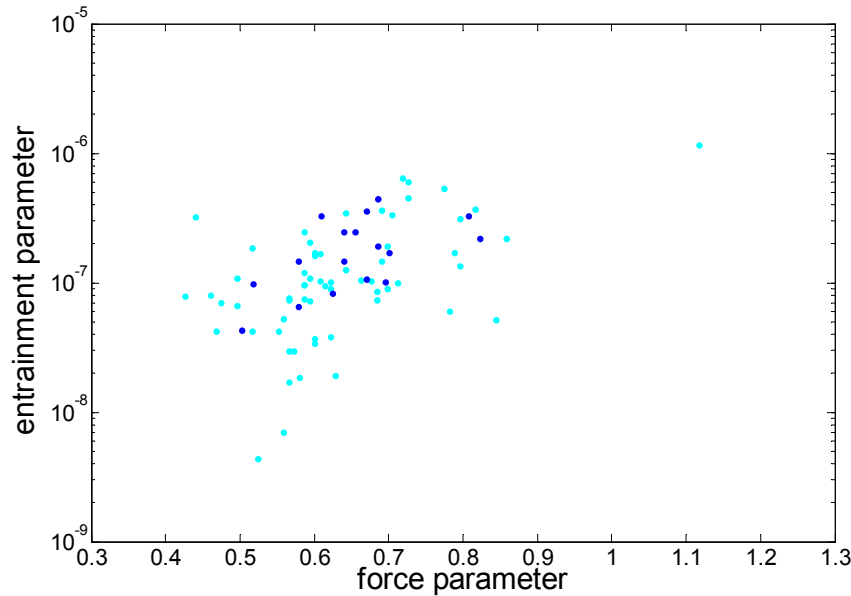


Figure 5.4-8 Plot that shows for all tested wave steepnesses the relation between the dimensionless entrainment parameter and the force parameters. The dark points are the tests carried out with the small stones. The light-colored points are found for the tests carried out with the large stones.

From the points in Figure 5.4-9 can be seen that an increase of the force parameter leads for both the stone diameters towards more entrainment. It can also be seen that this relation is the same for the small stones and for the large stones. This means that the parameters have been made dimensionless correctly. Also other ways have been used to create dimensionless parameters, but they never lead to an equal range of force and entrainment for both the small stones and the large stones.

There is however a large amount of scatter in the diagram. Reasons for this scatter can be: The experimental character of the tests. Experimental tests always show more scatter than numerical or analytical tests.

- To little data. To get better statistical data, all tests have to be repeated lots of times. Some data that has been used in the diagram was found as an average of only 3 tests.
- Number and placement of stones. Not always the same amount of stones was available for entrainment. For some tests a lot of stones already moved during the water-working time., while in other tests hardly any stones left during the water working.
- Combination of flow time and increase of wave steepness during a test. For every wave steepness the number of stones that moved have been registered after 50 and after 100 waves. The increase of wave steepness has not been uniform for all tests. It showed that for a large increase of wave steepness in a test the majority of stones did move during the first 50 waves. For small increases the amount of moved stones was the same over the first 50 and the second 50 waves. As entrainment is time-dependent other results would have been found when using wave steepness for a longer or shorter time. Also other results would have been found when using different steps of increase of wave steepness.

It is obvious that much extra research is required in order to find an entrainment parameter that is dependent on the wave forces.

5.5 Evaluation

Two different approaches have been used to predict the stability of stones, which are subject to wave forces. In section 5.2 an instantaneous approach has been used and in section 5.3 a waveform approach. Due to lack of time it was only possible to do profound research for the instantaneous approach.

Using an instantaneous approach leads to very satisfying results. With use of video monitoring it turned out that the stones started to move somewhere between 0.15s and 0.05s before passage of the wave top. This interval also happened to be the interval at which the velocities and accelerations have large values in the direction of the wave propagation. Using these velocities and accelerations in a Morison-like equation did proof that the threshold of motion is dependent on both the horizontal near-bed velocities and the accelerations.

A disadvantage of an instantaneous approach is that these instantaneous wave forces can only be found by using measurements of the horizontal velocities or by analysis of the surface elevation. Movement is considered to take place once the wave forces exceed the value of the gravity forces that try to keep the stone in place. So to know whether a stone starts to move, the wave forces have to be known at every momentary time. Once the velocity and the acceleration profiles are known, a wave force profile has to be constructed, to see at what intervals these forces exceed the gravitational forces. This is very time-consuming work and requires some skills. Another disadvantage is that the acceleration profiles are very steep at the intervals during which a stone starts to move. Therefore a very high measuring resolution is required; otherwise it will be impossible to determine the momentary accelerations accurately. A last disadvantage is that using momentary values doesn't give a lot of information about the present waves. A better method would be for instance to find a relation between the threshold of motion and wave steepness and water depth, because such a relation can be used by anyone and doesn't require special measurements.

The second used approach was by means of a waveform approach. Such an approach would be easier to use and has no problems of finding the exact momentary forces. Due to insufficient time however only little research could be done for this approach. Nonetheless, also with use of this approach it was possible to show that the threshold of motion depends in some measure on fluid accelerations in addition to fluid velocities. Furthermore it has been shown that the acceleration term becomes increasingly significant as the wave becomes more peaked.

Finally an attempt has been made to find a stability relation, in which both accelerations and velocities are present. A dimensionless entrainment parameter and force parameter have been designed, in order to use this relation for various stone sizes. The relation does show an increase of entrainment when the wave forces are enlarged, but there is still a lot of scatter in the diagram. Repeating the tests can find better statistical values and will certainly reduce the amount of scatter. Furthermore tests have to be performed with different stone densities and stone sizes to see whether they also show the same relation. And to see if their dimensionless form is in the same range.

6 Conclusions and recommendations

In this chapter the general conclusions and recommendations regarding the influence of accelerations on the threshold of motion will be reviewed. Technical remarks are not mentioned, they can be found in the relevant chapters.

6.1 Conclusions

It appears that both the fluid accelerations and the fluid velocities influence the threshold of motion. This has been shown for two different approaches. The most important findings and conclusions of these two approaches are reviewed. Furthermore an attempt has been made to create a dimensionless entrainment parameter that can be used to describe the entrainment as a function of the wave forces. Also the conclusions that can be drawn for that research are shown.

6.1.1.1 Instantaneous approach

- Just before passage of the wave top the fluid velocities and the fluid accelerations both have large values in the direction of the wave propagation
- Creating many scenarios of different velocities and accelerations shows that the initial movement of stones is caused by a combination of both.
- Grains start to move at 0.08s to 0.12s before passage of the wave top.
- Describing the wave forces with a Morison-like equation gives satisfying results.
- In this equation a bulk coefficient C_B has to be used to represent all forces that are generated by the horizontal velocities and a coefficient C_M must be used to represent all forces that are generated by the horizontal accelerations.
- For each stone diameter there is a critical force. If the wave forces exceed this force then the stone will start to move. If the wave forces remain smaller then this critical force then the stone will not move.

6.1.1.2 Waveform approach

- Describing the waveform with a_{spike} and u_{rms} can be used to find the threshold of motion.
- The threshold of motion is dependent on combinations of a_{spike} and u_{rms} .
- For every stone diameter there is a critical value of a_{spike} that will lead to movement of a stone once exceeded.
- The acceleration term becomes increasingly significant as the waves become more peaked.

6.1.1.3 Entrainment

- An increase of the wave force leads to larger values of entrainment
- This increase behavior is the same for different stone diameters.

6.2 Recommendations

In this section general recommendations will be given that will improve the results when performing a similar test. Also further studies that will give more insight in the matter will be recommended. Again the technical remarks are not mentioned, they can be found in the relevant sections.

- More tests have to be performed. This must be done in order to improve the statistical values used during the experiments.
- Also the tests performed at the initial water depths of 60 and 65 cm have to be analyzed. But before this can be done proper velocity measurements have to be taken for those water depths.
- A more profound research is required for the waveform approach. It appears that sharp wave crests generate strong horizontal pressure gradients. Describing the threshold of motion as a relation of the wave peakedness seems therefore a good option.
- When using an instantaneous approach more video images have to be made. They are very useful to detect the initial point of movement.
- Also video images have to be taken for different stone sizes.
- The water working time has to be enlarged. This will reduce the amount of stones that are in a unfavorable position during the tests.
- Only small increases of wave steepness must be used during the tests and the flow time of each wave steepness has to be increased. A flow time of one hour would be more appropriate.
Doing so makes leads to more uniform results.
- Tests have to be performed with stones that have a larger and with stones that have a much smaller density. This makes it possible to improve a dimensionless entrainment relation that can be used for designing.
- Velocity measurements have to be taken with laser Doppler or with PIV. These devices are more accurate. And it enables the user to find the velocities and accelerations much nearer to the stones.
- The sampling rate must be increased. During the experiments only every 0.05s a measurement has been taken. Just before the wave top the acceleration profile is very steep and therefore the used sampling rate of 20Hz was not able to find the exact values in this area.
- As a test concerning the waveform approach an irregular wave spectrum can be used. If this is done in combination with video monitoring it is possible to find more effects on movement and the presence of a waveform.
- Placing a constriction in a uniform current can also create an accelerating flow. By using different types of constrictions it is also possible to find the influence that accelerations have on the threshold of motion. Results from such tests can be compared to results from this experiment. Similarities between the results will also provide more understanding.
- A lot of data has been collected for the instantaneous approach. Maybe it is possible to work from this instantaneous approach towards an waveform approach.

7 References

ASCE, 2000. *Manual on hydraulic Modeling*. Reston, Virginia: American Society of Civil Engineers

BATTJES, J.A., 1991. *College manual CTWA 4320 Korte Golven*. Delft: Delft Faculty of civil engineering

BATTJES, J.A., 1993. *College manual CT2100 Fluid Mechanics*. Delft: Delft Faculty of civil engineering

CUR REPORT 169, 1995. *Manual on the use of Rock in Hydraulic Engineering*. Gouda: CUR.

HUGHES, G.J., 1993, *Physical models and laboratory techniques in coastal engineering*, World scientific publishing Co Pte ltd, River East, USA

DEAN & DALRYMPLE, 1991. *Water wave mechanics for scientists and engineers*. Singapore: Words scientific

SCHIERECK, G.J., 2001. *Introduction to Bed, bank and shore protection*. Delft: Delft University Press

VELDE, VAN DER, 2000. *College manual CT5309 Coastal Engineering*. Delft: Faculty of civil engineering

Articles:

CALANTONI AND DRAKE, september 2001. *Discrete particle mode for sheet flow sediment transport in the nearshore*. Journal of geophysical research. Vol 106. No C9 pages 19,859-19,868

ELGAR AND HOEFEL, march 2003. *Wave induced sediment transport and bar migration* Science. Vol 299. No C9 21 march 2003

HOFLAND.B., BATTJES J.A., BOOIJ R, to be published 2004. *Measurement of fluctuating pressures on coarse bed material*

KIRCHNER J.W., DITTRICH W.E., IKEDA H. AND ISEYA F., march 2003. *The variability of critical shear stress, friction angle, and grain-protrusion in water-worked sediments*. Sedimentology 647, 672

STIVE AND RENIERS, march 2001. *Sandbars in motion*. Science. Vol 299. 21 march 2003.

Internet:

November12, <http://physics.tamuk.edu/~suson/html/4323/super.htm>

January 16, <http://www.unc.edu/~rowlett/units/siderive.html>

TABLE OF CONTENTS	
APPENDIX A	III
SIGNAL AND DATA PROCESSING FOR EMS AND WAVE GAUGES	III
A.1 INTRODUCTION	III
A.2 DATA TRANSMISSION SYSTEMS	III
A.2.1 Linear (ideal) systems	iii
A.2.2 Real systems	iv
A.2.3 High pass filter behavior	iv
A.3 THEORY	V
A.4 HARMO	VIII
A.5 DATA PROCESSING FROM WAVE GAUGES	IX
A.6 ANALYZING EMS DATA	XII
A.6.1 Harmonical components	xii
A.6.2 Influence of the harmonically velocity components on complex velocity signal	xii
A.6.3 Quality of output data	xiv
A.7 UNDERESTIMATION OF EMS VELOCITIES	XVII
A.8 RECONSTRUCTION OF TRANSMITTED EMS SIGNAL	XX
A.9 FREQUENCY DEPENDENT TIME-DELAY	XXV
APPENDIX B	XXVII
PARAMETERS	XXVII
B.1 INTRODUCTION	XXVII
B.2 VARIABLE PARAMETERS	XXVII
B.3 CONSTANT PARAMETERS	XXVIII
APPENDIX C	XXX
APPENDIX D	XXXI
SIEVE CURVES	XXXI
APPENDIX E	XXXII
M-FILES AND LIST USED DURING THE EXPERIMENTS	XXXII
1.1 M-FILES	XXXII
1.2 LISTS USED DURING TESTS	XXXV
APPENDIX F	XXXVII
LARGE PLOTS OF STONE MOVEMENT FROM CHAPTER 5	XXXVII
APPENDIX G	XLIII
FLOW TIME ENTRAINMENT	XLIII
APPENDIX H	XLV
DETAILED WAVE ANALYSIS	XLV
H.1 INTRODUCTION	XLV
H.1 SHOALING	XLV
H.1.1 Breaking point of the waves	xlvi
H.2 REFLECTION	XLVII
H.3 VALIDATION OF EMS DATA	XLIX
H.3.1 RF wave	xliv

H.3.2	<i>Comparison between measured values and RF-wave</i>	<i>l</i>
H.3.3	<i>Final verifications</i>	<i>liv</i>
H.3.4	<i>Concluding</i>	<i>liv</i>
H.4	VELOCITY ANALYSIS	LV
H.4.1	<i>Validation of near-bed velocities</i>	<i>lvi</i>
H.4.2	<i>Behavior of near-bed velocities and phase lag</i>	<i>lvii</i>
H.4.3	<i>Phase shifts</i>	<i>lviii</i>
H.5	ACCELERATIONS	LXI
H.6	PROPORTIONALITY OF WAVE PROFILE TO HORIZONTAL VELOCITY PROFILE	LXIII

Appendix A

Signal and data processing for EMS and wave gauges

Horizontal velocity measurements are often carried out with use of an EMS. This EMS makes use of electro magnetic fields in flowing water. It is very difficult to check whether the measurements performed with an EMS are correct. For changing flows, like an orbital wave motion, this is almost impossible. Therefore as guidance to check the validity of EMS data, this manual has been written.

EMS measurements are often performed in addition to wave gauge measurements. As there are a lot of parallels in the signal processing of the wave gauges they will be discussed as well.

The data that are used are obtained from an experiment that used a malfunctioning EMS.

A.1 Introduction

Every continuous periodic function can be represented as an infinite sum of harmonic signals with differing angular frequencies ω_0 , whose amplitudes c_n , and phases φ , may also differ, but not necessarily. In the experiment the waves can be represented by an infinite sum of harmonic components of water surface elevations and the corresponding velocities under the waves can be made out of an infinite sum of harmonic components of wave velocities.

The velocities measured with an EMS are transformed with use of a signal conditioner devise [see appendix XX] into output signals. During this transmission of input to output signals the amplitude and the phase of the signal can change. Why and how this will be done is explained in the following sections as well as how the original input data can be reconstructed out of the output signal. The information in the following sections is partly obtained from Internet. [See Internet <http:///>].

A.2 Data transmission systems

A.2.1 Linear (ideal) systems

Digital measuring systems contain a measuring devise and a signal conditioner. The measuring devise sends the signals to the signal conditioner and this conditioner adapts the measured signals for usage. If the signal conditioner changes the amplitude of all harmonic input systems in the same manner independently of the frequency and if all signals undergo the same phase shift then we are dealing with a linear system. These linear systems fulfill the condition of linearity and therefore the transmission can change the amplitude and the phase of the signal but not the form. This means that the output factor is only amplified by a constant factor compared to the input signal. So by knowing this conversion factor the actual input signals can be reconstructed from the output signals and vice versa.

A.2.2 Real systems

These systems depend on the frequency (or the period) of the harmonic input systems. For every different frequency of the harmonic components of the input signal, different amplifications of the amplitude $C(\omega_n)$ and different phase shifts $\Delta\varphi(\omega_n)$ occur. This leads to a distortion in the output signal compared to the input signal. Now not only the amplitudes and the phases will change, but also the form of the input will change while transmitting the signal to an output signal.

$C(\omega_n)$ is the amplitude transfer function or the frequency response and $\Delta\varphi(\omega_n)$ is the phase transfer function of the system. Together both functions describe the frequency behavior of a real system.

When this frequency behavior of the used instruments is known it is possible to reconstruct the actual input data out of the output data for any given periodic signal. From the harmonic components that form the signal and from $C(\omega_n)$ and $\Delta\varphi(\omega_n)$ the original signal can then be reconstructed.

The frequency behavior is described in manuals of the used instruments. It is important to check the validity of these graphs with use of measurements.

A.2.3 High pass filter behavior

The purpose for this frequency behavior is to filter out disturbances. This is also known as high-pass filtering. These disturbances are mostly high frequent (have a small period) and have small amplitudes. In general the frequencies of these disturbances are much higher then the working range for these instruments. The basic idea is now that the low frequent amplitude regime (the working range of the instruments) has good transmission properties, because in this area the harmonic signals are amplified independent of the frequency by a constant factor. Outside this regime (the high frequent regime), the harmonic signals undergo a frequency dependent damping, which inevitably leads to a signal distortion.

A graph that shows this frequency behavior of an EMS is shown in Figure A-11. Three parameters that are susceptible to filtering are represented in the graph. These parameters are time-delay, phase shifts and amplification factors for the amplitude. The exact usage of the graphs will be discussed in the following sections.

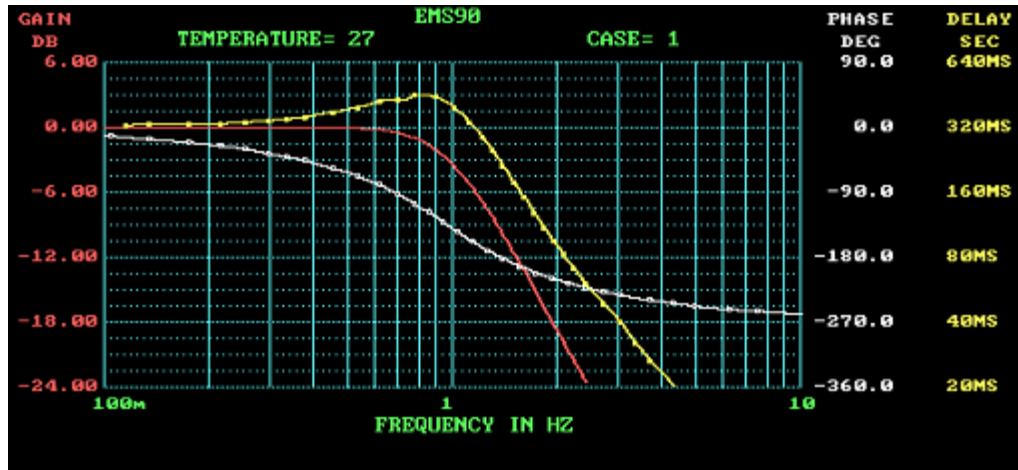


Figure A-1 frequency behavior of EMS10

A big disadvantage of this damping of high frequent harmonics arises when also the higher harmonics determine the shape of the complex waveform, i.e. shallow water waves. The amplitude of these higher order harmonics will now be damped and a distorted wave signal will be seen in the output data. In the worst case the higher harmonics will be reduced to zero and data will get lost. In this case it is impossible to reconstruct the actual velocity and the collected data will be useless. This will of course only be of significance when the high frequent higher order components have a big influence in the periodic, actual wave signal.

A.3 Theory

Harmonic analysis studies the representation of functions or signals as superposition of basic waves. To find the basic signals or functions a Fourier transform will be performed on the complex signal. Following the Fourier theorem, every periodic function $f(t)$ with period T can be represented as an infinite sum of harmonic functions. The individual terms of the infinite series are simple sine and cosine functions of t , with each term containing a distinct frequency in its argument. The sum of the infinite Fourier series form the original complex function $f(t)$. The Fourier series is given by:

$$f(t) = c_0 + \sum_{n=1}^{\infty} (a_n \cos n\omega_0 t + b_n \sin n\omega_0 t) \quad (\text{A.1})$$

In which

$f(t)$ = periodic function

C_0 = DC component (average of the function $f(t)$) also known as the offset.

a_n, b_n = Fourier constants

ω_0 = basic frequency

Determining the values of the Fourier constants is the subject of the Fourier analysis.

The representation of the Fourier series can be simplified by using the following relationships.

$$a_n \cos n\omega_0 t + b_n \sin n\omega_0 t = c_n \sin(n\omega_0 t + \varphi_n) \quad (\text{A.2})$$

with $c_n = \sqrt{a_n^2 + b_n^2}$ (A.4)

and $\varphi_n = \arctan\left(\frac{a_n}{b_n}\right)$ (A.5)

With this Eq(..) can be written in the following form:

$$f(t) = c_0 + \sum_{n=1}^{\infty} c_n \sin(n\omega_0 t + \varphi_n) \quad (\text{A.6})$$

In which $f(t)$ = periodic function
 C_0 = DC component (average of the function $f(t)$) also known as the offset.

c_n = amplitude spectrum
 ω_0 = basic frequency

The following example (Figure A-2) shows how a complex periodic signal can be split up into easy describable harmonic components. The complex waveform here is a rather simple example because only 2 sine waves have been added up. In reality for complex waveforms, tens of harmonical components determine the shape,

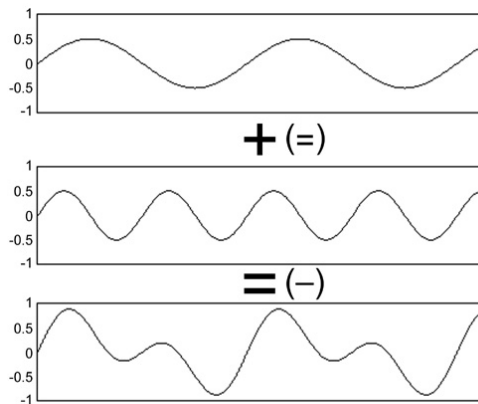


Figure A-2 Complex waves form by adding two simple sine functions

If the used data transforming system is a linear system, the data is not frequency dependent and therefore it won't be necessary to do a FFT (Fast Fourier Transformation). Multiplying the output data with the conversion factor can then easily change the amplified output data into the actual measured data.

When a real transforming system is used it becomes more complicated. The real system uses different amplitude amplifications and different phase shifts for the frequency-dependent transmissions. The output data then has to be split into harmonic components by FFT. The FFT gives for every frequency a sine (or cosine) with an amplitude and a phase (see equation..). In the output signal all these sine functions have been amplified with a different frequency-determined factor and are shifted by a frequency-determined phase. The values of this frequency behavior

are usually supplied by the manufacturer of the instruments and can be found in the systems manual.

To reconstruct the originally measured signal all the relevant harmonic output components have to be corrected for the instruments frequency dependence and then all these corrected and relevant components have to be summarized to retain the original signal. It has to be done as follows:

$$f(t) = c_0 + \frac{c_1}{k_1} \sin(\omega_0 t + \varphi_1 + \Delta\varphi_1) + \frac{c_2}{k_2} \sin(2\omega_0 t + \varphi_2 + \Delta\varphi_2) + \frac{c_3}{k_3} \sin(3\omega_0 t + \varphi_3 + \Delta\varphi_3) + \dots + \frac{c_n}{k_n} \sin(n\omega_0 t + \varphi_n + \Delta\varphi_n) \quad (\text{A.7})$$

This can be rewritten as:

$$f(t) = c_0 + \sum_{n=1}^{\infty} \frac{c_n}{k_n} \sin(n\omega_0 t + \varphi_n + \Delta\varphi_n) \quad (\text{A.8})$$

in which

- c_0 = Dc component (average value of function f)
- c_n = Harmonic amplitude for n^{th} frequency
- k_n = n^{th} frequency determined amplification of amplitude
- ω_0 = basic frequency
- φ_n = phase spectrum of n^{th} frequency
- $\Delta\varphi_n$ = n^{th} frequency determined phase shift
- $f(t)$ = original measured signal

A.4 Harmo

All continuously periodic output data can be split into its harmonical components by using the program Harmo.m. The program runs in Matlab.

Harmo performs a harmonic analysis of time series. By importing the measured data the program splits these periodic time series into the Fourier series and shows the following output.

As example a measurement signal has been chose that is obtained at the 4th of February with $h_0=55\text{cm}$, $T=2\text{s}$, $H=10\text{cm}$ at 18m distance from wave board. This data set can be found in the Msc-thesis of the author.

n	a_n	b_n	c_n	ϕ_n
0	-0.0184	0.0000	-0.0184	0
1	-0.0879	0.1036	0.1358	2.2743
2	0.0068	-0.0373	0.0379	-1.3904
3	0.0034	0.0067	0.0075	1.0952
4	-0.0005	-0.0008	0.0009	-2.0810
5	0.0003	0.0006	0.0007	1.1069

Table A-1 Output harmonical analysis on periodic velocity signal measured Feb. 4th with $h_0=55\text{cm}$, $T=2\text{s}$, $H=10\text{cm}$ at 18m distance from wave board.

In which:

- a : cosine Fourier coefficients, from 0 to m
- b : sine Fourier coefficients, from 0 to m
- c : amplitude of Fourier coefficients, from 0 to m
- phi : phase of Fourier coefficients (in radians), from 0 to m
- n : the number of harmonical components o be computed.

Section 0 showed that the n^{th} harmonical can be written as:

$$a_n \cos n\omega_0 t + b_n \sin n\omega_0 t = c_n \sin(n\omega_0 t + \phi_n) \quad (\text{A.9})$$

The values obtained when performing an harmonical analysis on the measured signal as seen in Table A-1 can now be used to reconstruct the original signal out of simple sine functions.

A.5 Data processing from wave gauges

The wave gauges and its signal conditioners as used in the experiment behave like a real system. All the used wave gauges and accompanying signal conditioners are of the same type and have the same data transmission characteristics. Every wave gauge is equipped with a filter. This filter is placed in order to filter out disturbances. The filter can damp signals that have a frequency, which is not in the range of the filter. For high frequencies it will even completely filter out all signals that have such a high frequency. The characteristics of the used wave gauge systems can be seen in Figure A-13.

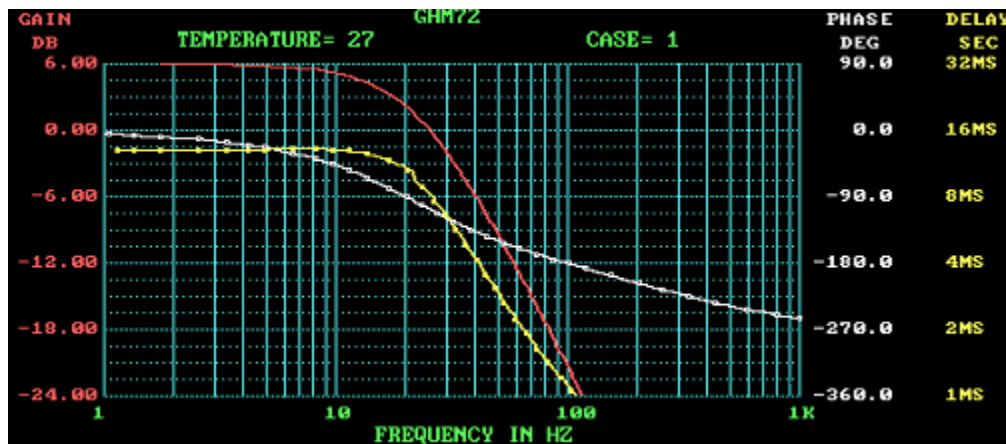


Figure A-3 Characteristics of wave gauge type 72, as used in the experiments

In this graph the phase shifts and amplitude amplifications that occur during transmission of the data can be seen for the various frequencies. The figure contains also a frequency-dependent time delay characteristic for the wave gauges.

The characteristics are represented as follows. The characteristic starting in the upper left corner (the red line) represents the gain factor for the amplitude. Its values are in DB and are listed at the left y-axes. The next characteristic (the white line), the line with the open squares in it, represents the frequency-determined phase shift and its values are in the first y-axes on the right in degrees. And finally the yellow line (the line with the closed squares) represents the frequency-dependent time-delays, whose values are in seconds and listed on the 2nd Y-axes on the right side.

As said the gain factor for the amplitude is represented in DB, which is a arbitrary dimension commonly used in electronics. It is a logarithmic factor that represents 20 times the gain factor. I.e. a gain of 0.50 will be equal to $20 \log(0.50) \approx -6.0 \text{ DB}$.

As said it's an arbitrary taken dimension. The maximum value of the gain factor (in this case 6.0DB) represents a gain factor of 1. So i.e. 0DB represents a gain factor, which is 6.0 DB lower. And -6.0 DB represents a gain factor, which is -12.0 DB (which is equal to a gain of 0.25).

From Figure A-3 it shows that the frequency-dependent range of a wave gauge is linear for frequencies up to a frequency of 3 Hz (see gain factor line). For frequencies between 3 Hz and 9 Hz only very small modifications of the amplitudes will arise. Furthermore, the frequency-dependent time delay remains constant up to frequencies up to 10 Hz.

This means that the harmonic components found in the range up to 3 Hz (or a period of 0.33s) or smaller (longer period) are transmitted without any changes of the amplitude. Periodic signals with a frequency of more than 3 Hz will be transmitted with modification of the amplitude, but up to 9 Hz this amplification is sufficiently small to be neglected.

Problems can arise for the phase shifts. Up to a range of 3 Hz this difference between the various frequencies will remain smaller than 10° , which is equal to 0.17 radians. But as the frequency of the signal increases the phase shift will grow more rapidly and output data needs to be corrected for this frequency-dependent phase-shift.

How this filter behavior will be of influence on the measured waves is explained in the following paragraph.

The regular waves used in the experiment have a period of at least 2 sec. Therefore the basic frequency of the used waves will always be in the non-modified range of the wave gauge and its signal conditioner. Splitting a complex surface elevation signal with a period of 2s up into harmonical components by FFT shows the following. All harmonics components up to the 6th harmonic have a frequency of 3 Hz or lower and with the used filter all these components then will be transmitted with hardly any loss or change of data.

Waves with a lower basic frequency than 0.5 Hz (period of 2s) have even more harmonic components with a frequency smaller than 3 Hz, i.e. for waves with a period of 3 sec the 8th harmonic component has a frequency of 3 Hz and will therefore still be transmitted with hardly any modifications of the amplitudes and the form.

It is obvious that the influence of the higher harmonics is detrimental for the quality of the output data. In the previous paragraphs the influence of the filter on the harmonical components has been laid out. Given that filter behavior and the influence of the higher harmonics now determines the quality of the output data.

For waves traveling in deep water only the first and maybe the second order harmonical components are of influence. In shallow water, however, this influence of the high order harmonic components becomes inevitable. Harmonic analysis on appearing shallow water waves in the wave flume however showed that the influence of 6th or even higher order harmonic components was very small and almost negligible. The influence of the harmonic components can be seen in Table A-2. The table shows the contribution of the higher order components. The influence of the higher order components will increase as the waves grow steeper. At breaking of the waves the influence of the higher order components will be at its maximum. Therefore the location and the form of the waves in table A-2 are chosen such that in most cases the waves are almost breaking.

	C1	C2	C3	C4	C5	C6	C7	C8
H=15cm;h=65cm;T=2s and X=18m	6.4896	2.7138	1.0534	0.3545	0.1493	0.0393	0.0058	0.0023
H=15cm; h=65cm; T=2s and X=20m	5.7756	3.3287	1.6603	0.9194	0.4177	0.2057	0.0774	0.0161
H=15cm; h=65cm; T=3s and X=18m	5.7856	4.1901	2.5600	1.4726	0.8322	0.5104	0.1695*	0.0948
H=15cm; h=65cm; T=3s and X=20m	4.6809	3.7821	2.6822	2.0683	1.4463	1.0555	0.6229*	0.389
H=10cm; h=55cm; T=2s and X=20m	3.6258	2.5119	1.4751	0.8751	0.5049	0.1517	0.0951	0.0159
H=10cm; h=55cm; T=3s and X=20m	2.8699	2.5499	1.9111	1.4273	1.1979	0.8459	0.5412*	0.2829
H=12.5cm; h=55cm; T=2s and X=19m	4.6958	2.9052	1.6666	0.9725	0.4879	0.2651	0.1496	0.0796
H=12.5cm; h=55cm; T=3s and X=18m	3.8851	3.2083	2.5072	1.8638	1.3334	0.7208	0.4845*	0.2866

Table A-2contribution of the harmonic components C1 to C8 on the waveform

Neglecting the influence of 7th and higher order harmonics leads to the assumption that the wave gauges behave linear and that the output data is of the same form and has the same values as the actual measured surface elevation.

*Note that in these cases, the influence of the 7th harmonic components is still be noticeable, but for these cases, with a basic frequency of 0.33 Hz, the 7th and even 8th harmonic components will still be transmitted without change of the data, because the frequency of those components is still lower then 3 Hz.

Figure A- shows the influence of the higher harmonic components on the shallow water waveform. From this figure can also be seen that the influence on the shape of the higher harmonical components is very small and can be neglected.

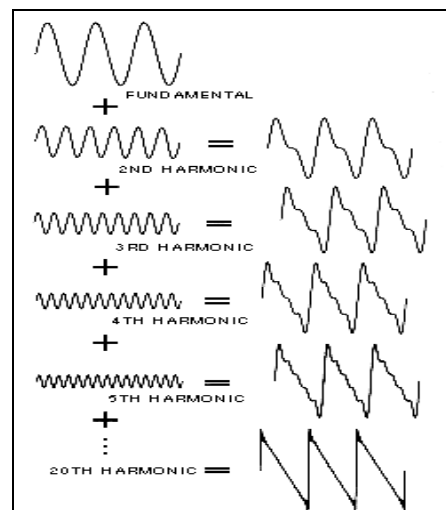


Figure A-4 Influence of harmonic components on wave shape

A.6 Analyzing EMS data

As with the wave gauges, the EMS-systems are also equipped with a frequency dependent filter. The function of the EMS is to measure the velocities and subsequently with these velocities, the accelerations will be determined. More details on EMS can be found in appendix XX.

Lots of attention is to be paid on the validity of this EMS data, because it forms the fundament of the experimental results. Before discussing the influence of the filter, first some important concepts of the velocities will be discussed.

A.6.1 Harmonical components

While a sine wave is constructed of only one frequency component, the measured velocity signal is a very complex periodic form composed out of many frequency components. As seen in the theory all continuous, periodic signals can be described mathematically as a Fourier series of individual sine components.

The Fourier series of such a complex velocity profile is:

$$f(t) = c_0 + \sum_{n=1}^{\infty} c_n \sin(n\omega_0 t + \varphi_n) \quad (\text{A.10})$$

Which can be written as:

$$f(t) = c_0 + c_1 \sin(\omega_0 t + \varphi_1) + c_2 \sin(2\omega_0 t + \varphi_2) + \dots + c_n \sin(n\omega_0 t + \varphi_n) \quad (\text{A.11})$$

This means that a complex velocity wave is an infinite series of harmonics, summed together to create the actual orbital horizontal velocity profile.

A.6.2 Influence of the harmonically velocity components on complex velocity signal

In deep water the influence of the high harmonic components is very small and the shape of the velocity profile will be largely determined by the lower harmonic components. In this case the influence of the higher harmonic components can be neglected. In shallow water, this influence of the higher harmonics becomes inevitable, and the shape of the velocity profile in shallow water will also be determined by the higher harmonics. This influence of harmonics on the shape of shallow water velocity profile is illustrated in Figure A.5. The figure shows the influence of the water depth on a wave with a period of 2s.

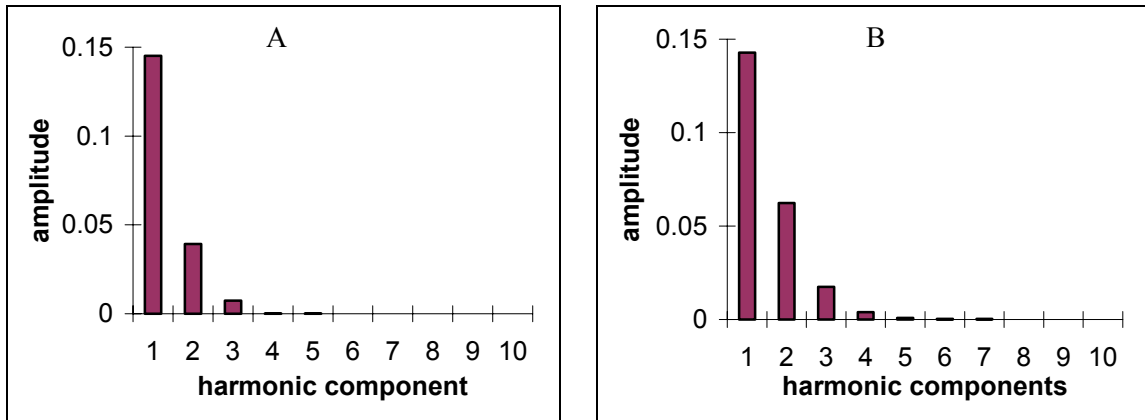


Figure A.5 mutations in amplitude- frequency spectrum of harmonical velocity components under regular waves traveling into water of less depth. The generated wave has the following properties: $H=10\text{cm}$, $T=2\text{s}$ and water depth at wave board is 55cm . Graph A is at 18m and graph B at 21m .

Enlarging the period will create a different velocity profile and the influence of the harmonical components on the summarized velocity profile will also change. Figure A-6 shows the influence of an enlarged period in the measuring area on to the significance of the harmonical components compared to those of Figure A.5.

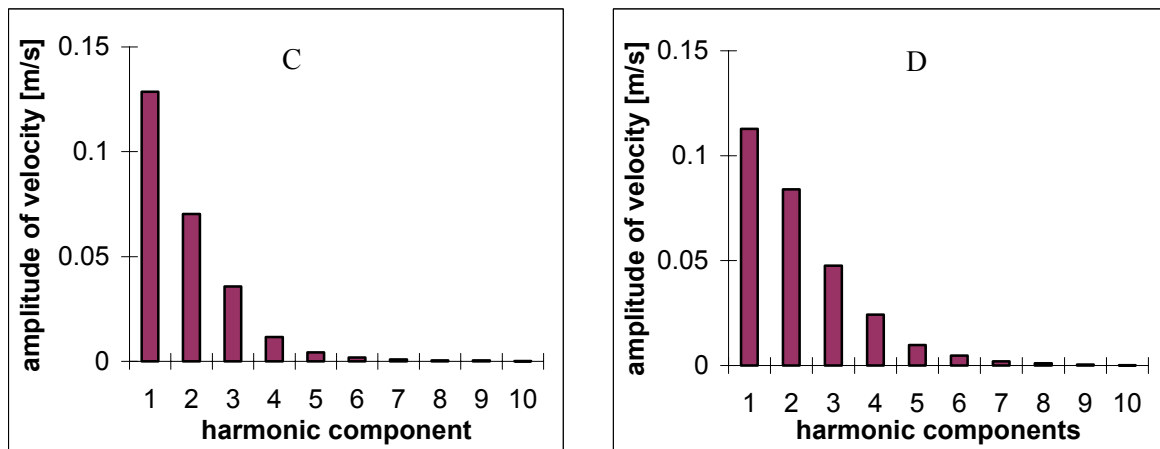


Figure A.6-mutations in amplitude- frequency spectrum of harmonical velocity components under regular waves traveling into water of less depth. The generated wave has the following properties: $H=10\text{cm}$, $T=3\text{s}$ and water depth at wave board is 55cm . Graph C is at 18m and graph D at 20m .

Here it shows that the influence of the higher harmonics becomes more significant. In case D the waves are almost breaking and the first 6 harmonics are important for the shape of the summarized velocity profile. In figure A-7 the same has been done for two other nearly breaking waves.

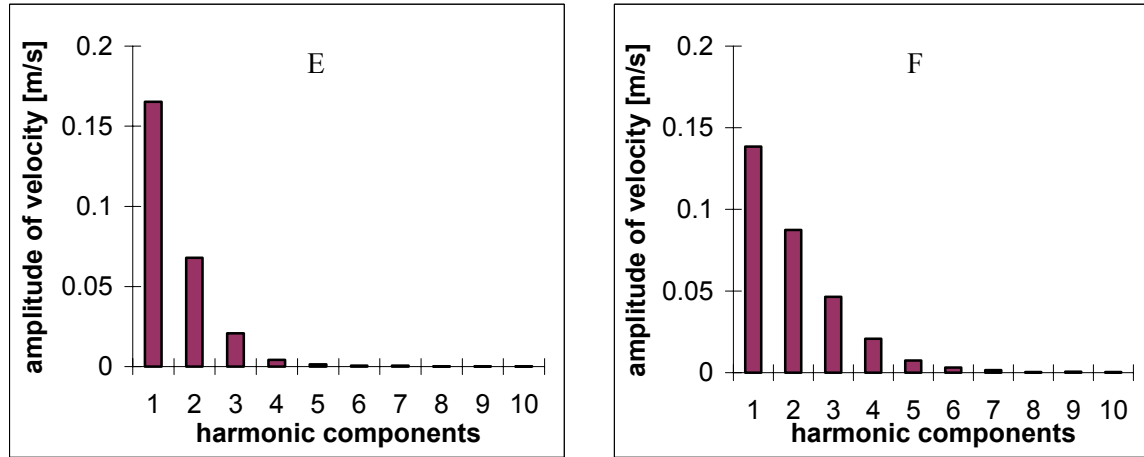


Figure A-7 mutations in amplitude- frequency spectrum of harmonical velocity components under regular waves just before breaking. Wave E has the following properties: $H=12.5\text{cm}$, $T=2\text{s}$ and water depth at wave board is 55cm . Graph F is the same wave with a period of 3 sec .

Obviously if a velocity profile in shallow water is to be transmitted without distortion, all the harmonics, onto infinity, must be transmitted. This is however impossible. Furthermore in the experiment for the given wave steepness it is also not necessary. As seen in the above amplitude-frequency spectra the shape of the horizontal velocity profile is mainly determined by the lower harmonic components. From the 7th harmonic or higher the influence will be assumed negligible for the shape of the velocity profile.

A.6.3 Quality of output data

The quality of the transmitted signal depends mainly on the filter used in the measuring equipment. Filtering is based on the assumption that the desired signal is composed out of a range of non-critical sinusoidal components. As with the wave gauges the process of filtering removes all data above or below a certain frequency.

Any filter function must take the harmonic structure of the wave into account. The removal or modification of any harmonic will affect the shape of the signal. [See Internet <http://www.web-ee.com/filters>] Modifications include amplitude, phase, and timing (delay) of each and every harmonic. As seen in the previous section the modification of higher order harmonics will have less effect on the shape of the waveform than modifying lower order harmonics. Elimination of higher harmonics usually leads to rounding of the corners of the signal. It is therefore the job of the designer of the filters to supply filters that meet the consumer's requests. I.e. to make a filter that only filters out the non-significant harmonical components.

The type of filtering that eliminates higher order components is called "Low-pass filtering". No noticeable changes in the signal transmission will occur, when this is performed for the proper frequencies.

The EMS instrument as used in the experiment was supposed to have a 5Hz filter. This meant that all data up to a frequency of 3 Hz were to be transmitted without loss or change of data. It would be the ideal range of the filter, because all significant harmonical components are within that

range and therefore no transmission modifications would occur. The filter characteristics of this filter were according to the manufacturer the following.

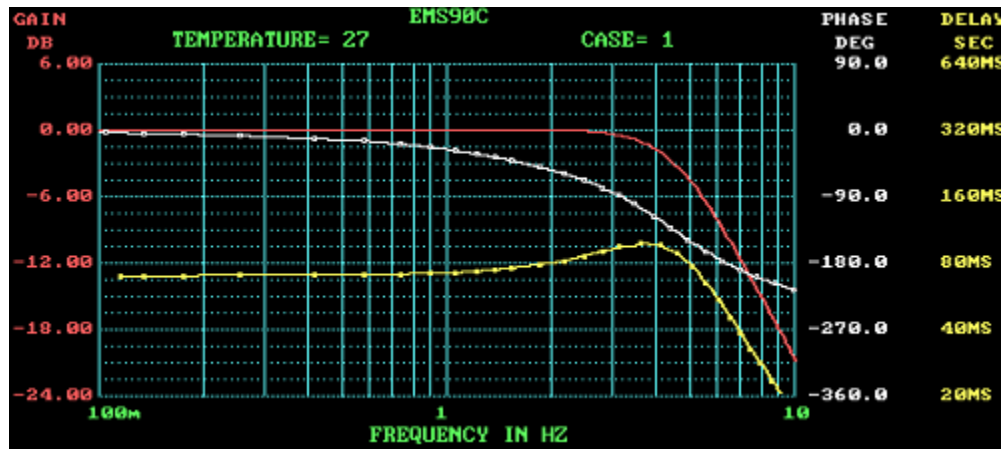


Figure A-8 Filter properties according to manufacturer of EMS90C

However after analyzing data obtained with this EMS, velocities were found that were much too low and velocity profile shapes were constructed from the output data, that didn't resemble to expected shapes. Opening the EMS and its signal conditioner revealed the origin of these assumingly wrong expectations. The filter as used turned out to be an unknown filter that had been in the EMS-system for an unknown period. After having the characteristics reconstructed of this filter, they turned out to differ enormously from the characteristics as provided by the manufacturer of the EMS. The truly filter properties turned out to be as follows:

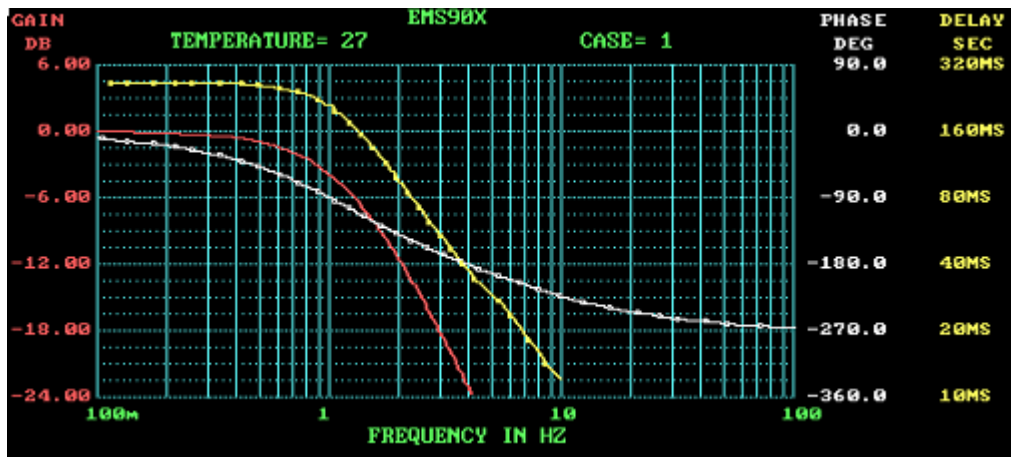


Figure A-9 Truly filter properties of used EMS

Analyzing this truly characteristics shows many peculiarities, which can explain the strange output data.

- The gain factor starts declining significantly at a frequency of 0.3 Hz. whether this damping will harm the complex signal is kept out of consideration.
- At a frequency of 1 Hz the gain factor is already 0.65, from here on the gain factor starts declining really fast. This leads to large output data modifications from the original signal.
- For frequencies larger then 3 Hz the signals will be completely damped and reconstruction is from here on impossible, because the signals haven't been transmitted to the output data.
- The time delay is 160ms, which is very large.
- For frequencies of 0.8 Hz this time-delay will keep on changing for higher frequencies.
- For low frequency rather large phase shifts occur. These phase shifts only grow as the frequency increases.

From the above peculiarities can be concluded that all these modifications take place in the range of the occurring horizontal velocities during the experiment. Therefore all output data obtained with this EMS needs to be reconstructed, whenever possible, into the original signals. This should be done as explained in the theory of section 0 and with the phase dependent filter modifications as found in the filter characteristics. More about this reconstructing of output data into the original data can be found in section 0.

Reconstructing all original signals is a time-consuming and not always reliable work. Therefore many measurements have been redone, with a new EMS and signal conditioner that have a for the range of the measurements more suitable filter. The characteristics of this filter can be seen in the following figure:

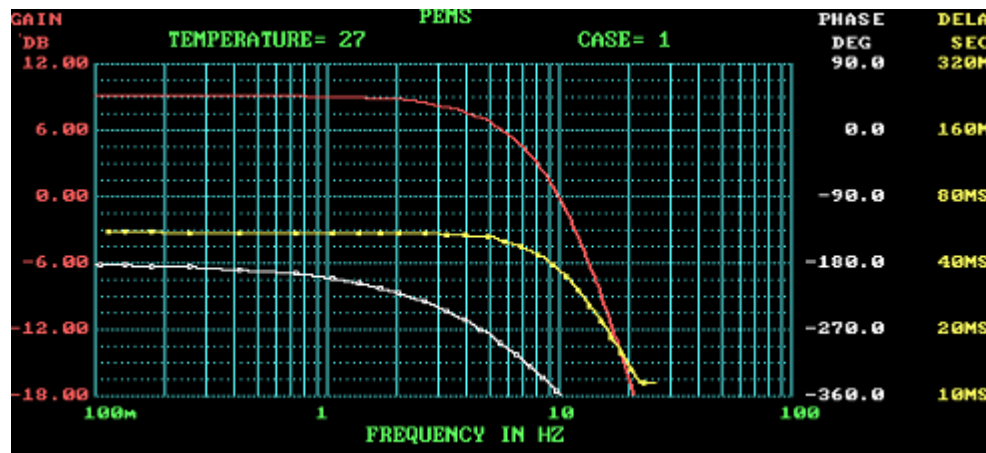


Figure A-10 Filter properties of 2nd EMS

This filter looks much more appropriate to do the velocity measurements with. Up to a frequency of 2Hz there is no modification of signals when transmitting the data. Little damping of the amplitude will be transmitted in the range for waves with a frequency of 2Hz up to 7Hz, par example for a wave with a basic frequency of 0.5 Hz ($T=2$ sec) there will be no modification of the amplitude up to the 6th harmonic and no hardly any data will be modified from signals up to a frequency of 7Hz, which corresponds to the 14th harmonical. When waves with a longer period are used even less modification of the profile are expected. The only modifications can arise for the waveform, because the phase becomes shifted for frequencies longer then 1 Hz. This phase shift influence will be investigated in the next chapter.

A.7 Underestimation of EMS velocities

A well-known problem for EMS measurements is that it sometimes underestimates the actual velocities.

To convert the output data to the actual velocity the following properties of the EMS have to be known.

$$U = a + b * \ddot{V} \quad (\text{A.12})$$

in which: U = velocity
 a = the offset
 b = gain factor

\ddot{V} = Voltage as transmitted through signal processor

If the electro magnetic field of the EMS gets disturbed the value of this gain factor can change and by doing so differences between the actual and measured velocity can occur. As mentioned in section XX the EMS has to be calibrated for changes in this gain factor before and after every day of testing. This has to be performed in the same manner as described in section XX, by dragging the EMS with various constant velocities in both directions of the flume.

When analyzing the data, it must primary be controlled whether this underestimation is a linear underestimation or not. If the underestimation is linear for all velocities then this gain factor must be determined. When it has a different non-linear underestimation for the various velocities then it becomes more difficult. A non-linear function that describes the underestimation at all velocities then has to be found.

The EMS that was initially used for the experiment, showed an in time increasing linear underestimation of the velocities. Cleaning the probe, refreshing the water and cleaning the cables every now and then leads to a reduction of the underestimations. So improper maintenance can be a reason for these underestimations, an other factor can be tiny cracks in the plastic cover of the probe.

Results of a test performed to check the underestimation of the velocities are shown in Table A-3..

4-Feb before experiment

Test nr.	U drag [m/s]	U ems [m/s]	U*	U**
1	0.30	0.206	0.300	0.305
2	-0.30	-0.207	-0.301	-0.307
3	0.20	0.135	0.197	0.200
4	-0.20	-0.140	-0.204	-0.207
5	0.10	0.064	0.093	0.095
6	-0.10	-0.065	-0.095	-0.096
7	0.05	0.028	0.041	0.041
8	-0.05	-0.029	-0.042	-0.043

4-Feb after experiment

test nr	U drag [m/s]	U EMS [m/s]	U*	U**
1	0.30	0.203	0.300	0.294
2	-0.30	-0.202	-0.299	-0.293
3	0.20	0.138	0.204	0.200
4	-0.20	-0.132	-0.195	-0.191
5	0.10	0.062	0.092	0.090
6	-0.10	-0.061	-0.090	-0.088
7	0.05	0.031	0.046	0.045
8	-0.05	-0.029	-0.043	-0.042

Table A-3 calibration of EMS by dragging the EMS in still water

Also in Table A-3 the relative velocities are set out against each other. It has been done for all dragging velocities. These relative velocities can be used to find whether the gain factor is constant.

$$U^* = U_{ems} * \frac{U_{drag}(0.30)}{U_{ems}(0.30)} \quad \text{and} \quad U^{**} = U_{ems} * \frac{U_{drag}(0.30)}{U_{ems}(0.30)} \quad (\text{A.13})$$

in which: U^* = relative velocity according to $U_{ems}(0.30)$ as true velocity.

U^{**} = relative velocity according to $U_{ems}(0.20)$ as true velocity.

$U_{ems}(0,30)$ = measured velocity with EMS while dragging it with 0.30m/s through flume.

$U_{ems}(0,20)$ = measured velocity with EMS while dragging it with 0.20m/s through flume.

$U_{drag}(0.30)$ = velocity at which the EMS is dragged through the flume.

$U_{drag}(0.30)$ = velocity at which the EMS is dragged through the flume.

The relative velocities measured at all days have been set out against each other. The graph for U^* can be seen in Figure . It shows that the gain factor is linear for all velocities.

For U^* all data comes through point (0,30, 0.30), this is because all data is shown relative to the underestimation of $U(0.30)$. If it's a linear underestimation the lines must also go through the other points of same x and y value. This is obviously the case. The points that do not lie exactly on these values of same X and Y, give an indication on the error in this linearization. It is as big as the widest spread of data through a point. In figure it is marked with the black arrows. For the other relative speeds the same graphs have been made and they all showed a linear underestimation with about the same error margin. This proves a linear underestimation of measured velocities.

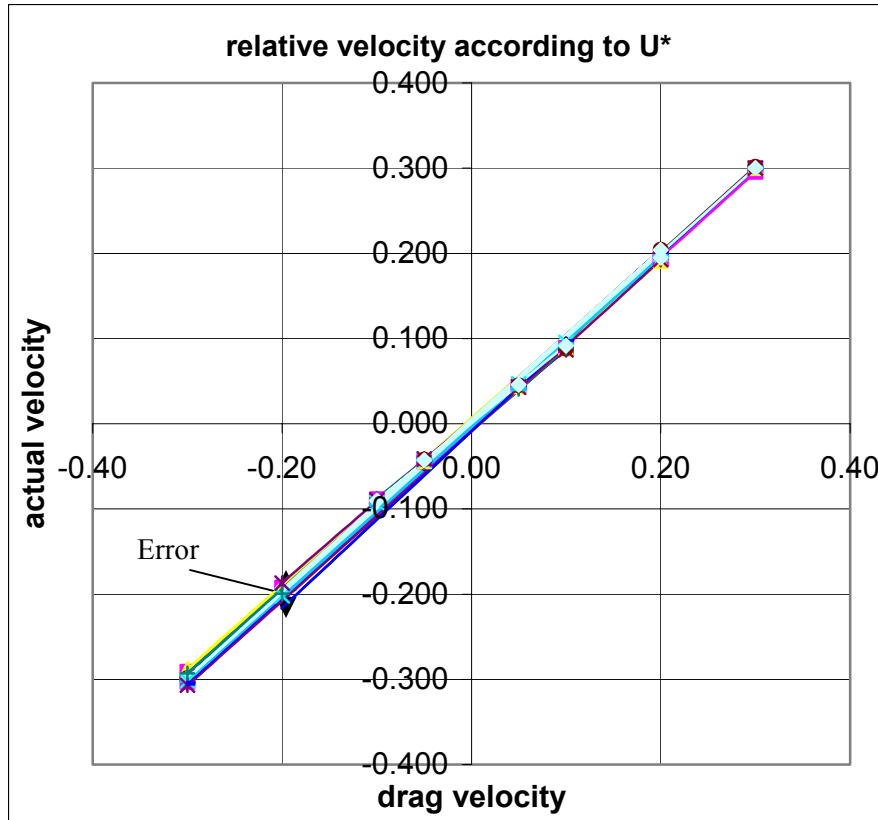


Figure A-11 Relative velocities according to the underestimation of $U_{\text{drag}}=30\text{cm/s}$

By dragging the EMS through the flume with constant speed, a uniform flow situation has been created. It is, though, not certain whether this underestimation is frequency dependent. Testing and comparing the frequency-related velocities of this EMS with an EMS that has no underestimations can only find this out. This has been another uncertainty that made the use of the EMS data dubious.

The EMS that replaced the old EMS showed no significant differences while dragging it through the flume at different velocities. This EMS has therefore no underestimation of velocities and the obtained data can be used without converting it for underestimations of the velocity.

In the next section with help of the new data from the second EMS it can be seen that the data was frequency dependent.

A.8 Reconstruction of transmitted EMS signal

Reconstruction of the transmitted signals into the original signals has to be done for most of the data. Section A.5, showed that the transmitted output data from the wave gauges showed no changes from the original signal. This means that the water surface elevation data can be used without converting it back to its original signal.

Though the data obtained with the EMS did modify during transmission. In section A.6 the changes that occur whilst transmitting the data through the filter have been explained for both the first and second used EMS. It appeared that the signal conditioner of the first used EMS was equipped with a wrong filter. Furthermore the first EMS showed an in-time increasing underestimation of the actual velocities.

Reconstruction of the original signal from the output data is still possible for the old data, but it can lead to inaccurate values. Therefore the reconstructed signals need to be compared to values obtained with a physical model. This will be done in section XX Validity of reconstructed data. As this chapter deals with the processing of signals an example of such a signal reconstruction for both the first and second used EMS will be given. The validity of this data does not come up in this chapter; this will be discussed in following sections. By comparing the results of the examples, we can also find whether the underestimation of the velocities of the first used EMS is frequency-dependent or not (see section A.7).

The waves as used in this example are the following:

- $H_0=10\text{cm}$, $T=2\text{s}$, $h_0=55\text{cm}$ measured on Feb. 4th with old EMS at 18m distance from wave board.
- $H_0=10\text{cm}$, $T=2\text{s}$, $h_0=55\text{cm}$ measured on Feb. 26th with new EMS at 18m distance from wave board.

The duration of both the measurements was 30 seconds. The data was sampled at 20 Hz; this means that values were recorded at every 0.05 s. The velocities are recorded as voltage. The uncorrected output signals for both waves are as follows. The values on the y-axis show the differences between the two measurements.

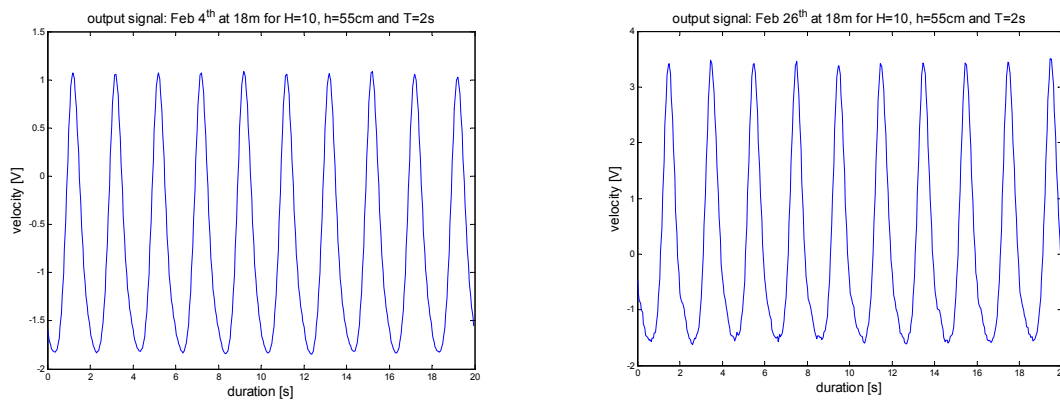


Figure A-12 Output signal measured with the 1st and the 2nd EMS

The uncorrected velocities must be corrected for the offset and for the gain factor. From the manual of both EMS's was known that $1\text{V} = 0.1\text{m/s}$. With use of this it is possible to get the uncorrected output velocities. It can be clearly seen that the measurements done with the old EMS

give lower velocities, this is partly due to the underestimation of the velocities and also because of the wrong filter.

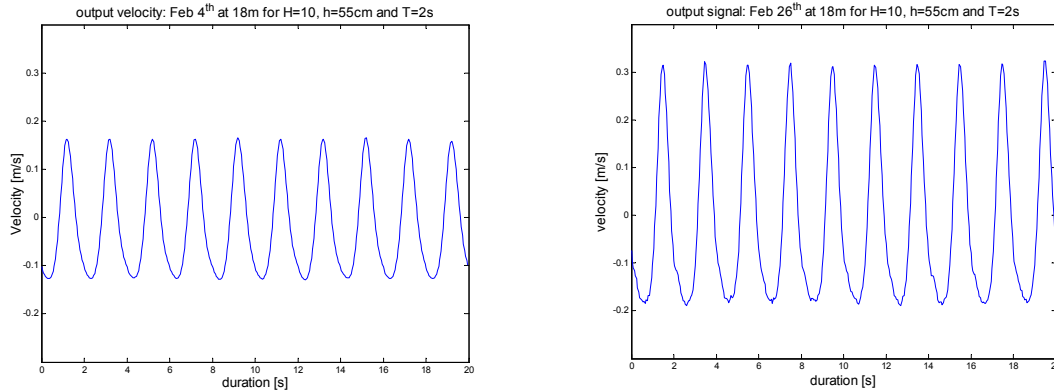


Figure A-13 Output velocities corrected for offset and gain factor

The output velocity is a continuous periodic function. Harmonical analysis with use of Harmo.m (see page viii) can represent the velocity function as an infinite series of simple sine components. Table A-4 shows the values of this harmonical analysis on both the old and new EMS signal for the first four orders.

	C_1	C_2	C_3	C_4	φ_1	φ_2	φ_3	φ_4
Old EMS	0.1358	0.0379	0.0075	0.0009	2.2743	-1.390	1.0952	-2.081
New EMS	0.2264	0.0804	0.0172	0.0021	1.3528	2.9841	-1.848	1.1317

Table A-4 Amplitudes and phases of 1st - 4th order harmonical components

Using the values of Table A-4 in the following equation makes simple cosine functions of the harmonical components.

$$n^{th} \text{ harmonic} = C_n \cos(n\omega_0 t + \varphi_n) \quad (\text{A.13})$$

It appears that the velocities are represented by a series of cosine functions instead of sine functions. Figure shows the graphical representation of these harmonical components. Once more the scale of the Y-axis shows the influence of the underestimation and of the filter on the transmitted signal.

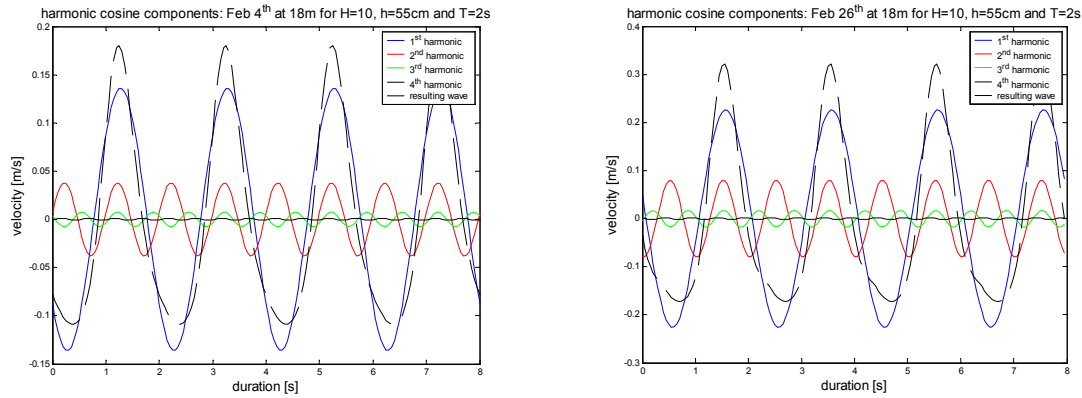


Figure A-14 significant harmonical components for measurements with old and new EMS

All harmonical components have different frequencies. The higher the order of the harmonical components becomes, the higher the frequency becomes. The filter influences both the phase of the transmitted signal as the amplitude of the harmonical components. As can be seen in both (the old and the new EMS) filter characteristics the modification of in the transmitted signal is much bigger for the old EMS. The filter creates a frequency dependent amplification (weakening) of the signal for the harmonical components.

For every harmonical component, the frequency is known, so by looking at the filter characteristics the amplification factor of the amplitude and the phase shift of that given frequency can be found. Adapting the harmonical components for these filter modifications now creates the non-filtered signal.

In the following table the frequencies of the 1st, 2nd, 3rd and 4th order harmonical components are given and the accompanying frequency-dependent phase shifts and amplitude amplifications.

		1 st order	2 nd order	3 rd order	4 th order
Frequency		0.5 Hz	1.0 Hz	1.5 Hz	2 Hz
old EMS	Amplification factor [k]	0.8	0.65	0.45	0.25
	$\Delta\phi$	-0.79	-1.57	-1.96	-2.36
new EMS	Amplification factor [k]	1	1	1	1
	$\Delta\phi$	0	-0.1	-0.3	-0.4

Table A-5 frequency-dependent phase shifts and amplitude amplifications

Correcting the harmonical components with this amplitude and phase shifts leads to the unfiltered signal. It has to be done as shown in section A.3. For every harmonical component this yields to the following expression:

$$n^{th} \text{ harmonical} = \frac{c_n}{k_n} \cos(n\omega_0 t + \varphi_n + \Delta\varphi_n) \quad (\text{A.14})$$

C_n and φ_n can be found in Table A-4 and k_n and $\Delta\varphi_n$ can be found from Table A-5. By doing so the following graphs for both the old and the new EMS can be made. Summarizing the four harmonical components leads to the complex velocity signal as seen in figure XX.

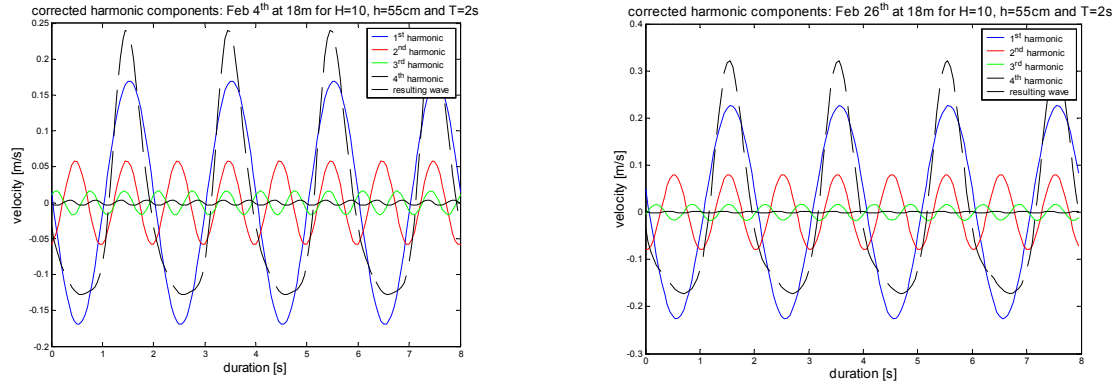


Figure A-15 harmonical components corrected for filter modifications. On the left the old EMS and on the right side the data found with the second EMS.

Still the original signal isn't completed. The original signal is a series of harmonical components, which has to be described as follows:

$$f(t) = c_0 + \sum_{n=1}^{\infty} \frac{c_n}{k_n} \cos(n\omega_0 t + \varphi_n + \Delta\varphi_n) \quad (\text{A.15})$$

In Figure this summation has been completed only the value of C_0 is still missing. This is the value for the average of the function $f(t)$ and is also given by Harmo.m. So to complete the Fourier series this average value C_0 has to be added to the summarized harmonical components. This has been done in figure XX. It appears that a little transport of water took place because the values of C_0 are negative, so the function $f(t)$ shifts a little downwards.

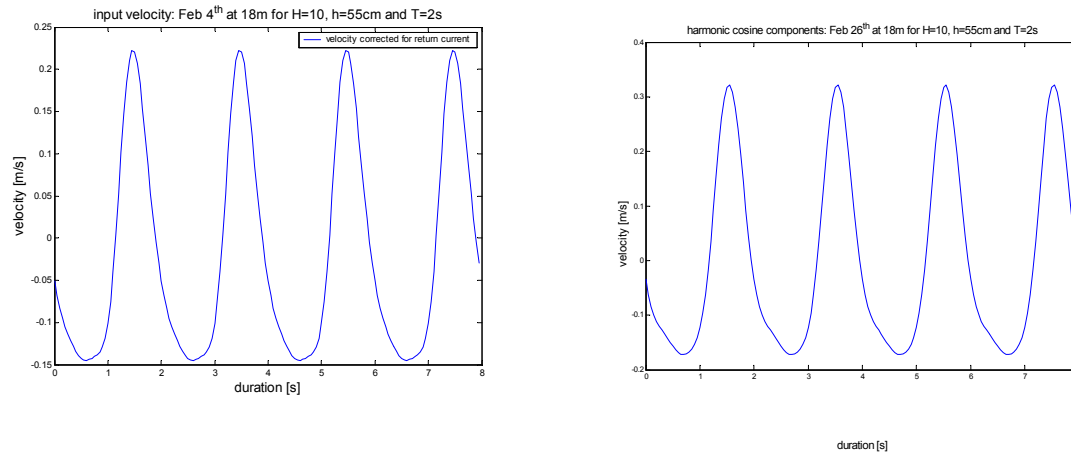


Figure A-1 input velocities corrected for return currents

The harmonical and summarized velocities still have smaller amplitudes for the measurements taken at the 4th of February with the first used EMS. This is because the firstly used EMS had a linear underestimation of the velocities. This linear underestimation was for a uniform current about 0.70 times the actual velocity. See appendix X for the calibration tests performed at the 4th of February.

So far it is not known whether this underestimation is also frequency dependent. This can be checked by comparing the underestimation of the various harmonical components of this test to the harmonical components obtained with an EMS that had no underestimation. The second EMS did not have such an underestimation. Comparing the results can clarify whether this underestimation is frequency-dependent

The tests will be compared for data that has been corrected for filter modifications. This must be done because the two EMS have different filters and therefore the filter has modified the output data in different ways.

Frequency-dependent underestimation can be found as follows:

$$\frac{c_1}{k_1} = a * \frac{c_1^{new}}{k_1^{new}} ; \quad \frac{c_2}{k_2} = b * \frac{c_2^{new}}{k_2^{new}} ; \quad \frac{c_3}{k_3} = d * \frac{c_3^{new}}{k_3^{new}} ; \quad \frac{c_4}{k_4} = e * \frac{c_4^{new}}{k_4^{new}} \quad (A.16)$$

In which:

- C_n = Amplitude of n^{th} -harmonic component measured with first EMS
- k_n = Frequency-determined amplification factor of n^{th} -harmonic of 1st EMS
- a, b, d, e = Frequency-determined underestimation-factor
- C_n^{new} = Corrected amplitude of n^{th} -harmonic component measured with second
- k_n^{new} = Frequency-determined amplification factor of n^{th} -harmonic of 2nd EMS

Doing so resulted in the following for comparison between two EMS's. The 1st EMS has an underestimation, while dragging the EMS through the flume, while the 2nd EMS shows no underestimation.

	C_1/k_1	C_2/k_2	C_3/k_3	C_4/k_4	$\Sigma(C_n/k_n)$
1 st EMS	0.1693	0.0578	0.0166	0.0036	0.2263
2 nd EMS	0.2264	0.0804	0.0192	0.0037	0.3176

Table A-6 values of corrected first harmonical order components for old EMS with underestimation and for new EMS without underestimation whilst dragging through the flume.

The underestimation whilst dragging the EMS is 0.70 times the velocity. This is for a uniform flow situation. See Table A-7. An formula can be used to find valued for a, b, d and e , which are the frequency dependent underestimation factors.

a	0.748
b	0.719
d	0.865
e	0.973

Table A-7frequency dependent underestimations

The values for a, b, d and e are not at all the same, which indicate an frequency-dependent underestimation of velocities. Therefore it is not possible to correct all data of different frequencies, with the same underestimation factor. Data of various frequencies has to be corrected with a factor that is frequency bounded. As seen this factor can only be found by comparing the data of the old EMS to the data of a same measurement done with an EMS that has no underestimations of the velocities. This leads to a lot of extra measurements. When possible, it can therefore be easier and more reliable to redo all relevant measurements with a proper filter and that has no underestimation of the velocities.

A.9 Frequency dependent time-delay

Finally, as mentioned all filters are equipped with a frequency-dependent time delay. This time delay may vary for the various instruments as used.

In the experiment there is a wave gauge placed next to the EMS. This has been done in order to find the velocities under the wave propagation. When analyzing the output data from the firstly used EMS, it occurred that the velocity and water surface elevation profiles were almost 300msec out of phase. See Figure A.

Initially the water is at rest, and then the first waves arrive at the position where the EMS and the wave gauge are placed. Already at the first changes of the still water surface elevation, the accompanying velocity arrives a little bit later. As the waves grow, the velocities grow as well, but the distance between the velocity function and the surface elevation function remains the same. Once the water movement stops this difference will also be still the same. This proves that it is not caused by reflection of the waves on the bed slope.

This phenomena occurred at various locations, and according to literature this was not possible

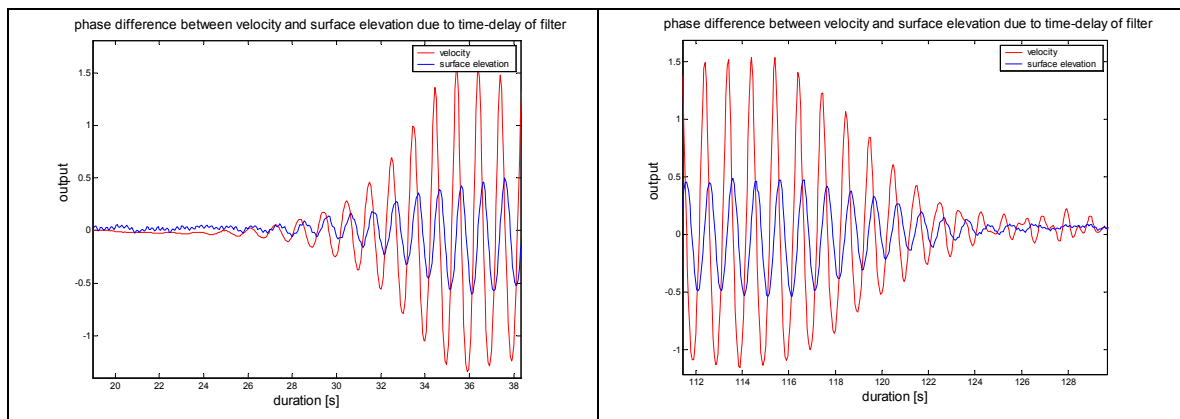


Figure A-16 phase differences between instruments caused by different time-delay of filters

It occurred that the time delay of the EMS was much bigger then the one of the wave gauge. This would not be a problem when this time-delay was constant, but this time delay was frequency-dependent and not linear between the wave gauge and the EMS. I.e. for a given frequency the time delay of the data from the EMS was 270ms, whilst for the same frequency this time-delay of the wave gauge was only 12ms. The time delay of a higher frequency now decreased to 220ms for the EMS and for the wave gauge it stayed 12ms at the higher frequency. Due to this behavior it becomes very difficult to predict the actual occurrence of the velocities under the wave propagation. The second EMS showed also a larger time delay then the wave gauge, but this delay stayed constant up to very high frequencies, just like the wave gauges. By knowing the difference in time-delay between the wave gauge and the EMS and assuming that this will be constant for all the relevant harmonic order components, it is possible to determine the exact occurrence of a velocity under a given part of the wave.

The time delay characteristics for the wave gauge, the firstly used EMS and the secondly used EMS have been set out to the frequencies in Figure 17. It is obvious that the time delay of the 1st EMS is impossible to use for determining the occurring velocities under the wave propagation.

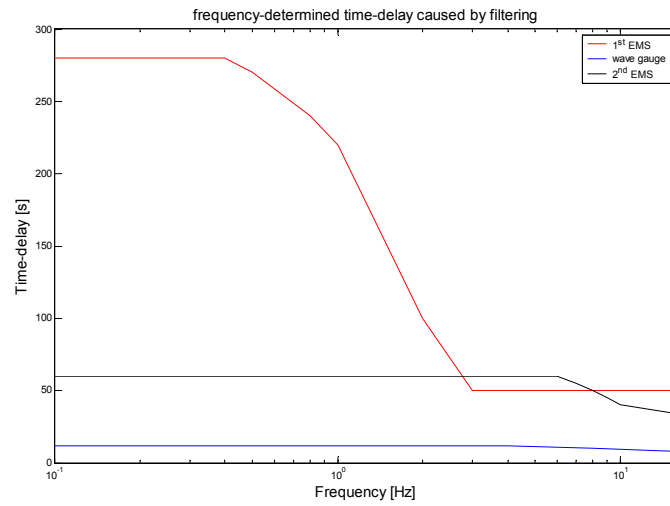


Figure A-17 Time delay caused by filtering

Appendix B

Parameters

B.1 Introduction

For the experiment many parameters are used. In this appendix a resume of all parameters will be given with a short description. The parameters will be divided into variable and constant parameters.

B.2 Variable parameters

The variable parameters are those parameters that change their values during the experiments. Therefore it is important to measure the values of these parameters during the various experiments in order to check whether the test was done with the correct values. The following parameters are used as variables.

The wave steepness S

A ratio of wave height to wavelength that shows the "peakedness" of a wave. The movements, velocities and accelerations near the bottom depend mainly on this peakedness of the waves and on the water depth. By changing the wave steepness, different velocities and accelerations can be generated near the bottom of the wave flume.

As mentioned, the wave steepness is a ratio of wave height to wavelength. So in order to vary the wave steepness there are two options.

1) Change of wave height H

Changing the wave height changes the ratio of the wave steepness.

2) Change of wave period T

The wavelength depends upon the water depth and the wave period. By keeping the water depth constant during a test, the wavelength can now easily be changed by changing the wave period.

A steering computer controls the wave board, which generates the waves. The software used by the steering computer wants the user to define the wave height and the wave period, so varying the wave height and the wave period can easily vary the wave steepness during the experiments.

The water depth h

This parameter mainly depends on the geometry of the wave flume, but some variations in the water depth are still possible. Changing the wave steepness can create different velocities and accelerations at a certain location; by changing the water depth even more different scenarios at this location can be created. This is very useful so that not the entire bottom of the flume has to be filled with stones and measuring equipment, but only some sections will be used for the experiments.

Velocity and accelerations near the bed

For every combination of wave steepness and water depth the waves will generate a different water movement onto the stones of the bed. This water movement is the driving force for the movement of the stones, and consists of a velocity and an acceleration, which also will vary for every different combination of wave steepness and water depth.

D_{n 50}

For a good investigation, multiple stone diameters have to be used, but because time is limited only two stone diameters will be used.

Location of the colored stones

The location of the colored stones (for details see report chapter 6) can be changed in order to see the effect of larger and smaller waves on these stones. The colored stones will be placed just in front of the breaking area of the waves. Because large waves break in deeper water than smaller waves, the colored stones have to be replaced sometimes. This depends on the breaking location of the waves to be used.

Number of moved stones

After every run of the wave machine the number of stones moved from the various color bands has to be counted. Maybe the distance the stones have moved can also be measured.

B.3 Constant parameters

These parameters have been set from the beginning of the experiment. During the entire experiment no changes have to be made to these parameters. Before starting the experiment it is important to measure them so that their values are known.

Bed slope

In water of constant depth the movements, velocities and accelerations of the water particles driven by the orbital wave motion will be the same for the entire bottom. As the experiment has been set up to investigate the influence of accelerations on stability of stones, it is important to create changing accelerations and velocities near the bed. A sloping bottom will meet this. In order to prevent large reflections and standing waves a mild slope 1:30 has been constructed in the wave flume.

Density of the stones

Density is defined as the ratio of dry mass of a stone to its volume, including the pores in it. If the stones in a test have the same diameter, they also need to have the same density so that all the stones have similar stability.

And because nearly all transport formulae require the density of the stones it is also very convenient to choose one single density for all the stones.

Gradation of the stones

For a proper transmission of force the stones have to be placed in a natural way. This can be created by water-working (see report) of the stones for a long time.

Shape of the stones

The shape of the rocks has to be equal. This is very hard to obtain, therefore from a sample the l/d has to be measured and if for that sample the l/d is smaller than 3 for 95% of that sample than the shape is nearly uniform.

Geometry of the flume

The wave flume to be used is a wave flume in the Fluid mechanics laboratory, with the following dimensions.

- ✓ $L = 40$ meters
- ✓ $w = 0.80$ meters
- ✓ $h = 0.90$ meters

The limited width, w , can be of influence on the development of wall friction, but because of the continuously changing conditions of the waves there will not be enough time for this friction to build up.

The limited height, h , will form a barrier to the water depth and the wave height.

Temperature of the water

The viscosity of the water depends among others on the temperature of the water. As it is impossible to cool down or heat the water in the flume, it is considered constant. Measurements have to be done regularly to ensure these assumptions. This is a parameter that can influence the EMS measurements, because they make use of viscosity.

Dimensions of the colored bands.

In every test bands of colored stones will be used. The width of these bands will cover the entire width of the flume. The length of these bands has to be larger than 5 times the D_{n50} . During the experiments a width of 15 cm will be used.

Appendix C

The EMS. Electro Magnetic Speed meters, which are used to measure flow velocities in currents or in orbital flows.

Fluid flow perpendicular to a magnetic field created by a pulsed electromagnet (coil) gives rise to an electric field perpendicular to the flow and magnetic vectors. Measuring the voltage difference between two electrodes senses this electric field. The voltage difference is directly proportional to the flow velocity.

The EMS has an analog voltage output that is converted to digital form for storage on computer disk. Two electrode pairs are situated on the prop to give orthogonal velocity components.

As said the measuring devices of the EMS are located in a prop, which is connected at its topside to a steel tube. This tube is attached to a trestle to keep the EMS in position. Raising and lowering this tube can position the prop at every required height.

From the EMS the data is send through a cable to the signal conditioner (Figure C). This signal conditioner transmits the measured analogue data into a digital output signal, which can be recorded with a computer.

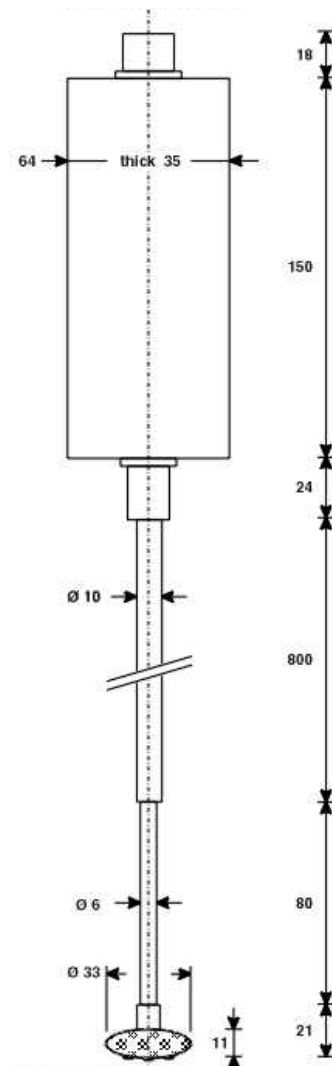
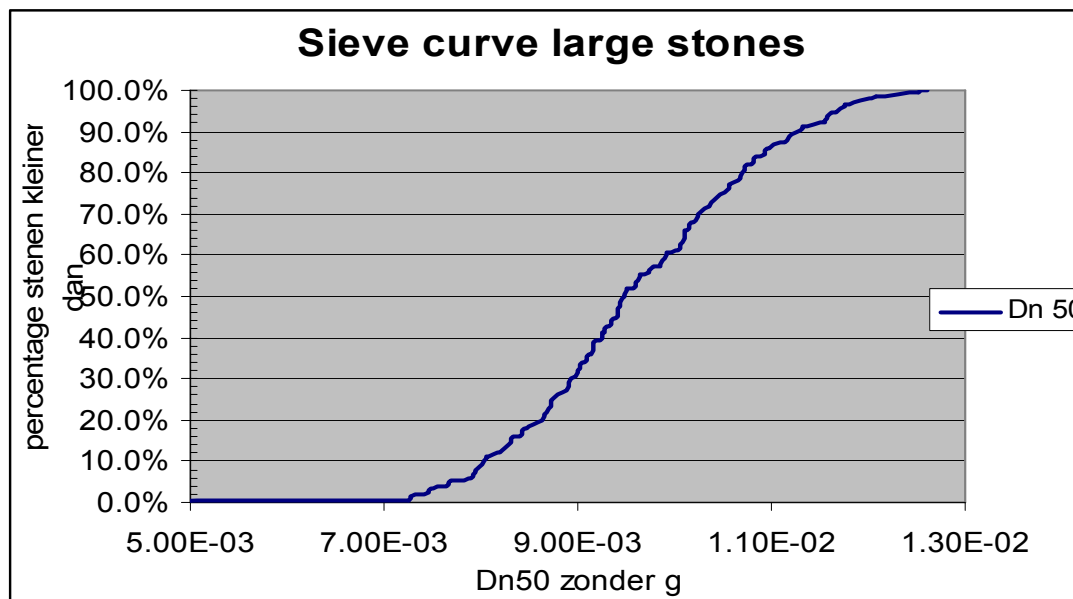
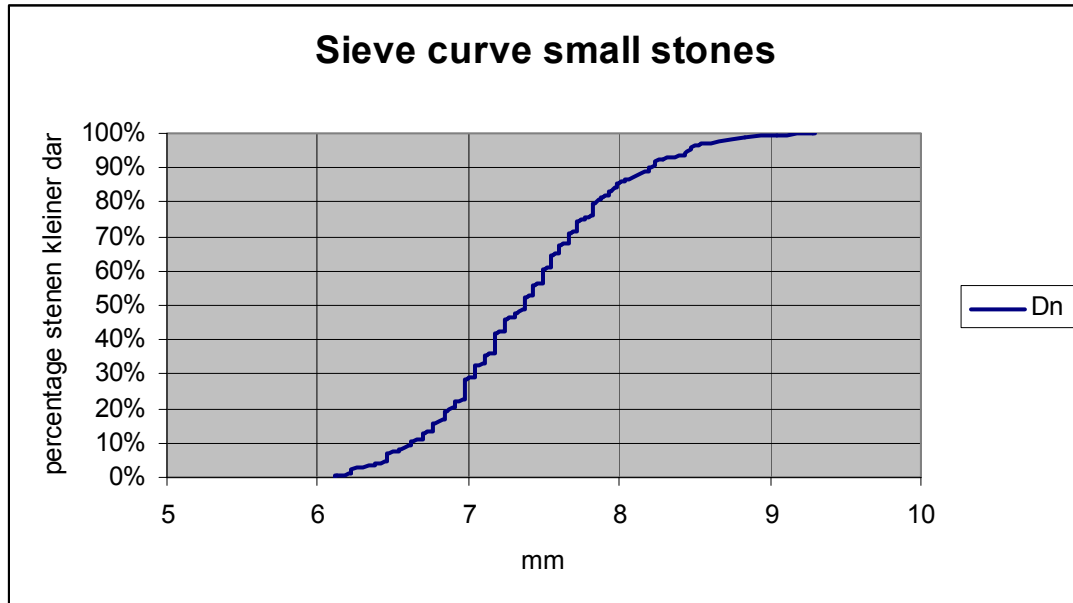


figure C

Appendix D

Sieve curves

The threshold of motion is a very delicate phenomenon. Little differences in forces form the border between movement and no movement. Therefore it is very important that the bed material is uniform. Both used stone diameters have been obtained by sieving. In order to get a small range of stone diameters the sieve curve must be steep. The sieve curves of both the stone diameters are shown in this appendix.



Appendix E

M-files and list used during the experiments

1.1 M-files

During the analysis of the experiment many Matlab files have been programmed in order to process the data. In this appendix the listings of some of those programs will be given. This will be done because after completion of this thesis someone else has to perform the same analysis, but then for different water depths. So sharing the m-files can help him.

Of each M-file also a short description will given.

The first m-file is the file that has been used to determine the momentary velocities and accelerations. It can also plot these values in a plot as seen in figure 5.2.2. The file can also be used to determine the values of a_{spike} and u_{rms} for each of the tested wave steepnesses. But before it can be used, first the velocity and acceleration profile of all wave steepnesses must be declared.

```
%uiiimport('H=0.1;T=2;X=21.00.asc')
%disp(' ')
T = input('give wave period')
%vul T in .....T=
n1=4*T/0.05
n2=n1+(T*20)-1
u=(data(:,8)-0.47)/10;
a=data(:,9)/10;
t=data(:,1);
u(n1:n2) = u(n1:n2)-mean(u(n1:n2));
[u_max,i]=max(u(n1:n2));
a_max = a(n1+(i-1));
t_beg0 = input('give time difference0')
u_beg0 = interp1(t(n1:n2),u(n1:n2),t(n1+i-1)-t_beg0)
a_beg0 = interp1(t(n1:n2),a(n1:n2),t(n1+i-1)-t_beg0)
t_beg1 = input('give time difference1')
u_beg1 = interp1(t(n1:n2),u(n1:n2),t(n1+i-1)-t_beg1)
a_beg1 = interp1(t(n1:n2),a(n1:n2),t(n1+i-1)-t_beg1)
t_beg2 = input('give time difference2')
u_beg2 = interp1(t(n1:n2),u(n1:n2),t(n1+i-1)-t_beg2)
a_beg2 = interp1(t(n1:n2),a(n1:n2),t(n1+i-1)-t_beg2)
t_beg3 = input('give time difference3')
u_beg3 = interp1(t(n1:n2),u(n1:n2),t(n1+i-1)-t_beg3)
a_beg3 = interp1(t(n1:n2),a(n1:n2),t(n1+i-1)-t_beg3)

% aiii=a(n1:n2).*a(n1:n2).*a(n1:n2)
% aii=a(n1:n2).*a(n1:n2)
aiii=a(n1:n2).^3;
aii=a(n1:n2).^2;
A3=sum(aiii);
A2=sum(aii);
N=length(u(n1:n2));
a3=A3/N;
```

```

a2=A2/N;
aspikes=a3/a2

%mu_u=mean(u(n1:n2))
%Xi=u(n1:n2).*u(n1:n2)
%var=sum((Xi-mu_u).*(Xi-mu_u))/N

Var = var(u(n1:n2));
urms = std(u(n1:n2))

figure(1)
plot(t(n1:n2),u(n1:n2),'r')
hold
plot(t(n1:n2),a(n1:n2),'b')
plot(t(n1+i-1)-t_beg0,u_beg0,'ro')
plot(t(n1+i-1)-t_beg0,a_beg0,'bx')
hold
figure(2)
plot(t(n1:n2),u(n1:n2),'r')
hold
plot(t(n1:n2),a(n1:n2),'b')
plot(t(n1+i-1)-t_beg1,u_beg1,'ro')
plot(t(n1+i-1)-t_beg1,a_beg1,'bx')
hold
figure(3)
plot(t(n1:n2),u(n1:n2),'r')
hold
plot(t(n1:n2),a(n1:n2),'b')
plot(t(n1+i-1)-t_beg2,u_beg2,'ro')
plot(t(n1+i-1)-t_beg2,a_beg2,'bx')
hold
figure(4)
plot(t(n1:n2),u(n1:n2),'r')
hold
plot(t(n1:n2),a(n1:n2),'b')
plot(t(n1+i-1)-t_beg3,u_beg3,'ro')
plot(t(n1+i-1)-t_beg3,a_beg3,'bx')
hold

```

The second m-file is a file that can be used to make the plots as seen in appendix F. Before it can be used the momentary accelerations and velocities have to be declared for all tested wave steepnesses. I did this by making a long list in which each row represented a tested wave steepness. And in the columns I declared all relevant momentary velocities and accelerations. (These matrices are also very useful when determining the maximum momentary wave forces. This will be discussed later.)

Now each movement parameter has to be declared manually. Interacting a file that contains the movement parameter to the program can of course make it fully automatic

```

close all;
n = input('give number of rows : ');
for i=1:n
    j=input([' give color and sign for row number ' num2str(i) ' :'],'s');
    figure(1);
    plot(u0(i),a0(i),j)

```

```

title('movement of at least one large stone, for U and a at t=0s','fontsize',16);
hold on;
figure(2);
plot(u5(i),a5(i),j)
title('movement of at least one large stone, for U and a at t=-0.05s','fontsize',16);
hold on
figure(3);
plot(u10(i),a10(i),j)
title('movement of at least one large stone, for U and a at t=-0.10s','fontsize',16);
hold on
figure(4);
plot(u15(i),a15(i),j)
title('movement of at least one large stone, for U and a at t=0.15s','fontsize',16);
hold on
figure(5);
plot(urms(i),aspikes(i),j)
title('movement of at least one large stone, for Urms and aspikes at t=0s','fontsize',16);
hold on
figure(6);
hu=max([a0(i) a5(i) a10(i) a15(i)]);
plot(u0(i),hu,j);
title('movement of at least one large stone, for Umax and amax','fontsize',16);
hold on;
if j=='r*'
    h=0;
elseif j=='m*'
    h=0.5;
else h=1;
end
figure(7);
plot(aspikes(i),h,'bo');
title('movement of at least one large stone, for aspikes','fontsize',16);
hold on
end

for t=1:6
    figure(t);
        xlabel('velocity (m/s)','fontsize',16);
        ylabel('acceleration (m/s^2)','fontsize',16);
        set(gca,'fontsize',14)
end
figure(7)
xlabel('aspikes (m/s^2)','fontsize',16);
ylabel('movement','fontsize',16);
set(gca,'fontsize',14)

```

The maximum momentary wave forces can be determined with use of the following file. Again each movement parameter has to be declared manually in it.

```

close all;

n = input('give number of rows : ');
bulk = input('contribution of velocity^2, bulkcoefficient Cb 1st choice : ');
cm = input('contribution of accelerations, coefficient Cm 1st choice : ');
d = input('diameter of stones : ');
for i=1:n
    j=input([' give color and sign for row number ' num2str(i) ':' ],'s');
    if j=='r.'
        h=0;
    elseif j=='g.'
        h=0.5;
    else h=1;
    end
    F1(i)=(0.5*u0(i)*u0(i)*d*d*1000*bulk)+(cm*a0(i)*1000*d*d*d);
    F2(i)=(0.5*u5(i)*u5(i)*d*d*1000*bulk)+(cm*a5(i)*1000*d*d*d);
    F3(i)=(0.5*u10(i)*u10(i)*d*d*1000*bulk)+(cm*a10(i)*1000*d*d*d);
    F4(i)=(0.5*u15(i)*u15(i)*d*d*1000*bulk)+(cm*a15(i)*1000*d*d*d);
    F(i)=max([F1(i) F2(i) F3(i) F4(i)]);
    figure(1);
    plot(F(i),h,j,'markersize',24);
    title ('Maximum forces for big stones, with Cb=1 and Cm=1 ','fontsize',16);
    hold on
end

for t=1
    figure(t);
    xlabel('Maximum force(N)','fontsize',16);
    ylabel('movement ','fontsize',16);
    set(gca,'fontsize',12)
end

```

Of course it is always possible to change these listing or to use other listings.

1.2 Lists used during tests

On the next page a list has been given. Such a list was used during the experiments. On it all steps to be taken are listed. During each test the number of moved stones had to be registered on these forms.

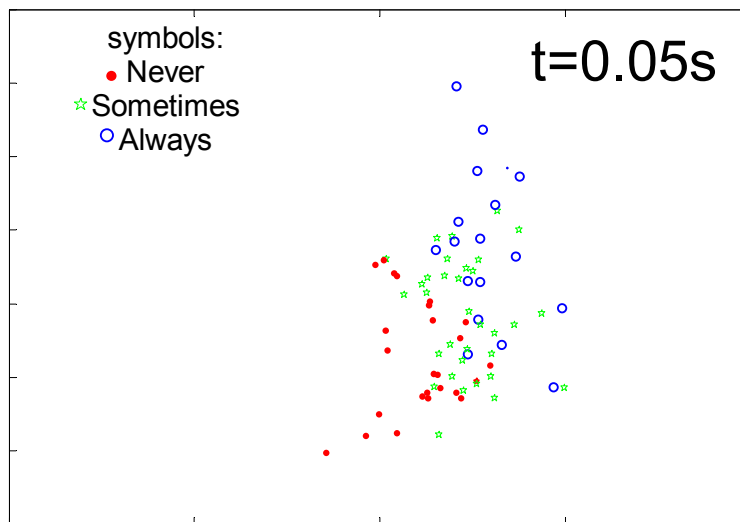
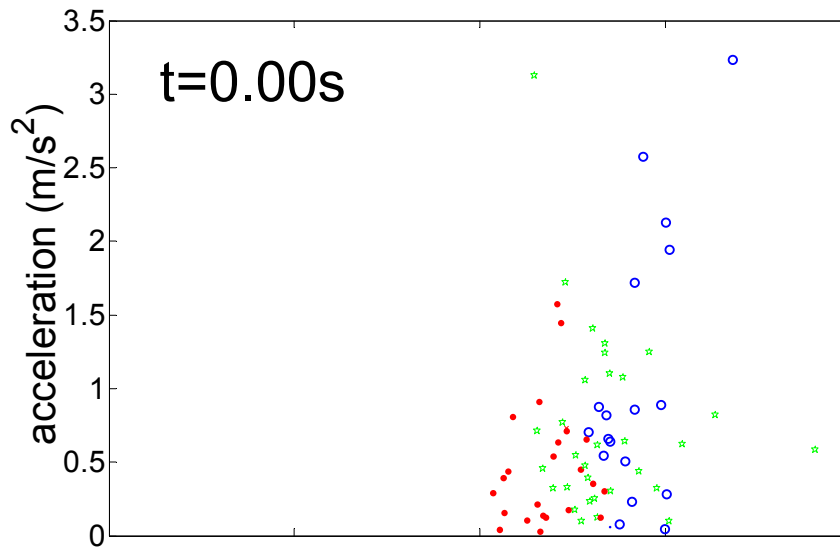
Experiment nr. ; date , h0 = cm									nr. of stones moved	
run nr.	color	average distance	period	wave height	breaking point	breaker type	max. velocity	max. acceleration	after 50 waves	after 100 waves
1	blue	21.60	2	10						
	orange	20.95	2	10						
	yellow	20.30	2	10						
	green	19.65	2	10						
	pink	19.00	2	10						
2	blue	21.60	2.25	10						
	orange	20.95	2.25	10						
	yellow	20.30	2.25	10						
	green	19.65	2.25	10						
	pink	19.00	2.25	10						
3	blue	21.60	2.5	10						
	orange	20.95	2.5	10						
	yellow	20.30	2.5	10						
	green	19.65	2.5	10						
	pink	19.00	2.5	10						
4	blue	21.60	2.75	10						
	orange	20.95	2.75	10						
	yellow	20.30	2.75	10						
	green	19.65	2.75	10						
	pink	19.00	2.75	10						
5	blue	21.60	3	10						
	orange	20.95	3	10						
	yellow	20.30	3	10						
	green	19.65	3	10						
	pink	19.00	3	10						
6	blue	21.60	3.2	10						
	orange	20.95	3.2	10						
	yellow	20.30	3.2	10						
	green	19.65	3.2	10						
	pink	19.00	3.2	10						
7	blue	21.60	3.4	10						
	orange	20.95	3.4	10						
	yellow	20.30	3.4	10						
	green	19.65	3.4	10						
	pink	19.00	3.4	10						
8	blue	21.60	3.6	10						
	orange	20.95	3.6	10						
	yellow	20.30	3.6	10						
	green	19.65	3.6	10						
	pink	19.00	3.6	10						

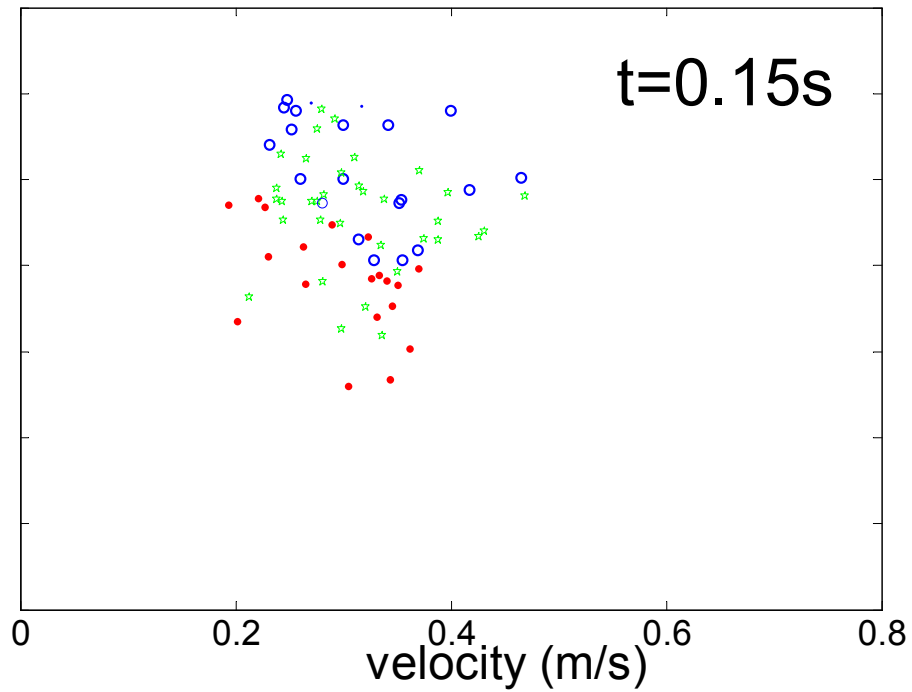
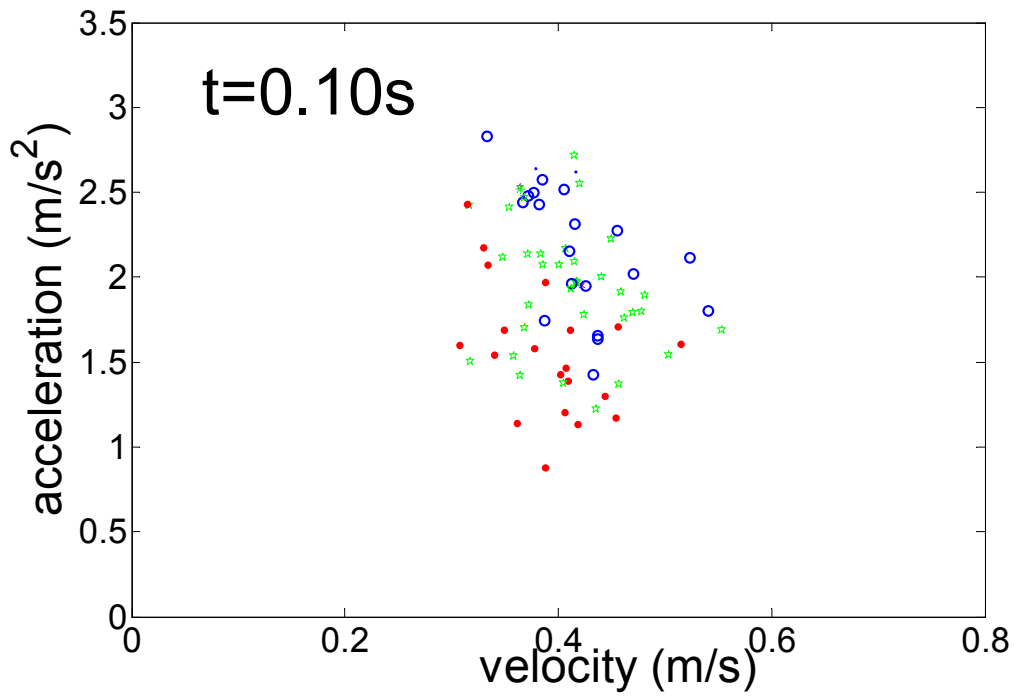
Appendix F

Large plots of stone movement from chapter 5

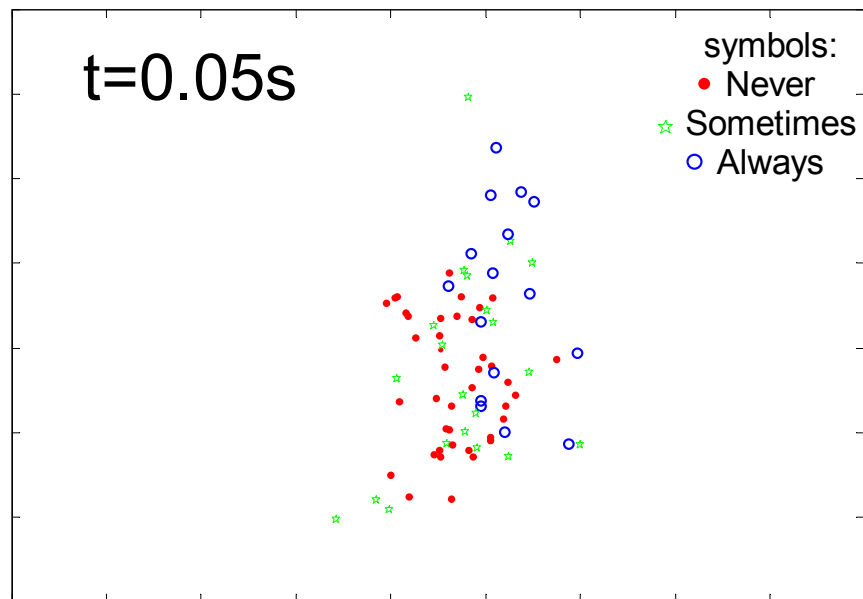
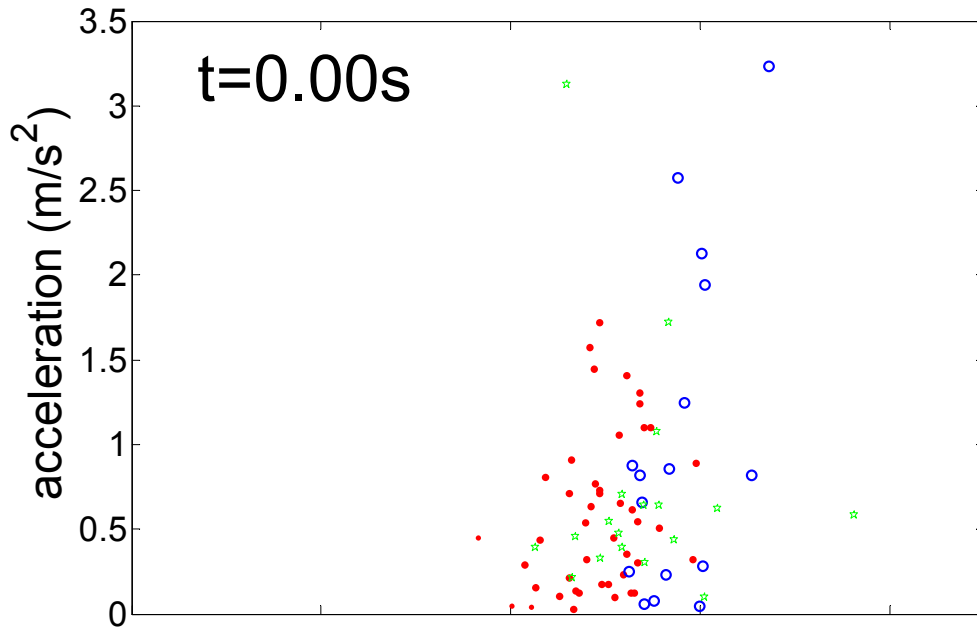
In this appendix some plots that are shown in the report in chapter 5 are represented larger. It are the plots that describe the statistical movement parameter of a stone as a function of the velocity and of the acceleration. Each time the same figure nr. will be used as in the report. Also the used definition of threshold of motion is given for each plot.

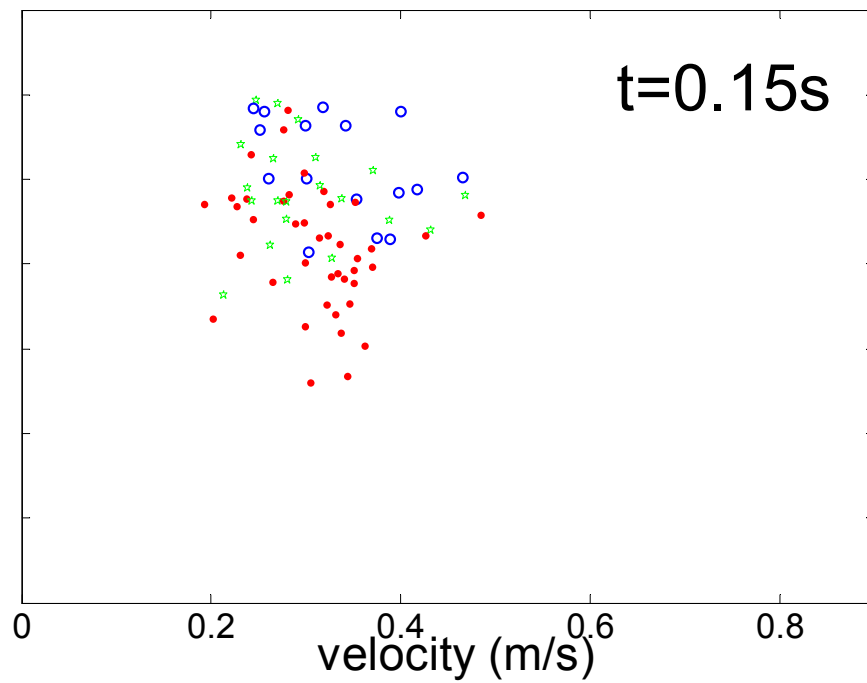
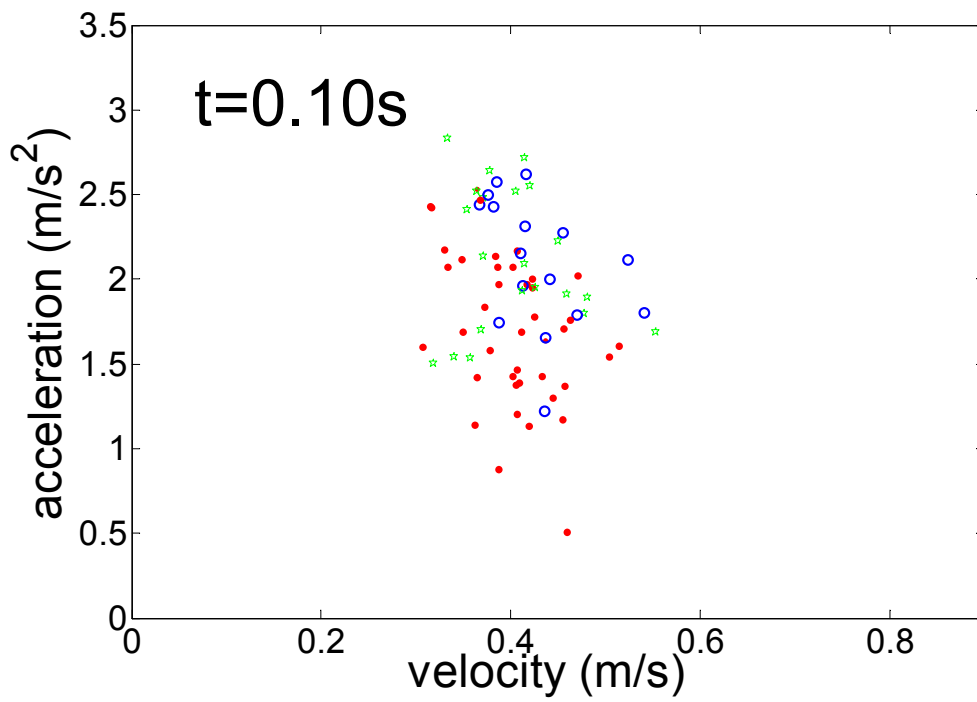
Movement of at least one large stone, which is Figure 5.2-2



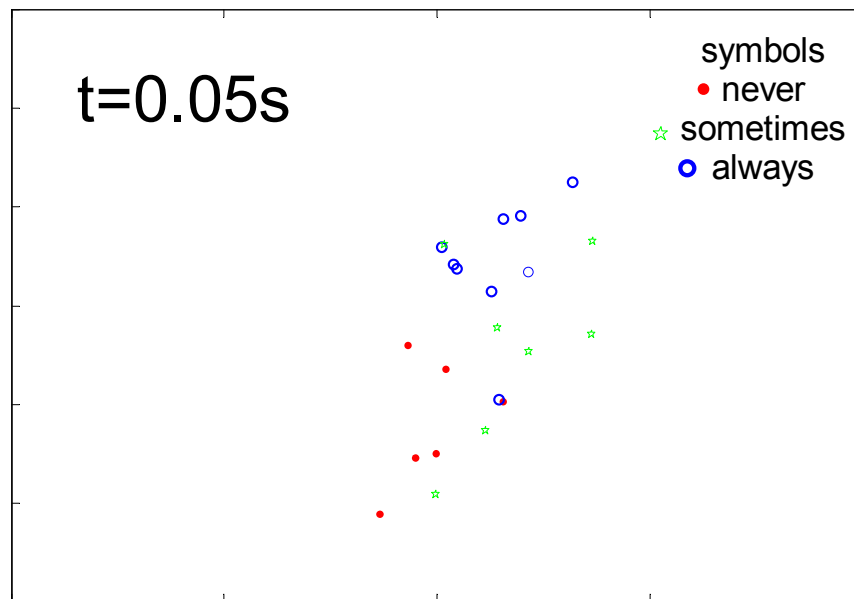
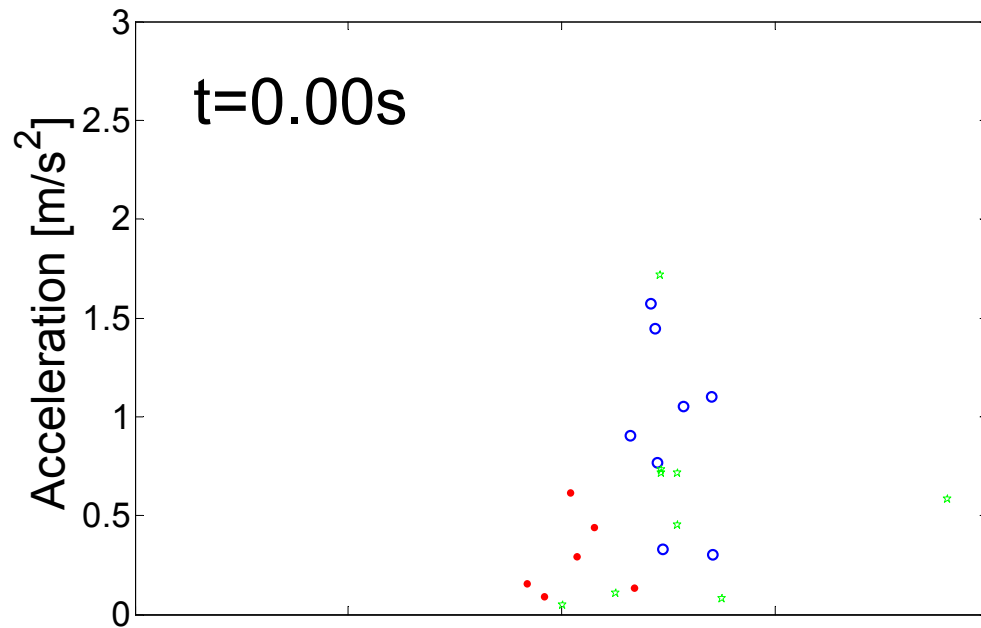
More movement of at least one large stone of Figure 5.2-2

Cumulative movement of at least 4 large stones which is Figure 5.2-3

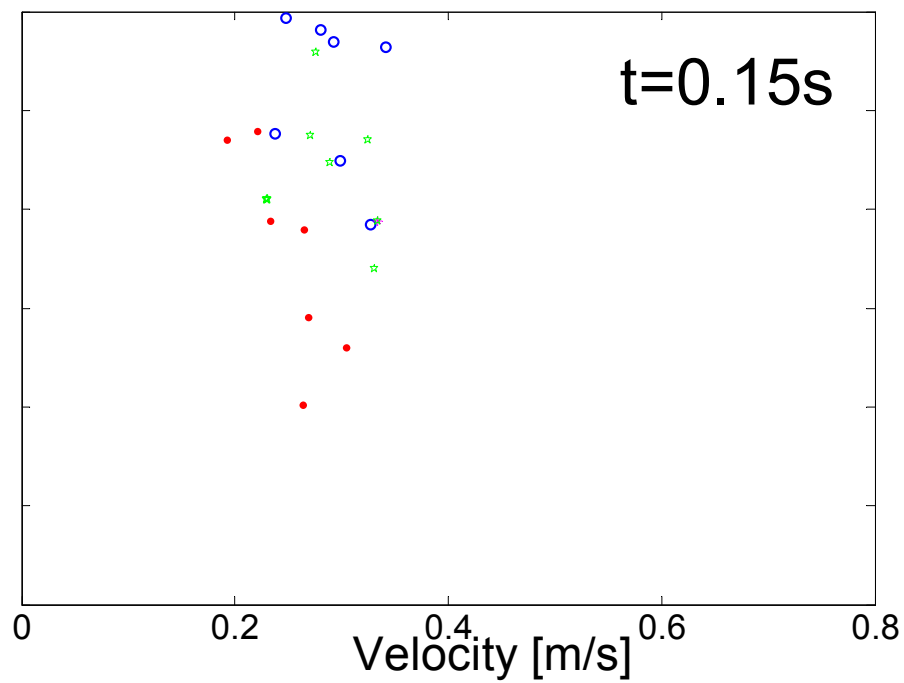
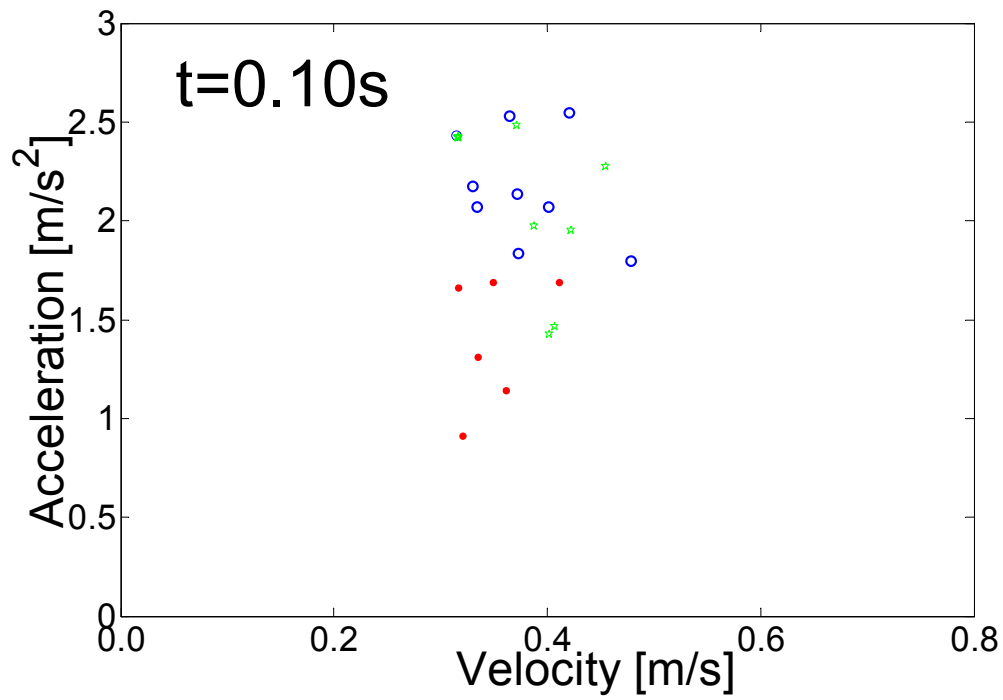


More Cumulative movement of at least 4 large stones

Movement of at least 1 small stone, which is Figure 5.2-4 in report



More movement of at least 1 small stone



Appendix G

Flow time entrainment

Entrainment has been defined as the number of stones that move per unit area per unit time:

$$E = \frac{n}{AT} \quad (G.1)$$

All parameters that are required for usage of this formula are available. A problem however arises when determining the time for which the stones are subject to the wave flows.

As the wave steepness is increased after every 100 waves it becomes difficult to predict what time should be used. Consider the following:

If a stone starts to move for the first series of waves as used in a test it is easy to tell, that the required time is the time of the first series of waves. Now consider stones that have not moved during the first series of waves, but that do start to move in the second series of waves, which has increased wave steepness. Because most times the increase of wave steepness is rather small, it is unknown whether the stones did start to move because of the increased wave forces, or that the stones now move because of a combination of both the wave series. To find this out is not in the scope of this thesis and therefore the following time values will be used.

Two opposite times will be considered

- Only the time for which the required wave steepness has been tested. This is for every tested wave steepness equal to:

Wave period*100*number of tests, in which 100 is the number of used waves

- The total tested time up to the required wave steepness. For each test during which the required wave steepness has been tested this will be the time of the required wave steepness + the time of all previously used wave steepness. So this is a cumulative time.

The actual time, during which a stone is subject to the wave forces, will be a time somewhere between these two boundary values.

For every tested wave steepness an entrainment parameter can be found. This can be done with use of the following steps.

1. Make a long list that contains all tested wave steepnesses. Make for both tested stone diameters such a list. List also for each wave steepness the number of times it has been tested.
2. Count the number of stones that moved for all tested wave steepnesses. This number of stones has to be the number of stones that moved during all tests performed with the same wave steepness. The following should however be considered.
A tests starts by using a mild wave steepness for 100 waves, then the wave steepness is increased and this will also be used for 100 waves. Again the wave steepness will be increased and this goes on and on. The stones that move during the first used wave steepness of a test are no longer available to move for the upcoming waves that have an

increased steepness. In most cases the wave forces will become stronger when the wave steepness is increased. Therefore it will be assumed that the stones that already moved for a milder wave steepness would also have moved for the following steeper wave steepness. (This is not exactly true because due to phase shifts the wave forces are not always stronger for steeper waves, but this has just been done as a pilot research, so future investigations should consider these phase lags).

Because of the above, the number of moved stones for a tested wave steepness should also contain the number of stones that already left for wave steepness that have been used before in the same test series.

3. Determine for all wave steepness the duration of the acting flow. As mentioned this must be done in two ways. Doing so results in two different entrainment times. The actual value should be somewhere between these values.

With use of the above steps it is now possible to determine the entrainment parameter for all the tested wave steepness. The two different times result in two different entrainment values.

Both methods have been tried. The cumulative time resulted in high values of the entrainment parameter and the other method had much lower values. However they both showed more entrainment for larger values of the wave forces. The direction of the cloud of points was also similar. So probably the actual value will probably be a flow time somewhere between the two explained times.

It is obvious that more research has to be done to find a correct method of testing the threshold of motion in an orbital wave motion.

Appendix H

Detailed wave analysis

H.1 Introduction

The wave behavior in the flume is very important during the experiments. Therefore in advance of the analysis on the influence that fluid accelerations have on the threshold of motion, has been performed, a detailed wave analysis has been performed. Its most relevant details have already been discussed in the report.

In this appendix the entire analysis will be shown.

H.1 Shoaling

As waves travel into water of decreasing depth the wave height increases and the wave profiles become more peaked. This effect is known as shoaling. The waves used in the experiments will also shoal due to the presence of the slope.

An example of such a shoaling wave in the wave flume can be seen in figure H.1.1.

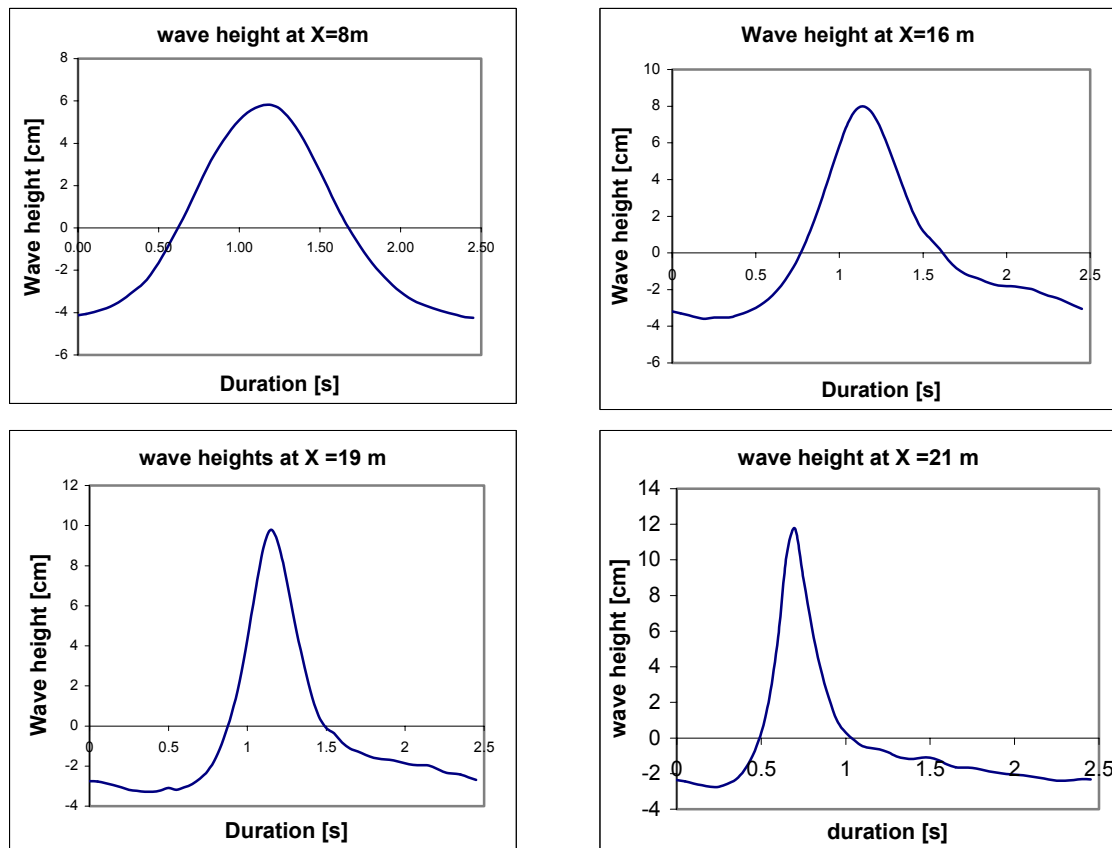


Figure 0-1 Wave heights and wave forms at various locations for $H=0.1$ m, $T=2.5$ sec and $h=0.55$ m

It can be clearly seen that an asymmetric wave pattern develops as the water depth decreases. The wave front (the left side of the wave) becomes steeper and the wave tops grow, while the troughs get smaller amplitudes. It can also be seen that the waveform becomes skewed. This will be discussed later.

H.1.1 Breaking point of the waves

Only movement under waves that haven't broken yet will be investigated. During the experiments the breaking point of the waves was observed visually. This was not a very accurate manner, and it was hard to determine this breaking point. In case of doubt, it is now possible to determine the breaking point with the use of the collected wave heights. When the waves break, a drop in the wave height arises. Figure XX shows the development of the wave heights in the longitudinal direction.

The distance in cm between the maximum height and the minimum height line corresponds to the amplitude of the wave height at that location. For example in figure A, the wave height before the slope is $6+4 = 10\text{cm}$. And the wave height grows due to shoaling towards $11,8\text{ cm}$ at $X=16$ and even to $14,4\text{ cm}$ at $X=21\text{m}$. The origin of the toe of the slope is at $X=8,70\text{ m}$. The wave height there is about 10 cm ; this is also what was expected, because the wave generator was instructed to make a wave with a wave height of $0,1\text{m}$.

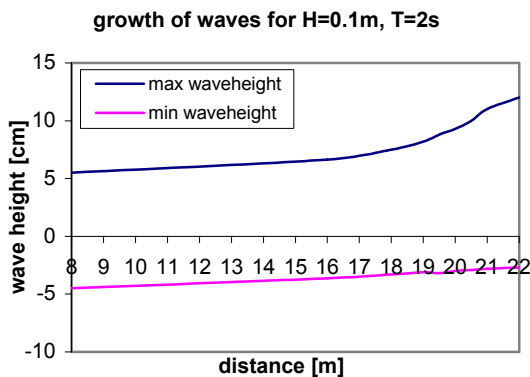


Figure A

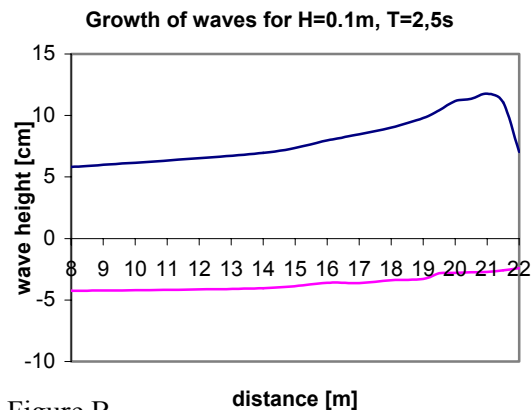


Figure B

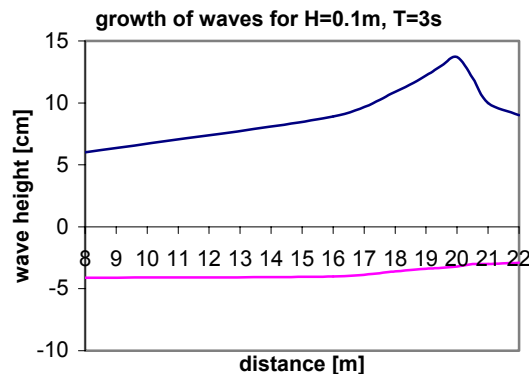


Figure C

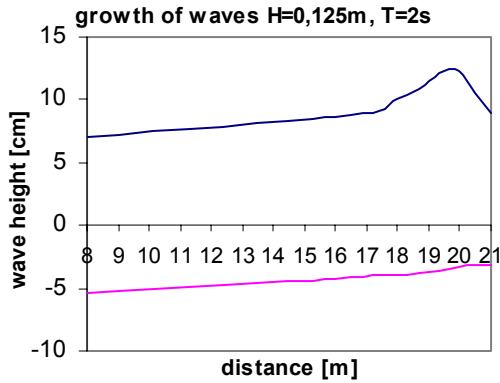


Figure D

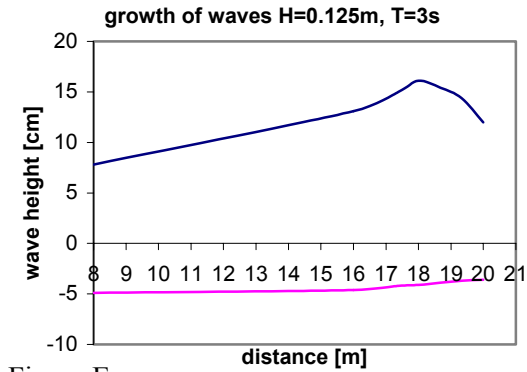


Figure E

Figure H.2-0-2 Growth of wave height for various waves in depth of $h_0=55\text{cm}$

It can be seen that for increasing wave heights the breaking point moves towards the wave board (compare figure A vs. D and figure C vs. E). The same phenomenon occurs for increasing wave periods (note the steeper wave growth of waves with same height but larger period; compare figure A, B and C and compare figure D and E).

For relative deep water the increase of the wave height grows linear along the slope. This linearity however is not valid for the entire growth. From a certain depth this growth increases. In theory this will also yield to increasing horizontal near-bed velocities. The waves are chosen such that this increasing growth of both waves and velocities occurs in the measuring area, between $X=16$ and $X=21\text{m}$.

H.2 Reflection

The reflection of regular waves on the slope is assumed to be negligible. To ensure this a test with two wave gauges has been conducted. Doing so, two wave gauges must be placed at a distance of about $\frac{1}{4}$ wavelength from each other just before the toe of the slope. The gauges have been placed at the following locations for the different wave scenarios. Longer periods couldn't been used, because the wave pattern needs some distance to be fully grown and if longer periods were tested the first wave gauges would be placed in a location where the waves haven't been fully grown yet.

Test	GHM 1	GHM 2	Wave Test
1	$X = 7,87 \text{ m}$	$X = 8,60 \text{ m}$	$T = 1.5\text{s}; H = 0.15\text{m}; h = 0.55\text{m}$
2	$X = 7,55 \text{ m}$	$X = 8,60 \text{ m}$	$T = 2\text{s}; H = 0.15\text{m}; h = 0.55\text{m}$
3	$X = 7,55 \text{ m}$	$X = 8,60 \text{ m}$	$T = 2\text{s}; H = 0.10\text{m}; h = 0.55\text{m}$

Table H-1 Location of wave gauges (GHM)

The elementary equation for a regular wave passing a wave gauge at location $X=x_1$ is given by the following equation *Goda and Suzuki, (1973)*.

$$\eta(x_1, t) = \sum_{n=1}^N a_{i,n} \cos(k_n x_1 - \omega_n t + \phi_{i,n}) + \sum_{n=1}^N a_{r,n} \cos(k_n x_1 + \omega_n t + \phi_{r,n}) \quad (\text{H.1})$$

in which:

η = surface elevation of water
 t = time
 $a_{i,n}$ = amplitude of the n^{th} - harmonic of the incoming wave
 $a_{r,n}$ = amplitude of the n^{th} - harmonic of the reflecting wave
 k_n = wave number of the n^{th} - harmonic
 ω_n = angular frequency of the n^{th} - harmonic
 $\phi_{i,n}, \phi_{r,n}$ = phase of the n^{th} - harmonic of the incoming and the reflecting wave,
 respectively

Only the first harmonic has to be considered, when determining the reflection. So no higher harmonics, nor free or bounded harmonics have to be taken into account.

If only the first harmonic has to be considered then (1) can be written as follows

$$\eta(x_1, t) = a_i \cos(kx_1 - \omega t + \phi_i) + a_r \cos(kx_1 + \omega t + \phi_r) \quad (\text{H.2})$$

This can be rewritten as:

$$\eta(x_1, t) = a_i \{ \cos(kx_1 + \phi_i) + \sin(kx_1 + \phi_i) \sin(\omega t) \} + a_r \{ \cos(kx_1 + \phi_r) \cos(\omega t) - \sin(kx_1 + \phi_r) \sin(\omega t) \} \quad (\text{H.3})$$

or :

$$\eta(x_1, t) = A_1 \cos(\omega t) + B_1 \sin(\omega t) \quad (\text{H.4})$$

in which:

$$A_1 = a_i \cos(kx_1 + \phi_i) + a_r \cos(kx_1 + \phi_r) \quad (\text{H.5})$$

$$B_1 = a_i \sin(kx_1 + \phi_i) + a_r \sin(kx_1 + \phi_r) \quad (\text{H.6})$$

The above holds for every wave that passes wave gauge number one. As there are two wave gauges, the waves will also pass the location of the second wave gauge. Here the same formulae can be applied as for the waves passing the first gauge, except that x_1 becomes x_2 . After performing the same steps for location $X = x_2$, this leads to the following complex equations for the waves at the two wave gauges.

$$A_1 + B_1 = a_i e^{ikx_1} e^{i\phi_i} + a_r e^{-ikx_1} e^{-i\phi_r} \quad (\text{H.7})$$

$$A_2 + B_2 = a_i e^{ikx_2} e^{i\phi_i} + a_r e^{-ikx_2} e^{-i\phi_r} \quad (\text{H.8})$$

With use of the program “Refreg” these equations can be solved.

The results are as follows:

Test	Wave Test	Reflection
1	T=1.5 sec; H=0.15m; h=0.55m	1.3 %
2	T=2 sec; H=0.15m; h=0.55m	1,2 %
3	T=2 sec; H=0.10m; h=0.55m	1,2%

Table H-2 reflection of the slope

As seen in table H-1 the influence of reflections from the slope is sufficiently small to be neglected. So the assumption to neglect the influence of reflection has been justified.

H.3 Validation of EMS data

In the appendix A the problems that arise when transmitting EMS data have been discussed. It became clear that the quality of the EMS data was dependent on the range of the filter. Appendix A also made clear how the original signal could be reconstructed out of the filtered output data. So far it has been left out of consideration whether the obtained data will be valid or not to use in the analysis. This section will treat with this problem and will lead to rejection or approval of specific EMS data.

Harmonical analysis and correction for the frequency-dependent filter capacities can lead to reconstruction of the original measured data. To find out whether these reconstructed values are corrected properly the corrected values will be compared to values obtained with the use of a computer calculation.

H.3.1 RF wave

The computer calculation that will be used as reference is known as RF-wave. It is a program, which can be used to compute the velocities under waves and Ab van Dongeren has developed it. In the program can be used to calculate near-bed velocities by higher order Stokes computations. How the program works is explained below. Only for this experiment relevant use of RF-wave will be discussed in this section

The first relevant menu of RF-wave is the declaration of the parameters. The following parameters can be used as input data

- Mean water depth h
- Wave period T
- Wave height H
- Number of Fourier components N
- Water mass density ρ
- Gravitational acceleration g

The gravitational acceleration g and the Water mass density ρ are constant during all tests. The other parameters will be used as varying parameters.

The model applies for water of constant depth and not for sloping beds. But because of the mild slope the water depth at a given distance of the wave board can be assumed as constant for a small stretch.

Knowing the slope and the location of the toe of the slope can determine the Still water level at every required location. After taking snap checks at some locations these calculated values

seemed to be smaller than the actual measured water depths, inclination of the concrete of the slope is probably the main reason for these differences. Hence, a leveler must be used to find the exact water depth at the required positions.

Doing so the values for the variable parameter h have been found.

The maximum number of Fourier components to be used in the program is 32. This has also been chosen as default. Sometimes in very shallow water the program jammed, when using 32 Fourier components, in these cases less components have been used. As a check on the influence of the harmonical components, sometimes, the same case has been calculated, with a varying number of components. It turned out that in both cases the velocities were equal and that the influence of the low order harmonics was also quite similar.

The wave period T is the easiest to find variable parameter. It is of course the wave period of the generated waves, which horizontal velocities are to be controlled.

Finally, the wave height has to be given as variable parameter. This is the wave height at location of the required velocity. It can be obtained from the wave gauge data. From this data the wave height at location X can be found as this value needs to be given as parameter to RF-wave.

After declaring the parameters it is possible to give the elevations at which the horizontal velocity has to be computed. Because the near-bed velocity measurements with EMS have been performed at an height of 4-5 cm above the bed, these elevations are easy to find with use of parameter h . Note that the elevations are negative.

After completing the above steps the program RF-wave will compute the required velocities and much more. Relevant for the experiment are of course the velocities at an elevation of 4cm above the bed and furthermore, the value of the first four Fourier components.

For many wave steepness, multiple water depths and at various locations these values have been calculated with use of RF-wave.

H.3.2 Comparison between measured values and RF-wave

In the ideal case, the velocities calculated with the computer program will have the same values as the from output data reconstructed velocities (the measured velocity before transmission of data). In shallow water and on a slope as in the wave flume during the experiment, this is however not the case.

Waves traveling in shallow water are built up out of many harmonical components. Summarizing all these components leads to the complex velocity profile.

The complex signal can be represented as:

$$f(t) = c_0 + \sum_{n=1}^{\infty} c_n \cos(n\omega_0 t + \varphi_n) \quad (\text{H.9})$$

In which each harmonical order component can be written as

$$c_n \sin(n\omega_0 t + \varphi_n) \quad (\text{H.10})$$

As seen in the above equations each harmonical component consists of a frequency, which is related to the basic frequency ω_0 , and each component consists of a phase. The frequency will remain constant for waves traveling into water of decreasing depth, but the phase will change. Due to this change of phases from the various harmonical components the summarization of the harmonical components will almost never be a summarization of the maximum values for the amplitudes of the harmonics. More of this Phase lag will be discussed in this appendix. The amplitude of the horizontal velocities obtained from RF-wave is a summarization of the amplitudes of all computed harmonical components and the mean Eulerian velocity (\bar{u}). This summarized velocity will of course be larger than the velocities found with measurements, which have phase lags. This leads to the following approach, in which the amplitudes of the first four harmonical components, obtained with RF-wave will be compared with the first four harmonical components of the measured signal. The harmonical components of the measured signal must be obtained by doing harmonical analyses on the output signal and need to be corrected for damping of the EMS filter. As explanation, this comparison will be made for the following cases. [See appendix A for finding and correcting harmonical components]

In the last column the summarization of all harmonical order components has been made. This is equal to the velocity that would occur when all harmonics are in phase (and stay in phase). Also the average velocity \bar{u} (which is equal to the 0th Harmonic order component and is always negative) has been included in this summarization.

	1 st component	2 nd component	3 rd component	4 th component	Max velocity
1 st EMS	0.1693	0.0578	0.0166	0.0036	0.2263
2 nd EMS	0.2264	0.0804	0.0192	0.0037	0.3176
RF-wave	0.2304	0.0867	0.0221	0.0048	0.3164

Table H-3 Comparison of first four harmonical components for H=0.10m, T=2s, h=55cm at X=18m, waves break at 21.6m

	1 st component	2 nd component	3 rd component	4 th component	Max velocity
1 st EMS	0.1665	0.0886	0.0367	0.0132	0.2738
2 nd EMS	0.2163	0.1244	0.0550	0.0170	0.3888
RF-wave	0.2125	0.1227	0.0563	0.0222	0.3840

Table H-4 Comparison of first four harmonical components for H=0.10m, T=2s, h=55cm at X=20m, waves break at 21.6m

It can be seen that the values obtained with the first EMS are much lower than the values obtained with RF-wave and the values of the second EMS. Furthermore it appears that the values of the second EMS are about the same as the values from the physical model. Only the fourth harmonical order component is smaller for the 2nd EMS, the cause of this is probably that the first frequency-dependent damping of the filter will occur for these frequencies (about 2 Hz). By doing the same for a wave with a period of 3 seconds this can be checked, because the frequency of the fourth component is 1,33 Hz, so the difference between the 2nd EMS and the physical should be much smaller in this case. In the tables the period has been increased and the same comparison between the data from the EMS and the RF-wave data will be made.

	1 st component	2 nd component	3 rd component	4 th component	Max velocity
1 st EMS	0.1308	0.0847	0.0534	0.0239	0.2768
2 nd EMS	0.1942	0.1243	0.0779	0.0356	0.4387
RF-wave	0.206	0.1396	0.0785	0.0387	0.4563

Table H-5 Comparison of first four harmonical components for H=0.10m, T=3s, h=55cm at X=18m waves break at 20.4m

	1 st component	2 nd component	3 rd component	4 th component	Max velocity
1 st EMS	0.1208	0.0978	0.0699	0.0428	0.3313
2 nd EMS	0.1632	0.1437	0.0925	0.0560	0.5114
RF-wave	0.1358	0.1148	0.0888	0.0642	0.472

Table H-6 Comparison of first four harmonical components for H=0.10m, T=3s, h=55cm at X=20m waves break at 20.4m

It appears that when the waves become very steep and almost break, that the values of the 2nd EMS and RF-wave are no longer of the same magnitude. Because it is impossible to draw conclusions from only the above example an analysis of this phenomena has been made. For waves with a constant period and a constant wave height, the influence of the first four Fourier components has been investigated for both the measured signal with the 2nd EMS and the RF-wave programl, at various locations. The locations are chosen such, that every location is nearer to the breaking point and that the in the final location the waves are already broken. The results are:

	1 st component	2 nd component	3 rd component	4 th component	Max velocity
2 nd EMS	0.2628	0.0836	0.0208	0.0048	0.3431
RF-wave	.2550	.0851	.0195	.0034	0.3298

Table H-7 Comparison of first four harmonical components for H=0.125m, T=2s, h=55cm at X=16.73m. Break at 19.8m

	1 st component	2 nd component	3 rd component	4 th component	Max velocity
2 nd EMS	0.2703	0.0981	0.0240	0.0069	0.3743
RF-wave	0.2598	0.0977	0.0262	0.0055	0.3531

Table H-8 Comparison of first four harmonical components for H=0.125m, T=2s, h=55cm at X=17.38m. Break at 19.8 m

	1 st component	2 nd component	3 rd component	4 th component	Max velocity
2 nd EMS	0.2595	0.1108	0.0341	0.0087	0.3836
RF-wave	0.259	0.1141	0.0369	0.0096	0.3789

Table H-9 Comparison of first four harmonical components for H=0.125m, T=2s, h=55cm at X=18m. Break at 19.8 m

	1 st component	2 nd component	3 rd component	4 th component	Max velocity
2 nd EMS	0.2708	0.1218	0.0416	0.0149	0.4175
RF-wave	0.2489	0.1254	0.0482	0.0156	0.3968

Table H-10 Comparison of first four harmonical components for H=0.125m, T=2s, h=55cm at X=18.68m. Break at 19.8m

	1 st component	2 nd component	3 rd component	4 th component	Max velocity
2 nd EMS	0.2462	0.1296	0.0556	0.0200	0.4239
RF-wave	0.196	0.1173	0.0581	0.0262	0.3689

Table H-11 Comparison of first four harmonical components for H=0.125m, T=2s, h=55cm at X=19.33m. Break at 19.8 m

	1 st component	2 nd component	3 rd component	4 th component	Max velocity
2 nd EMS	0.2436	0.1422	0.0664	0.0274	0.4681
RF-wave	0.176	0.1187	0.0682	0.0359	0.3754

Table H-12 Comparison of first four harmonical components for H=0.125m, T=2s, h=55cm at X=20m. Break at 19.8 m

The first thing that occurs is that the velocities of the 2nd EMS are larger than the velocities found with the physical model. For waves far away of the breaking point, this difference is very small, but as the waves near the breaking point this difference increases. When looking at the 2nd to the 4th order component, it can be seen that the values of both model and measurement are equal, before breaking (see table 1-8 to 1-11). So it appears that only the values of the 1st order harmonical component of the measured signal are larger than the 1st order harmonical components of RF-wave. This difference between the values of the 1st harmonical component increases as the waves near their breaking point.

A second striking difference is that the measured velocities increase, as the waves near their breaking point, while in the model the velocities decrease as the water becomes shallower. Even when the waves are already broken the velocities in the measurement still increase and are still a lot higher compared to those of the model.

The second phenomenon can be explained by the fact that the output of RF-wave is related to the wave height. As the wave height increases the velocities will also increase. After the waves have broken the wave height becomes less, so in RF wave the velocities will become less, while in reality, the velocities are still large under breaking waves.

The first phenomenon is probably caused due to differences between model and reality and therefore it doesn't mean that wrong velocities have been measured. Some reasons that can give cause to the differences between model and measurements near the breaking zone are:

- Model uses a horizontal bed, while in the experiment there is sloping bed.
- The phase lag in both waves and velocities
- Influence of the bed roughness, which is not used as a parameter in RF
- Presence of breaking waves in the experiment, that causes turbulent velocities and return currents, which are not present in the model.

Despite the differences, that occur near the breaking zone of the waves the velocities of the measured waves are more or the less equal to those found with a model. The velocities of waves

at a distance of the breaking zone even show exact the same values for the first four harmonical components. So using data obtained with the second EMS can be considered, as using data that has sufficient resemblances with the actual occurring velocities in the wave flume.

H.3.3 Final verifications

Finally before accepting or rejecting data the influence of the harmonical components needs to be analyzed. As the influence of the higher order harmonics is relatively small, then no problems will arise when reconstructing the original signal. If the higher harmonical components have a great influence on the complex velocity signal, then the data will probably not be able to be reconstructed, because the filter has damped some harmonics to a value of zero. For the new EMS, the data seems comparable to the data found with RF-wave, especially for waves that are at some distance from their breaking point. Even the values off the fourth order harmonical components are of the same magnitude. At locations where the influence of the higher order harmonical components becomes inevitable the velocities of the higher order harmonics are still of the same magnitude as the ones obtained from the model. As the difference between the model and the measurements is mainly caused by the difference of the amplitudes of the 1st order harmonics there seems no problem in accepting the data obtained with the second EMS.

Precautions still have to be taken for phase and time delays because of the filtering.

The data obtained with the primary used EMS, however, shows for every harmonical component big differences. This can be partly subscribed to the underestimation of the velocities, but mainly due to the wrongly installed filter. For deep water the data can still be reconstructed, because the declination due to the frequency-dependent filtering of the harmonical signals is known, but as the water depth decreases this becomes (almost) impossible.

Especially the shape of the velocity profile, required for finding the accelerations will be influenced by the higher harmonical components. This is of course valid for both, the old and the new EMS, but the new one has a filter that has better properties for the given frequencies*. The range of the old EMS is up to a frequency of 3 Hz. For higher frequencies the data will be filtered out. To find proper velocities probably a range up to 3 Hz is enough, because the influence of the harmonical order components with a frequency bigger than 3 Hz can surely be neglected. The shape, however, required to find the accelerations, will in some cases still be influenced when data larger than 3 Hz is filtered out. This uncertainty whether the correct shape can be reconstructed makes use of the data unreliable.

*Note: The range of the new EMS is up to higher frequencies. In the previous section has been proved that up to the 4th order components no filtering problems have arisen. If filtering takes place from on in the worst case the 5th and higher order components this will not lead to large deviations of the shape, because the firstly filtered components will only be damped a little and that shouldn't harm the profile a lot. The first truly damage due to filtering will then occur from on the 8th order components. The values and influence of these 8th or higher order components are negligibly small, so no problems are to be expected when using the new EMS.

Additionally the old EMS also showed a large frequency-dependent time delay. Using the EMS simultaneously with the wave gauges now becomes very inaccurate, because of the frequency-dependent time-delay differences between the two instruments.

H.3.4 Concluding

After the verification steps decisions can be made whether data is to be accepted or rejected. The data obtained with the old EMS proved to be unreliable because of the uncertainties in reconstructing the signal. This, and the fact that reconstruction of all measured signals for, the frequency-dependent filtering, the frequency-dependent time-delay and the frequency-dependent underestimation of velocities (see appendix A) will take a very big effort, that isn't feasible in the

time estimated for this project, will lead to rejection of all data obtained with the firstly used EMS.

Data obtained with the second EMS can be accepted. In cases of doubt it can be useful to do a harmonical analysis onto the data to check whether this doubt is justified, but normally no problems will arise when using data obtained with the 2nd EMS.

Because of the unexpected rejection of the primary obtained data and the limited time, it is no longer viable to complete the experiment as intentioned. Therefore in the context of this thesis only the measurements and experiments with a water depth of 55cm at the wave board will be fulfilled. To do so all required measurements with a water depth of 55 cm have been redone with the new EMS.

Emmanuel Terile will do the measurements required for the tests in a water depth of 65cm. He will also analyze that data. After completion of both thesis's, the results can be compared and a eventual influence of water depth on the results can be found.

H.4 Velocity analysis

The vertical and horizontal fluid motion differ 90° in phase. This corresponds to a revolting turn along a circle, the so-called orbital motion, *Battjes* (1990) Due to non-linear movement, these circles are not entirely closed, but describe in one period a relative small net horizontal movement.

The values of kh (the product of the wave number and water depth) determine the relative quantities of the water motion velocities.

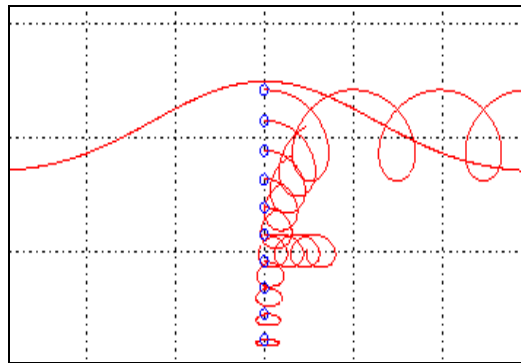


Figure H.4-0-1 non linear orbital movements of water particles

The vertical water motion reduces to zero near the bottom. The vertical accelerations on the bed are also assumed to be infinitely small, and can therefore also be neglected. This doesn't mean that no vertical water motion forces try to move the grains in the bed. Turbulent movements near the bed due to irregularities of the bed and flow irregularities create turbulent forces that can act on the grains and try to lift up the grains. Creating a uniform slope, with carefully placed grains of the same size and by sufficient water working time this influence can be minimized.

In the experiment it is assumed that the horizontal water motion generates the forces that try to move the grains. With an EMS the horizontal flow velocities have been measured during all the tests at various locations near the bed for all types of generated regular waves. The accelerations follow from differentiating these velocities.

H.4.1 Validation of near-bed velocities

The force acting on the stones can be directly related to the orbital horizontal fluid motion near the bed. So the most logical thing to measure will be the horizontal orbital velocity at the bed. This is though, not possible with the EMS. The EMS is based on the Faraday principle of electromagnetic induction. For accurate measurements the probe, in which the measuring electrodes are situated, must be surrounded by a sufficiently big body of water in order to prevent disturbances in the created the electronically fields. This implies for the EMS that it cannot be placed too close to the bed. The minimum height at which the EMS can do its measurements without disturbances of the electronically field is approximately 4 cm above the bed. It is of course important to know whether the values measured at 4 cm above the bed are representative for the near-bed velocities.

The vertical distribution of orbital horizontal velocities can give an insight in this representation of the measurements at 4 cm altitude.

For two waves the horizontal velocities have been measured at an elevation of respectively 4, 6, 8, 10 and 12 cm above the bed. The amplitude of those horizontal velocities at every elevation shows the development of the horizontal distribution in the vertical. If the increase of velocities is gradually between the various heights, then we are dealing with velocities outside the boundary layer. On the contrary if the increase of velocities is very big between the various heights then we know that most of the previously done near-bed measurements have been taken, within the boundary layer.

Note that under waves the boundary layer is growing and declining due to the orbital motion. Therefore the amplitude is a good criterion, because it is the largest value, and hence the biggest boundary layer.

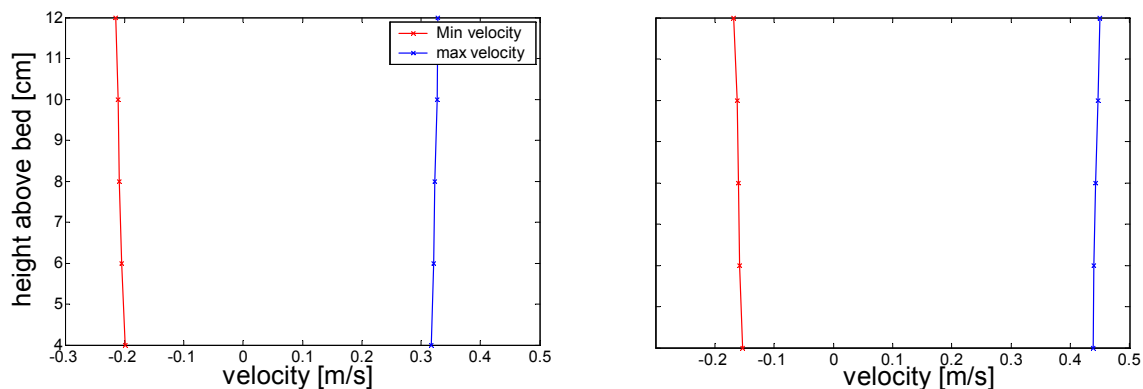


Figure H.4.1-0-2 amplitudes of horizontal velocities at various elevations at 18m for a wave of $H_0 = 0.1\text{m}$, $h_0 = 55\text{cm}$ and on the left $T = 2\text{s}$ and in the right graph $T = 3\text{s}$.

Both graphs show a very small increase of velocities and therefore it can be assumed that the near-bed velocity measurements have been taken outside the boundary layer. The fact that all near-bed velocities have been taken outside the boundary layer means that it's assumable that no velocity fluctuations can be expected due to irregularities in the bed.

It will also be very useful for determining the velocities at the bed, because now common accepted relations can be used to determine the velocities within the boundary layer at the height of the stones.

Booij (1992) found an approximate height of this boundary layer.

$$\frac{d\delta}{dt} = \kappa u_* \approx 0.4 u_* \quad (\text{H.11})$$

In which $u_* \approx 0.1 * u_b$

For the above two examples this leads to a maximum boundary layer height of respectively 1.2cm for the 2s wave and 1.8cm for the 3s wave. This is indeed be very small and verifies the assumption that the velocities that have been measured at 4cm above the bed, were taken outside the boundary layer.

H.4.2 Behavior of near-bed velocities and phase lag

In section H.1 has been shown that the wave front becomes steeper due to shoaling. This shoaling also influences the horizontal velocities and accelerations. Figure H.4.2-1 shows the growth of the near-bed horizontal velocity profile at various locations along the slope. The distances are distances from the wave board, which leads to a decreasing water depth.

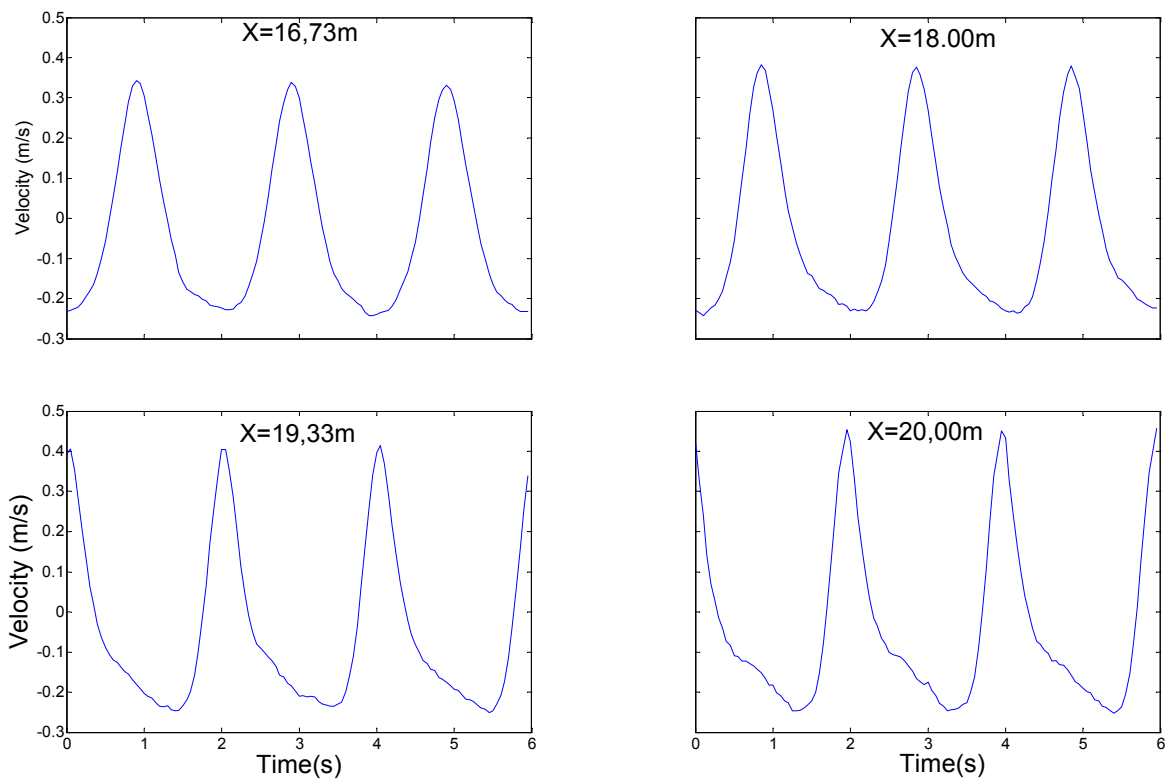


Figure H.4-2-1 Near-bed velocity as waves travel into shallower water for $H=0.125\text{m}$, $T=2\text{s}$ and $h=55\text{cm}$

It can be seen that just like the wave profiles, the velocity profile becomes more peaked at the top and gets a flatter trough. The waves break at $X=20\text{ m}$, this can also be seen in the velocity profile around $X=20\text{m}$. The profile there is very sharply peaked.

It also seems that the velocities will keep increasing due to shoaling. This is however not exactly true. The reason for this is the occurrence of phase shifts.

H.4.3 Phase shifts

The shape of deep-water waves is sinusoidal. The reason for this is that waves in deep water are constructed of only one frequency component. As waves travel into water of decreasing depth the influence of the higher order frequency components becomes more and more evitable and the wave evolves to a more peaked and skewed form. This is represented in figure H.4.3. -1.

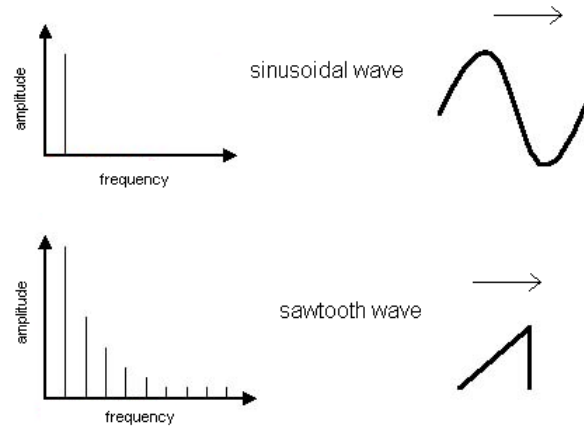


Figure H.4.3-1 Frequency-amplitude spectra and accompanying waveforms.

From harmonical analysis (see appendix XX) it is known that every continuous periodic function can be represented as an infinite sum of harmonic signals with differing angular frequencies ω_0 , whose amplitudes c_n , and phases φ , may also differ, but not necessarily.

So in the experiment the waves can be represented by an infinite sum of harmonic components of water surface elevations and the corresponding velocities under the waves can be made out of an infinite sum of harmonic components of wave velocities.

All these harmonical components of the surface elevations and the near-bed velocities have an amplitude and a phase. The phases of the harmonical components are however not always equal. As the waves travel into water of decreasing depth the phases of the various harmonical components will change independently of each other.

Effects of components that are in phase and components that are out of phase can be seen in

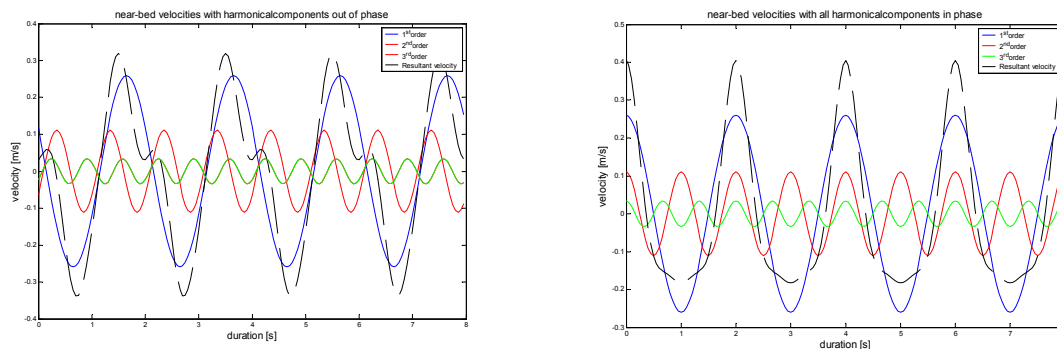


Figure H.4.3-2 Different velocity profiles created out same harmonical components but the figure on the left has phase differences between the harmonical components and the right figure is in phase.

Due to these changing phases of the various harmonical order components, the horizontal near-bed velocities will not grow linearly towards the breaking point of the waves, where the surface elevation of the wave is maximal. The graph that represents the increase of velocities can look very bumpy due to these ever changing phase lags. This is represented in figure H.4.3-2.

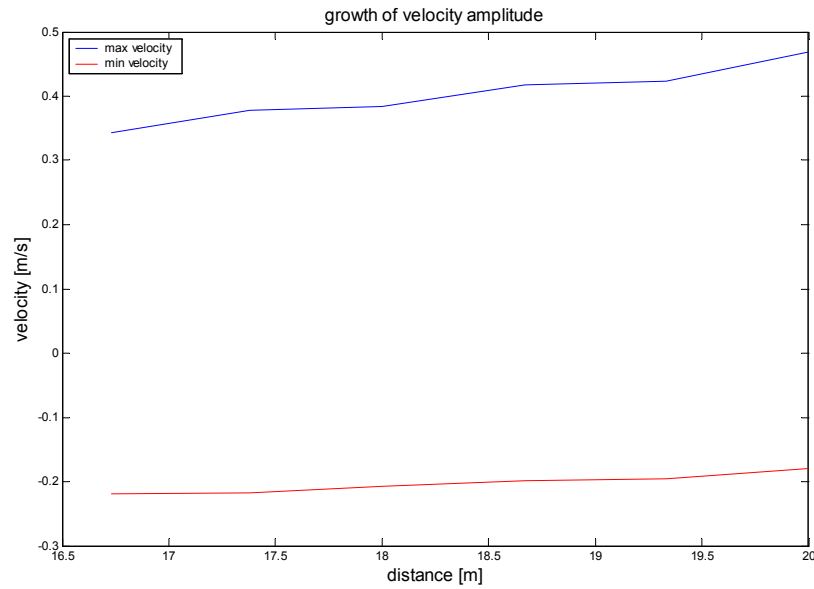


Figure H.4-3-3 Growth of velocities in decreasing water depth for $H_0=0.125\text{m}$, $T=2\text{s}$ and $h_0=55\text{cm}$

When plotting the phases of the first three harmonical components of this wave the phase shifts look arbitrary.

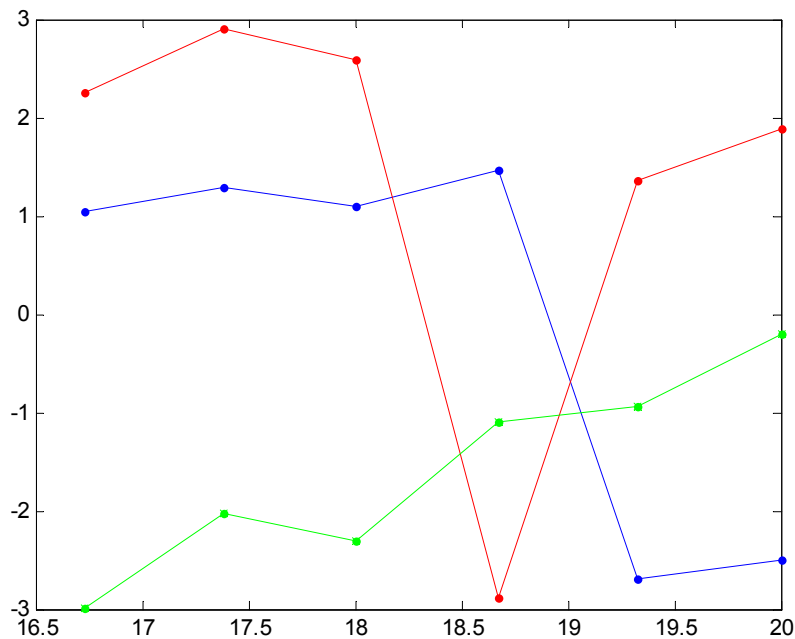


Figure H-4.3.5 Phase shifts of first three harmonical components

When bearing in mind that every point can be shifted upwards 2π the same values for the harmonical components can be represented in the following manner.

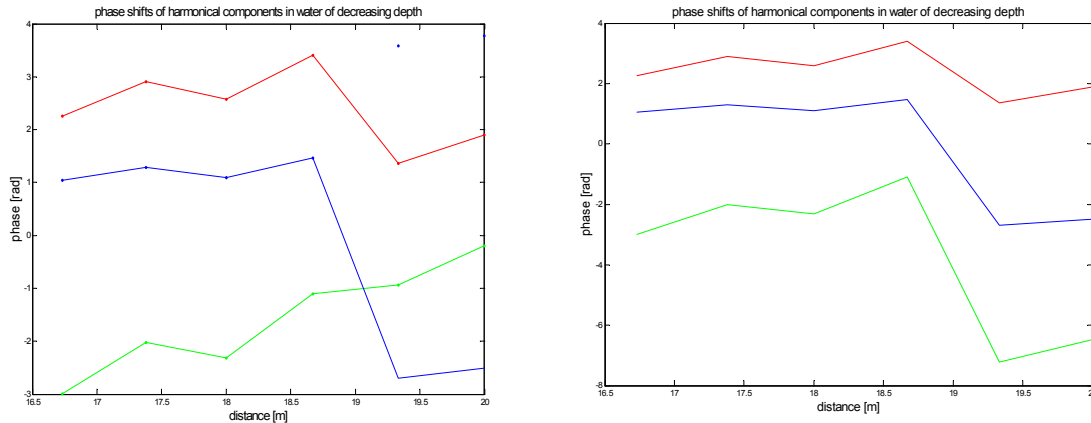


Figure H.4.3.6 Phase shifts of three largest harmonical components

Here a sudden decrease of the phase of the first two components can be found and in the second graph even a decrease of all three harmonical components. A reason for this is that at that point the form of the wave changes in a saw tooth form. Note that the waves break at 19.8m, so just before breaking the waves have transformed into a saw tooth profile.

This did however not occur for all waves, so this requires more research. But that is beyond the scope of this thesis.

H.5 Accelerations

As mentioned the velocities are not the only forces that act upon the grains. Accelerations create pressure gradients that also try to move the grains from their initial position. The accelerations are found by differentiating the velocities profile as a function of the time. As said in the previous section the changing waveform leads to changing bed velocities. Therefore also the bed accelerations will change. As seen in the previous section, the near-bed horizontal velocity profile becomes steeper at the wave front for a decreasing water depth. This will therefore yield to increasing accelerations in water of decreasing depth, because the derivative of a steeper profile has a larger value, then the derivative of a mild slope.

The increase of accelerations along the slope can be seen in Figure H.4.2-1. The accelerations are found from derivation of the velocity profile that has been shown in figure H.3.1.1.

From the plots it becomes clear that in the experiment the biggest acceleration (or pressure) gradients can be found just before breaking of the waves. After breaking these accelerations still increase, but the experiment only deals with waves that haven't broken yet.

In the plots the measured waves did break at a distance of 20 m from the wave board. This can be seen in the plot of $X=20\text{m}$ as it shows a lot of turbulence.

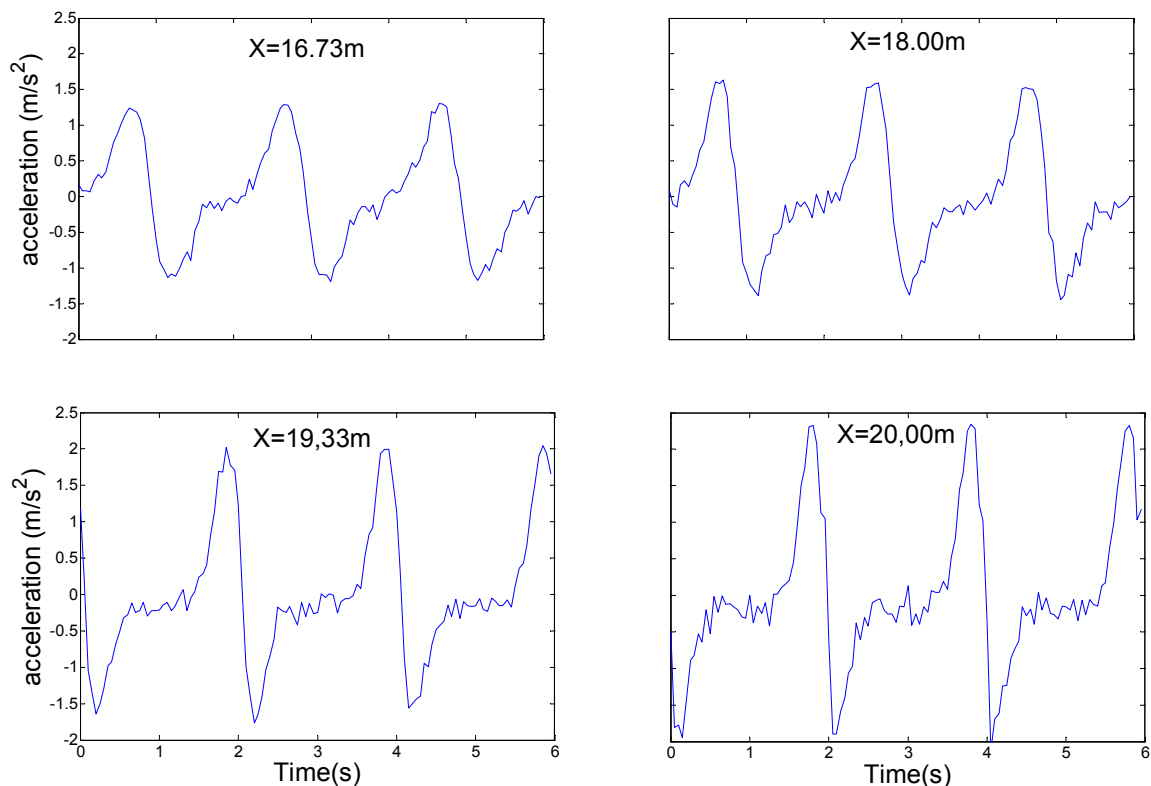


Figure H.5-1 Accelerations at various locations for $H_0=0.125\text{m}$, $T=2\text{s}$ and $h_0=0.55\text{m}$

The growth of accelerations increases more rapidly as the waves near their breaking point, this is shown in the following figure. Values before the measuring area are not available. This is because

the values are all taken from the measurements with the new EMS and there was little time, so only the measurements in the measuring area have been taken.

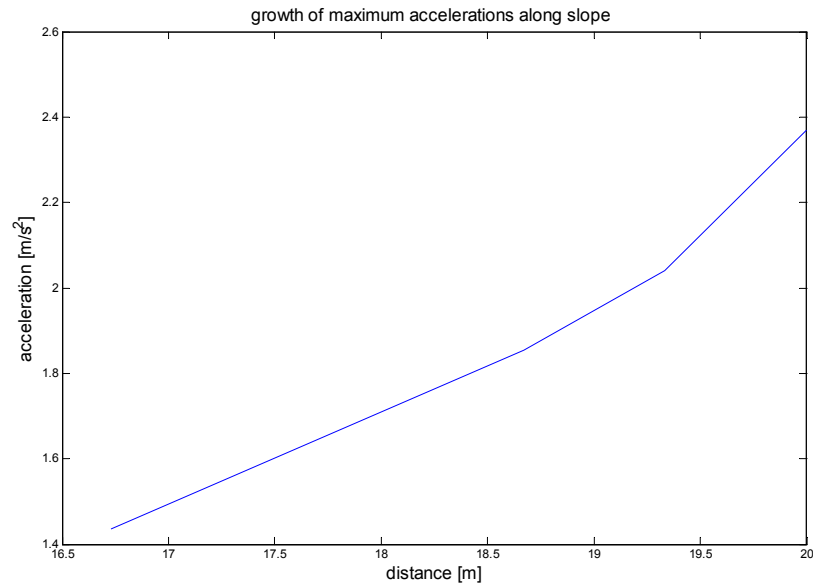


Figure H5-0-1 Values of maximal accelerations obtained in the measuring area for $H_0=0.125\text{m}$, $T=2\text{s}$ and $h_0=55\text{cm}$. Waves break around 20m.

H.6 Proportionality of wave profile to horizontal velocity profile

Both the EMS and the wave gauge have a frequency dependent time-delay. In appendix A can be seen that this time-delay is constant for the relevant frequencies that occur in the experiment. The values of both time delays however are different for the EMS and the wave gauges. From the characteristics, delivered by the manufacturer of the EMS (shown in appendix A), can be seen that the time delay of the wave gauge is 12ms and the time delay of the EMS is about 60ms. This has been illustrated in figure H.6-1

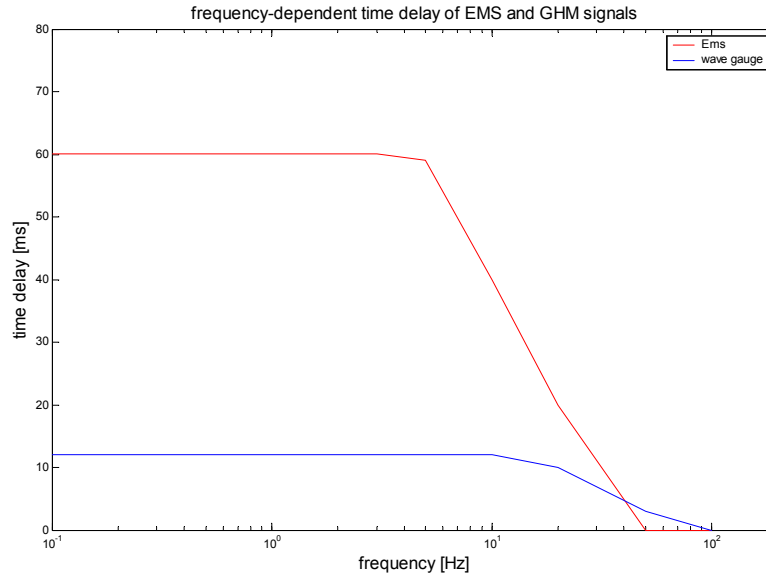


Figure H.6-1 Time delay of both EMS and wave gauge

As this time delay is constant for all relevant frequencies (up to a frequency of 5 Hz), the time delay between the wave gauge data and the EMS data will also be constant. The value of this delay can be found in the above figure. Its value is as big as the distance between the two time delay graphs. This implies that all data measured with the EMS will be recorded $60 - 12 \approx 48\text{ms} \approx 0.05\text{s}$ later. So a surface elevation measured at time t has a corresponding velocity registered at $t+0.05\text{s}$.

For the experiment the assumption has been made that the maximum velocity will be found at the same time as the maximum value of the surface elevation. This lead to the assumption that:

$$\frac{dv}{dt} \equiv \frac{dh}{dt} \quad (\text{H.12})$$

This means that the change of surface elevation in time is proportional to the change of velocity in time. The fact that the time delay between the wave gauges and the EMS is constant at all relevant frequencies and the known behavior of this delay makes it possible to check the validity of the above assumption.

For four different waves and locations the EMS and a wave gauge have been placed next to each other. When there was no wave movement yet the EMS and the wave gauge started their measuring. Subsequently the wave board has been instructed to generate the required regular waves. After 50 waves the wave board was stopped and finally, when there was no more water

movement the measuring instruments were switched off. Doing so allows a verification of the above assumption. By doing the EMS measurements at various heights it also becomes possible to invest whether the height at which the measurements have been taken do influence this time-delay.

The following cases have been investigated, for all cases the initial water depth at the wave board $h_0=55\text{cm}$

1. $T=2\text{s}$, $H_0=0.1\text{m}$ wave gauge and EMS at $X=20\text{m}$. EMS was placed at respectively 4,6,8,10 and 12cm above the bed
2. $T=3\text{s}$, $H_0=0.1\text{m}$, wave gauge and EMS at $X=20\text{m}$. EMS was placed at respectively 4 and 10 cm above bed
3. $T=2\text{s}$, $H_0=0.125\text{m}$, wave gauge and EMS at $X=18\text{m}$. EMS was placed at respectively 4 and 10 cm above the bed
4. $T=2.5\text{s}$, $H_0=0.15\text{m}$, wave gauge and EMS placed at 17.38m. EMS was placed at respectively 4 and 10 cm above the bed.

For all cases the EMS and the wave gauge have been plotted in one figure. When zooming in on the plot it showed that the time delay between the EMS and the wave gauge remain constant over the entire duration of the measurement. This is shown in the following figure for waves with $H_0=0.10\text{m}$ and $T=2\text{s}$ at $X=20\text{m}$.

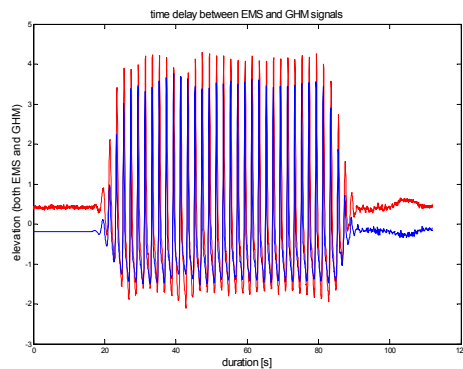


figure A

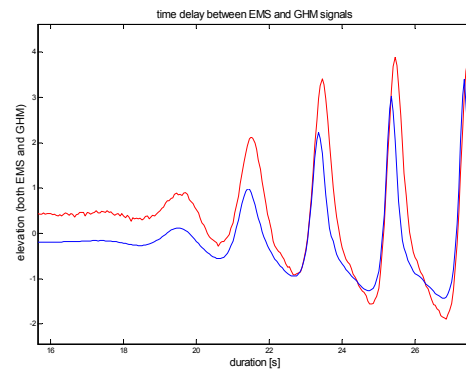


figure B

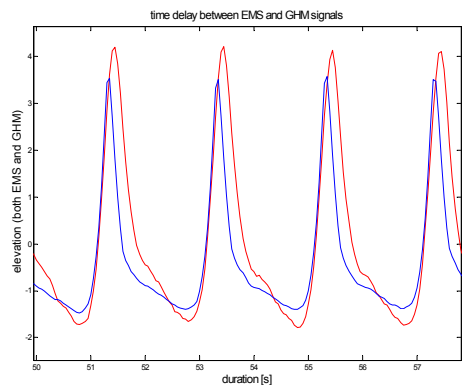


figure C

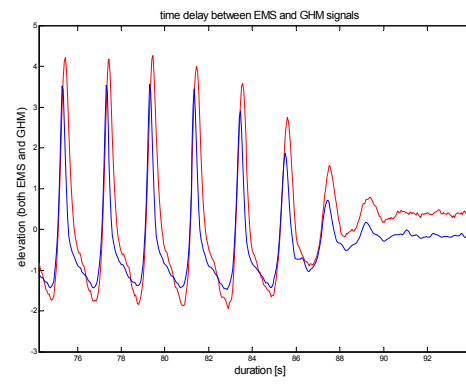


figure D

Figure H.6-1 Time delay between EMS signal and GHM signal. Figure A shows both measured signals over the entire duration of the measurement. Figure B shows the time delay between the EMS

and wave gauge signals as the waves arrive at $X=20\text{m}$. Figure C shows the time delay between EMS and wave gauge signals for waves, which have been completely adapted. Figure D shows the time delay when the waves are no longer generated.

As said it shows that in figure B, C and D the distance between peak-values of the EMS and the wave gauge signal remain constant. Zooming in more closely at two peaks can show the value of this delay between the peak values of the EMS and the wave gauge. This has been done in figure H.6-3

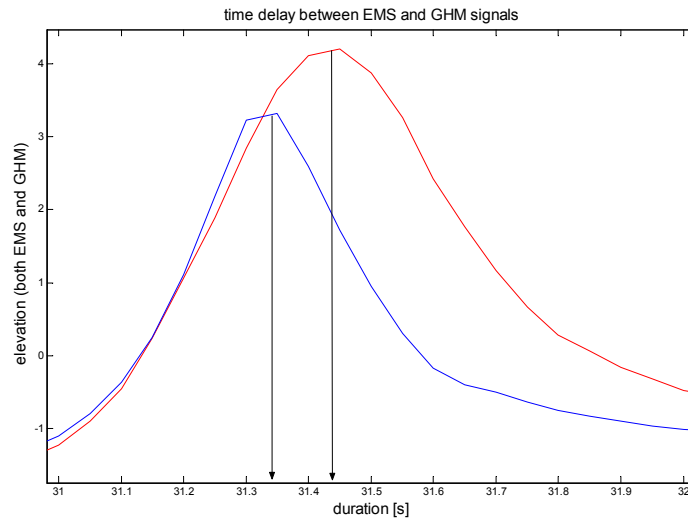


Figure H.6-2 Time delay between wave gauge and EMS at passage of wave top

Here it shows that the distance between the two peaks is about 0.10 seconds. As the time-delay found from the characteristics was 0.05s there will be still a difference of 0.05 s between the peak of the surface elevation and the peak of the near-bed velocity.

For the various elevations of the EMS and the other cases the same analysis has been performed.

Case	Elevation of EMS	Dist. between peaks
$H_0=0.1\text{m}$, $T=2\text{s}$, $X=20\text{m}$	4 cm	0.10s
$H_0=0.1\text{m}$, $T=2\text{s}$, $X=20\text{m}$	6 cm	0.10s
$H_0=0.1\text{m}$, $T=2\text{s}$, $X=20\text{m}$	8 cm	0.10s
$H_0=0.1\text{m}$, $T=2\text{s}$, $X=20\text{m}$	10 cm	0.10s
$H_0=0.1\text{m}$, $T=2\text{s}$, $X=20\text{m}$	12 cm	0.10s
$H_0=0.1\text{m}$, $T=3\text{s}$, $X=20\text{m}$	4 cm	0.15s
$H_0=0.1\text{m}$, $T=3\text{s}$, $X=20\text{m}$	10 cm	0.15s
$H_0=0.125\text{m}$, $T=2\text{s}$, $X=18\text{m}$	4 cm	0.10s
$H_0=0.125\text{m}$, $T=2\text{s}$, $X=18\text{m}$	10 cm	0.10s
$H_0=0.15\text{m}$, $T=2.5\text{s}$, $X=17.38\text{m}$	4 cm	0.10s
$H_0=0.25\text{m}$, $T=2.5\text{s}$, $X=17.38\text{m}$	10 cm	0.12s

TableH-13 Distance between signal peaks

It showed that the elevation of the EMS doesn't lead to different delays between the peaks of the two signals. Nor did the other cases lead to different values of this delay.

The assumption, that the change of velocity in time is proportional to the change of surface elevation in time, is therefore not entirely correct, or the actual time-delay from the EMS is somewhat higher than mentioned in the manual. Nonetheless, because of the very small difference the assumption seems justified. This assumption is even more justified when is considered that previous research showed a velocity profile, which peak value occurred before or equal (instead of after as shown above) to the peak of the surface elevation.